Advanced Theory of Plasmas - EPDY Autumn 2011

- Week 1: Derivation and limitations of the MHD model. Conservation of Flux, The Grad-Shafranov Equation. Coordinate systems in tokamak equilibrium.
- Week 2: Tokamak equilibrium. Analytical expansions. Shafranov Shift. Shaping, and shaping penetration into the torus.
- Week 3: Linearised ideal MHD stability, energy principle, stability boundaries, Internal ideal kink mode
- Week 4: External Kink modes, singular layer calculations (ideal, FLR, resistive), tearing modes
- Week 5: Toroidal effects: Interchange stability (Mercier) and ballooning. Infernal Modes
- Week 6: Parallel dynamics: compressibility in MHD, and analogous kinetic compressibility in hybrid kinetic MHD formulation.
- Week 7: Kinetic-MHD instabilities in tokamaks

Relevant Texts

- J. Freidberg, Ideal MHD
- R. B. White, The Theory of Toroidally Confined Plasmas (Second! edition).
- R. O. Dendy, Plasma Physics, An Introductory Course (Chapter 4 by K. I. Hopcraft)
- Various academic papers, pointed out along the way

The Ideal MHD Model

The following is an alternative derivation, The model is constructed piece by piece, and allowing simple adaptation to more realistic (e.g. kinetic - MHD) models. In essence, the standard ideal MHD model is highly restrictive. It assumes that the plasma is collisional, despite the fact that ideal MHD is often applied to the dynamics of almost collisionless tokamak plasmas.

Nevertheless, ideal MHD does well describe perpendicular (to the equilibrium magnetic field) dynamics of macroscopic instabilities. Cross-magnetic field behaviour is relatively slow. Ideal MHD is not a good descriptor of dynamics parallel to the magnetic field, which for collisionless plasmas, occurs too rapidly for the ideal MHD model.

Luckily, parallel dynamics are often stabilising, or they introduce other classes of instabilities which can be distinguished experimentally from ideal MHD. For this reason, ideal MHD can be used in order to assess the lowest level (necessary but not sufficient) stability of a magnetised plasma. Despite its limitations, it remains an extremely complex and powerful tool to investigate stability. It is also a closed system, enabling non-linear effects (beyond the scope of this course), and other effects to be studied which are too complicated for any other model.

ÉCOLE POLYTECHNIQUE
FÉDÉRALE DE LAUSANNE

The Ideal MHD Model

$$
\begin{aligned}
\frac{d\rho}{dt} + \rho \boldsymbol{\nabla} \cdot \boldsymbol{u} &= 0 \text{ (Conservation of mass)} \\
\rho \frac{d\boldsymbol{u}}{dt} + \boldsymbol{\nabla} P - \boldsymbol{J} \times \boldsymbol{B} &= \mathbf{0} \text{ (Equation of motion)} \\
\frac{d}{dt}\left(P\rho^{-\gamma}\right) &= 0 \text{ (Adiabatic equation of state)} \\
\boldsymbol{E} + \boldsymbol{u} \times \boldsymbol{B} &= \mathbf{0} \text{ (Ideal Ohm's law)} \\
\boldsymbol{\nabla} \cdot \boldsymbol{B} &= 0 \text{ (Field lines have no sources or sinks)} \\
\boldsymbol{\nabla} \times \boldsymbol{B} - \mu_0 \boldsymbol{J} &= \mathbf{0} \text{ (Ampère's law)} \\
\frac{\partial \boldsymbol{B}}{\partial t} + \boldsymbol{\nabla} \times \boldsymbol{E} &= \mathbf{0} \text{ (Faraday's law),}
\end{aligned}
$$

where $\boldsymbol{u}$ is the fluid velocity, ρ is the mass density, P is the plasma pressure, $\boldsymbol{J}$ is the current density, γ is the adiabaticity index and the convective derivative $d/dt = \partial/\partial t + \boldsymbol{u} \cdot \boldsymbol{\nabla}$. The electric and magnetic fields $\boldsymbol{E}$ and $\boldsymbol{B}$ consist of externally applied fields and averaged fields arising from long-range inter-particle interactions.

The Ideal MHD Model

$$\frac{d\rho}{dt} + \rho\boldsymbol{\nabla}\cdot\boldsymbol{u} = 0$$ Exact - no assumptions on gyro radius or collisionality

$$\rho\frac{d\boldsymbol{u}}{dt} + \boldsymbol{\nabla}P - \boldsymbol{J}\times\boldsymbol{B} = \boldsymbol{0}$$ Parallel component poor model in collisionless plasmas

$$\frac{d}{dt}\left(P\rho^{-\gamma}\right) = 0$$ Poor model for system closure in collisionless plasma

$$\boldsymbol{E} + \boldsymbol{u}\times\boldsymbol{B} = \boldsymbol{0}$$ Good providing $r_L \ll a$

$$\boldsymbol{\nabla}\cdot\boldsymbol{B} = 0$$ Exact - Maxwell's

$$\boldsymbol{\nabla}\times\boldsymbol{B} - \mu_0\boldsymbol{J} = \boldsymbol{0}$$ Pre-Maxwell - good for MHD relevant timescales

$$\frac{\partial\boldsymbol{B}}{\partial t} + \boldsymbol{\nabla}\times\boldsymbol{E} = \boldsymbol{0}$$ Exact

Luckily, near marginal stability (small growth rates), plasma motions are incompressible. It will be seen that for incompressible motions, neither the parallel momentum equation, nor the energy equation play an important role (though this is only true when there is no plasma rotation - advanced topic outside e.g. Freidberg). With this in mind, we derive the MHD model in a non-standard way.

Appropriate Assumptions and Variables

The neglect of $\epsilon_0 \boldsymbol{\nabla} \cdot \boldsymbol{E}$ (Poisson equation $\epsilon_0 \boldsymbol{\nabla} \cdot \boldsymbol{E} = \rho$, with ρ the charge distribution) implies that QUASI NEUTRALITY is valid everywhere:

$$\sum_j n_j = n_e \quad \text{with } j \text{ summed over ion species, and } n \text{ is density}$$

It is customary to introduce a mass density ρ rather than number density. Due to quasi-neutrality, and electron/ion mass ratio, fluid mass density in MHD is essentially:

$$\rho = m_i n \tag{1}$$

where we have assumed one ion species i, and employed $n = n_i = n_e$. Likewise, the momentum of the fluid is carried by the ions, so that

$$m_i u_i + m_e u_e \approx m_i u_i$$

Electrons do make an appearance in the fluid like quantity of the current (difference between ion and electron velocity):

$$\boldsymbol{J} = en(\boldsymbol{u}_i - \boldsymbol{u}_e) \tag{2}$$

Guiding Centre Motion

The orbit of a single particle, with velocity components $v_\parallel$ and $v_\perp$ and mass m_i (m_e for an electron) and charge e, in an electro-magnetic field can be written as

$$\boldsymbol{v} = \boldsymbol{v}_{\perp \text{gyro}} + v_\parallel \boldsymbol{e}_\parallel + \boldsymbol{v}_{\perp g}$$

where $\boldsymbol{v}_{\perp \text{gyro}}$ is the rapid gyro motion about a field line, $v_\parallel \boldsymbol{e}_\parallel$ is the streaming along a field line (basic confinement) and the remainder is the slow guiding centre drift velocity, comprising the sum of $\boldsymbol{E}\times\boldsymbol{B}$, $\boldsymbol{\nabla} B$, curvature $\kappa = (\boldsymbol{e}_\parallel \cdot \boldsymbol{\nabla} \boldsymbol{e}_\parallel)$ (where $\boldsymbol{e}_\parallel = \boldsymbol{B}/B$), and polarisation drifts for ions and electrons:

$$\boldsymbol{v}_{\perp gi} = \frac{\boldsymbol{E}\times\boldsymbol{B}}{B^2} + \frac{\boldsymbol{e}_\parallel}{\Omega_{ci}} \times \left[\frac{v_\perp^2}{2}\frac{\boldsymbol{\nabla} B}{B} + v_\parallel^2 \kappa + \frac{d}{dt}\left(\frac{\boldsymbol{E}\times\boldsymbol{B}}{B^2}\right)\right] \tag{3}$$

$$\boldsymbol{v}_{\perp ge} = \frac{\boldsymbol{E}\times\boldsymbol{B}}{B^2} - \frac{\boldsymbol{e}_\parallel}{\Omega_{ce}} \times \left[\frac{v_\perp^2}{2}\frac{\boldsymbol{\nabla} B}{B} + v_\parallel^2 \kappa + \frac{d}{dt}\left(\frac{\boldsymbol{E}\times\boldsymbol{B}}{B^2}\right)\right] \tag{4}$$

where $\Omega_{e,i} = eB/m_{i,e}$. So, some important properties to note: the $\boldsymbol{E}\times\boldsymbol{B}$ drift is in the same direction for both ions and electrons, and forms the basis for the MHD fluid velocity. Corrections are in the opposite direction for electrons and ions, so thus, create the MHD current. Corrections are r_L/a smaller, where $r_L = v_\perp/\Omega_c$.

Take the distribution function of ions F_i and F_e (recall that $\int dv^3 F_{i,e} = n_{i,e}$) and evaluate the first moment of the distribution functions in order to obtain the 'fluid' velocity to leading order in gyro radius (this neglects Hall terms and resulting diamagnetic effects):

$$\boldsymbol{u}_{\perp i,e} = \frac{1}{n_{i,e}} \int dv^3 F_{i,e} \boldsymbol{v}_{\perp gi,e} \approx \frac{\boldsymbol{E}\times\boldsymbol{B}}{B^2}, \tag{5}$$

which can be re-written as Ohm's law, which states that the electric field in a frame moving with the plasma (fluid velocity $\boldsymbol{u}$ is zero:

$$\boldsymbol{E} + \boldsymbol{u}\times\boldsymbol{B} = 0$$

Ohms Law: Conservation of Flux in Ideal MHD

Consider a closed loop C of surface S drawn in the fluid. A magnetic field $\boldsymbol{B}$ passes through the loop, bounded by l, and so the flux Φ linking the loop is

$$\Phi = \int_S \boldsymbol{B} \cdot \boldsymbol{dS}$$

The flux can change in two ways.

1) The loop can deform, and by altering its shape, it can lose or capture field lines. If the loop moves with velocity $\boldsymbol{v}_c$, and $\boldsymbol{\delta l}$ is an elemental length tangential to the loop L, then in time δt it will sweep out an elemental area:

$$\boldsymbol{\delta S}_c = \boldsymbol{v}_c \, \delta t \times \boldsymbol{\delta l} = \boldsymbol{v}_c \, \delta t \, \delta l \, \sin\theta$$

and the flux linking this element is

$$\delta\Phi_c = (\boldsymbol{v}_c \, \delta t \times \boldsymbol{\delta l}) \cdot \boldsymbol{B} = -(\boldsymbol{v}_c \times \boldsymbol{B}) \cdot \boldsymbol{\delta l} \, \delta t.$$

2) Alternatively, the flux can change through $\boldsymbol{B}$ itself changing in time. The change in flux through a stationary element of area $\boldsymbol{\delta S}$ in time δt is

$$\delta\Phi_t = \frac{\partial \boldsymbol{B}}{\partial t} \cdot \boldsymbol{\delta S} \, \delta t$$

and the total rate of change of flux is therefore the sum of 1) and 2):

$$\frac{\delta\boldsymbol{\Phi}}{\delta t} = \frac{\delta\boldsymbol{\Phi}_c}{\delta t} + \frac{\delta\boldsymbol{\Phi}_t}{\delta t}.$$

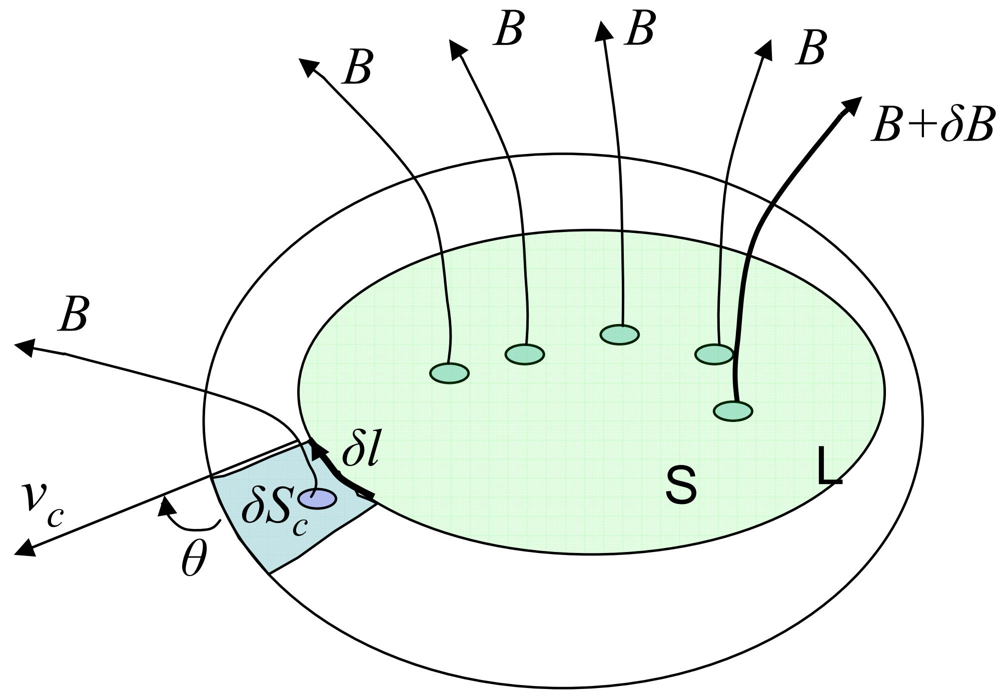

Concept of Conservation of Flux in Ideal MHD

On proceeding to the limit where δt, $\boldsymbol{\delta S}$ and $\boldsymbol{\delta l}$ tend to zero, and summing the contributions from the elemental loops, it follows that,

$$\frac{d\boldsymbol{\Phi}}{dt} = \oint_L (\boldsymbol{v}_c \times \boldsymbol{B}) \cdot \boldsymbol{dl} + \int_S \frac{\partial \boldsymbol{B}}{\partial t} \cdot \boldsymbol{dS},$$

where the line integral evaluated around the loop L. Use Faraday's law $\partial \boldsymbol{B}/\partial t = -\boldsymbol{\nabla} \times \boldsymbol{E}$, and employ Stoke's theorem $\int_S (\boldsymbol{\nabla} \times \boldsymbol{A}) \cdot \boldsymbol{dS} = \oint_L \boldsymbol{A} \cdot \boldsymbol{dl}$ to obtain,

$$\frac{d\boldsymbol{\Phi}}{dt} = \oint_L (\boldsymbol{v}_c \times \boldsymbol{B}) \cdot \boldsymbol{dl} - \oint_L \boldsymbol{E} \cdot \boldsymbol{dl}$$

Apply now resistive Ohm's law $\boldsymbol{E} + \boldsymbol{v} \times \boldsymbol{B} - \eta \boldsymbol{J} = 0$, with η the resistivity and $\boldsymbol{v}$ the *fluid* velocity, giving:

$$\frac{d\boldsymbol{\Phi}}{dt} = -\oint_L \{(\boldsymbol{v}_c - v) \times \boldsymbol{B} + \eta \boldsymbol{J}\} \cdot \boldsymbol{dl}$$

Concept of Conservation of Flux in Ideal MHD

On proceeding to the limit where δt, $\boldsymbol{\delta S}$ and $\boldsymbol{\delta l}$ tend to zero, and summing the contributions from the elemental loops, it follows that,

$$\frac{d\boldsymbol{\Phi}}{dt} = \oint_L (\boldsymbol{v}_c \times \boldsymbol{B}) \cdot \boldsymbol{dl} + \int_S \frac{\partial \boldsymbol{B}}{\partial t} \cdot \boldsymbol{dS},$$

where the line integral evaluated around the loop L. Use Faraday's law $\partial \boldsymbol{B}/\partial t = -\boldsymbol{\nabla} \times \boldsymbol{E}$, and employ Stoke's theorem $\int_S (\boldsymbol{\nabla} \times \boldsymbol{A}) \cdot \boldsymbol{dS} = \oint_L \boldsymbol{A} \cdot \boldsymbol{dl}$ to obtain,

$$\frac{d\boldsymbol{\Phi}}{dt} = \oint_L (\boldsymbol{v}_c \times \boldsymbol{B}) \cdot \boldsymbol{dl} - \oint_L \boldsymbol{E} \cdot \boldsymbol{dl}$$

Apply now resistive Ohm's law $\boldsymbol{E} + \boldsymbol{v} \times \boldsymbol{B} - \eta \boldsymbol{J} = 0$, with η the resistivity and $\boldsymbol{v}$ the *fluid* velocity, giving:

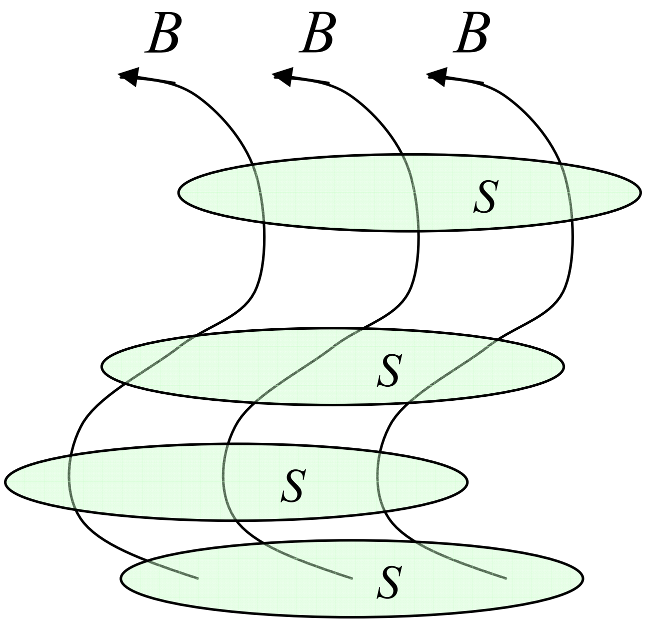

$$\frac{d\boldsymbol{\Phi}}{dt} = -\oint_L \{(\boldsymbol{v}_c - v) \times \boldsymbol{B} + \eta \boldsymbol{J}\} \cdot \boldsymbol{dl}$$

If we define the boundary $\boldsymbol{S}$, and the increment $\boldsymbol{\delta S}$ as those of the fluid, such that the fluid moves with velocity $\boldsymbol{v}_c$, then

$$\frac{d\boldsymbol{\Phi}}{dt} = -\oint_L \eta \boldsymbol{J} \cdot \boldsymbol{dl}.$$

Plainly in the ideal limit we have the conceptually appealing notion of field lines being frozen into the fluid. For, if the fluid elements retain their identity it follows that the magnetic field topology is necessarily invariant. This constraint has a profound effect on the allowable class of MHD motions. Clearly, a small amount of resistivity would allow the field lines to diffuse through the fluid (e.g. sun spots and solar flare activity, as well as tearing modes in tokamaks).

Current and Momentum Equation

Evaluate the guiding centre current by subtracting Eqs. (3) and (4) and evaluating the first moments of the electron and ion distributions

$$\boldsymbol{J}_{\perp g} = e\int dv^3(F_i\boldsymbol{v}_{\perp gi} - F_e\boldsymbol{v}_{\perp ge}) = \frac{\boldsymbol{e}_{\parallel}}{B}\times\left[P_{\perp}\frac{\boldsymbol{\nabla}B}{B} + P_{\parallel}\kappa + \rho\frac{d}{dt}\left(\frac{\boldsymbol{E}\times\boldsymbol{B}}{B^2}\right)\right] \quad (6)$$

where

$$P_{\perp} = P_{\perp i} + P_{\perp e} = m_i\int dv^3 F_i\frac{v_{\perp}^2}{2} + m_e\int dv^3 F_e\frac{v_{\perp}^2}{2}$$

$$P_{\parallel} = P_{\parallel i} + P_{\parallel e} = m_i\int dv^3 F_i v_{\parallel}^2 + m_e\int dv^3 F_e v_{\parallel}^2$$

$$\rho \approx m_i\int dv^3 F_i$$

We also need to consider the magnetisation (diamagnetic) current

$$\boldsymbol{J}_M = -\boldsymbol{\nabla}\times\left(P_{\perp}\frac{\boldsymbol{B}}{B^2}\right)$$

The total current is the sum $\boldsymbol{J} = \boldsymbol{J}_{\perp g} + \boldsymbol{J}_M$. The trick is so substitute the Ohm's law (5) into the guiding centre current (6) and form the cross product with $\boldsymbol{B}$ in order to obtain the momentum equation:

$$\rho\left(\boldsymbol{e}_{\parallel}\times\frac{du_{\perp}}{dt}\right)\times\boldsymbol{e}_{\parallel} = \boldsymbol{J}\times\boldsymbol{B} - \boldsymbol{\nabla}_{\perp}\cdot\underline{\underline{P}}$$

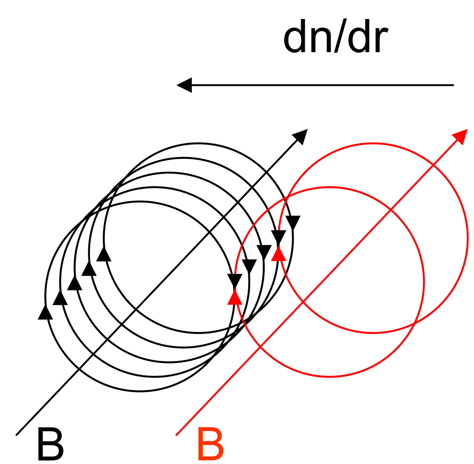

If there is a density gradient, a current is generated perpendicular to B and dn/dr. Larmor radius (and currents) also affected by temperature (v^2) and field strength.

Momentum Equation continued

Here we have

$$\underline{\underline{P}} = P_\perp \underline{\underline{I}} + (P_\| - P_\perp)\boldsymbol{e}_\|\boldsymbol{e}_\| = \begin{pmatrix} P_\perp & 0 & 0 \\ 0 & P_\perp & 0 \\ 0 & 0 & P_\| \end{pmatrix} \quad \text{and} \quad \boldsymbol{\nabla}_\perp = \boldsymbol{\nabla} - \boldsymbol{e}_\|(\boldsymbol{e}_\| \cdot \boldsymbol{\nabla}) \tag{7}$$

where $\underline{\underline{I}}$ is the unit dyadic. This diagonal pressure tensor, and properties of curvature vector reveal the useful result:

$$\boldsymbol{\nabla}_\perp \cdot \underline{\underline{P}} = [\boldsymbol{\nabla} - \boldsymbol{e}_\|(\boldsymbol{e}_\| \cdot \boldsymbol{\nabla})]P_\perp + (P_\| - P_\perp)\boldsymbol{\kappa}$$

Let us recap the model equations so far:

$$\begin{aligned} \frac{d\rho}{dt} + \rho\boldsymbol{\nabla}\cdot\boldsymbol{u} &= 0 \\ \rho\frac{d\boldsymbol{u}_\perp}{dt}\bigg|_\perp - \boldsymbol{J}\times\boldsymbol{B} + \boldsymbol{\nabla}_\perp\cdot\underline{\underline{P}} &= \boldsymbol{0} \\ \boldsymbol{E} + \boldsymbol{u}\times\boldsymbol{B} &= \boldsymbol{0} \\ \boldsymbol{\nabla}\cdot\boldsymbol{B} &= 0 \\ \boldsymbol{\nabla}\times\boldsymbol{B} - \mu_0\boldsymbol{J} &= \boldsymbol{0} \\ \frac{\partial\boldsymbol{B}}{\partial t} + \boldsymbol{\nabla}\times\boldsymbol{E} &= \boldsymbol{0} \end{aligned} \tag{8}$$

We note that we need to close the system with an energy equation (giving $\underline{\underline{P}}$), and an equation for $u_\|$. Depending on the application, we will close the system as appropriate.

MHD Equilibrium

We initially look at a static equilibrium, meaning that there are no equilibrium flows $\boldsymbol{u} = 0$ and $\partial\boldsymbol{u}/dt = 0$. Consider the isotropic case where $P_\perp = P_\parallel = P$. Thus we have to solve

$$\boldsymbol{J} \times \boldsymbol{B} = \boldsymbol{\nabla} P \tag{9}$$

On taking the divergence of Amperes law $\boldsymbol{\nabla} \times \boldsymbol{B} = \mu_0 \boldsymbol{J}$ it follows that $\boldsymbol{\nabla} \cdot \boldsymbol{J} = 0$, indicating that there are no sources or sinks in the current, in accordance with charge neutrality. It is evident from Eq.(9) that $\boldsymbol{J} \cdot \boldsymbol{\nabla} P = 0$ and $\boldsymbol{B} \cdot \boldsymbol{\nabla} P = 0$ which means that lines of magnetic field and current lie on surfaces of constant pressure. In a tokamak these isobaric surfaces are known as flux surfaces

- The so called 'hairy ball' theorem ,attributed to Poincare, states that the only smooth surface which can be covered by a non-vanishing vector field (i.e. current of magnetic field vectors) is a toroidal one.
- Hence toroidal surfaces of constant pressure (flux surfaces) will have the attractive property that the fields of $\boldsymbol{B}$ and $\boldsymbol{J}$ be non-zero everywhere on the surface.
- This indicates that the $\boldsymbol{J} \times \boldsymbol{B}$ force can, in principle at least, balance the pressure everywhere.

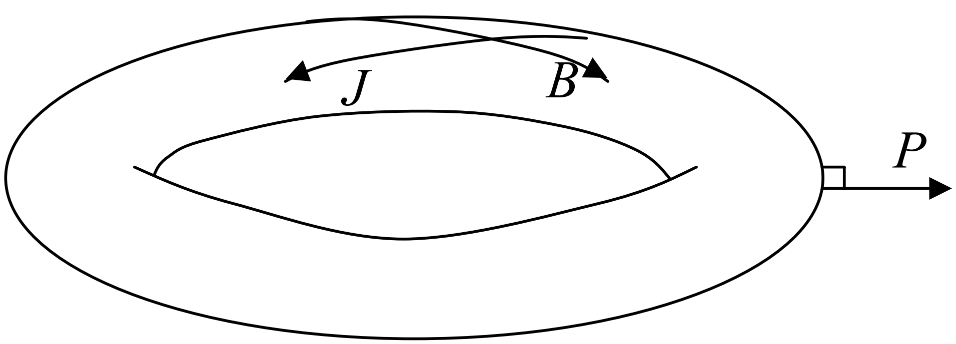

Definitions of Cylindrical Coordinates

We note that there are two types of cylindrical coordinates used in our field. The first type represents a cylindrical system which is an un-approximated (though not very useful for stability considerations) definition of toroidal geometry, and is the baseline or standard definition of the equilibrium. The other type is used in stability studies, and involves approximating to an infinite aspect ratio ratio ($R/a \to \infty$), and circular nested flux surfaces. We must not confuse these very different meanings of 'cylindrical.'

Cylindrical coordinates of un-approximated torus looking down from above

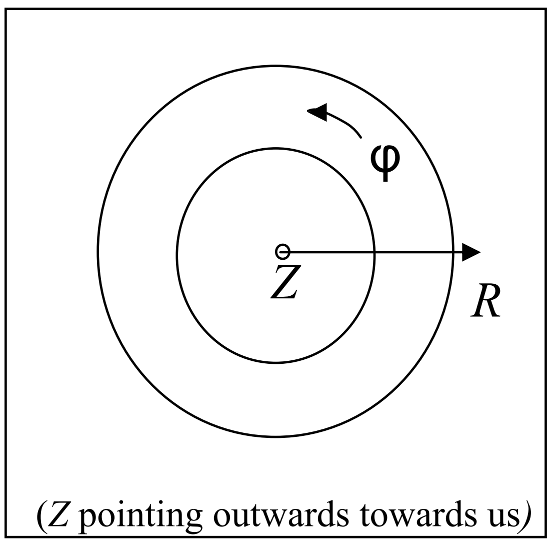

Approximated cylindrical tokamak used in stability studies

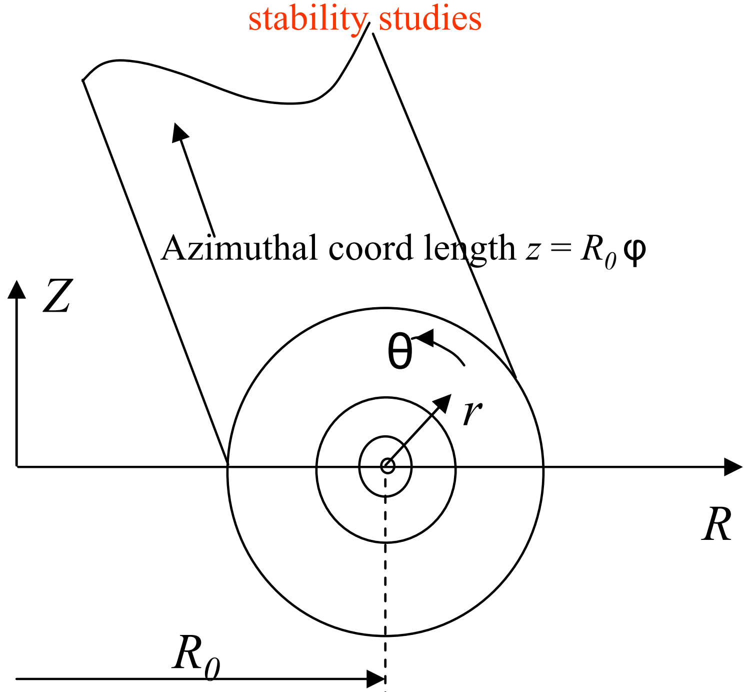

Axisymmetric Toroidal Equilbria

We employ the cylindrical coordinate system (R, ϕ, Z) which in these coordinates give

$$\boldsymbol{\nabla}\cdot\boldsymbol{B} = \frac{1}{R}\frac{\partial(RB_R)}{\partial R} + \frac{\partial B_Z}{\partial Z} + \frac{1}{R}\frac{\partial B_\phi}{\partial \phi} = 0$$

We assume equilibrium axisymmetry, which means that all equilibrium quantities (e.g. pressure magnetic field and current) are independent of ϕ, so that $B = B(Z, R)$. This then allows us to introduce a stream function to represent the field components in the poloidal plane

$$RB_R = \frac{\partial\psi}{\partial Z} \quad and \quad RB_Z = -\frac{\partial\psi}{\partial R}$$

or more succinctly,

$$\boldsymbol{B} = \boldsymbol{B}_p + B_\phi\boldsymbol{e}_\phi \;\text{ with }\; \boldsymbol{B}_p = \boldsymbol{\nabla}\psi\times\boldsymbol{\nabla}\phi \;\text{ and }\; \boldsymbol{\nabla}\phi = \frac{\boldsymbol{e}_\phi}{R} \tag{10}$$

It is clear that toroidal and poloidal fields are perpendicular to $\boldsymbol{\nabla}\psi$, i.e. the field lines lie on surfaces of constant ψ. It is now clear why these surfaces are named flux surfaces, since ψ is related to the poloidal flux ψ_p, for instance through a ring in the equitorial plane defined by $S = \{Z = 0, R(\psi_1) < R < R(\psi_2)\}$

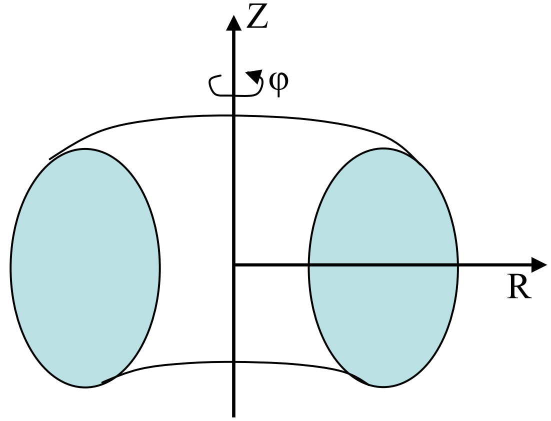

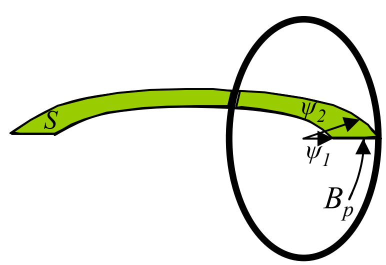

$$\psi_p = \int_S \boldsymbol{B}_p\cdot d\vec{S} = \int_S \boldsymbol{\nabla}\times(\psi\boldsymbol{\nabla}\phi)\cdot\boldsymbol{dS}$$
$$= \oint \psi\boldsymbol{\nabla}\phi\cdot\boldsymbol{dl} = 2\pi(\psi_2 - \psi_1)$$

The total poloidal flux (vacuum as well as plasma field) through the circular magnetic axis is found by taking $R(\psi_1) = R_0$ and $R(\psi_2) = 0$, where $R = R_0, Z = 0$ defines the magnetic axis whereby $\psi = 0$.

ÉCOLE POLYTECHNIQUE
FÉDÉRALE DE LAUSANNE

Axisymmetric Toroidal Equilibria

Applying Amperes law in the cylindrical system we obtain

$$\mu_0 J_R = \frac{\partial B_\phi}{\partial Z} \quad , \quad \mu_0 J_Z = -\frac{1}{R}\frac{\partial (R B_\phi)}{\partial R} \quad , \quad \mu_0 J_\phi = -\frac{\partial}{\partial R}\left(\frac{1}{R}\frac{\partial \psi}{\partial R}\right) - \frac{1}{R}\frac{\partial^2 \psi}{\partial Z^2}.$$

Grouping the poloidal and toroidal currents, identified in Eq. (10), one obtains the compact expression

$$\mu_0 \boldsymbol{J} = \frac{1}{R}\boldsymbol{\nabla}(R B_\phi) \times \boldsymbol{e}_\phi - \frac{1}{R}\Delta^* \psi \boldsymbol{e}_\phi \tag{11}$$

with Δ^* the Laplacian-like Grad-Shafranov operator, which in general coordinates is given by

$$\Delta^* = R^2 \boldsymbol{\nabla} \cdot \left(\frac{1}{R^2}\boldsymbol{\nabla}\right) \tag{12}$$

while in the cylindrical coordinate system, we have

$$\Delta^* = R\frac{\partial}{\partial R}\left(\frac{1}{R}\frac{\partial}{\partial R}\right) + \frac{\partial^2}{\partial Z^2}.$$

Now, substituting the field Eq. (10) and the current Eq. (11) into force balance $\boldsymbol{J} \times \boldsymbol{B} - \boldsymbol{\nabla} P = 0$, and forming the dot product with $\boldsymbol{e}_\phi$, (for which $\boldsymbol{\nabla} P \cdot \boldsymbol{e}_\phi = 0$) yields an equation for the toroidal field that is independent of pressure,

$$\frac{\partial (R B_\phi)}{\partial R}\frac{\partial \psi}{\partial Z} - \frac{\partial (R B_\phi)}{\partial Z}\frac{\partial \psi}{\partial R} = 0.$$

This states that the Jacobian of the functions $R B_\phi / \mu_0$ and ψ is zero. The vanishing of the Jacobian implies that

$$F(\psi) = R B_\phi / \mu_0 \quad \text{is constant on a flux surface} \tag{13}$$

Axisymmetric Toroidal Equilibria

Now use the fact that field lines lie on isobaric surfaces $\boldsymbol{B}\cdot\boldsymbol{\nabla}P=0$:

$$\boldsymbol{B}\cdot\boldsymbol{\nabla}P=\frac{1}{R}\boldsymbol{\nabla}\psi\times\boldsymbol{e}_\phi\cdot\boldsymbol{\nabla}P=\frac{1}{R}\frac{\partial\psi}{\partial R}\frac{\partial P}{\partial Z}-\frac{1}{R}\frac{\partial\psi}{\partial Z}\frac{\partial P}{\partial R}=0$$

which is the Jacobian of P and ψ, which again vanishes, so that $P=P(\psi)$. Finally, forming the dot product of $\boldsymbol{J}\times\boldsymbol{B}-\boldsymbol{\nabla}P=0$, with $\boldsymbol{e}_R$ we obtain

$$\frac{\partial P}{\partial R}=-\left(\frac{1}{\mu_0 R}\frac{\partial(RB_\phi)}{\partial R}\right)B_\phi-\frac{1}{\mu_0 R}\Delta^*\psi\left(\frac{1}{R}\frac{\partial\psi}{\partial R}\right).$$

Using the fact that both P and RB_ϕ are functions of ψ only:

$$\frac{\partial P}{\partial R}=\frac{\partial\psi}{\partial R}\frac{dP}{d\psi}=-\frac{\partial\psi}{\partial R}\frac{1}{R^2}\mu_0F\frac{dF}{d\psi}-\frac{\partial\psi}{\partial R}\frac{\Delta^*\psi}{\mu_0R^2},$$

which directly gives the Grad-Shafranov Equation

$$\Delta^*\psi=-\mu_0R^2\frac{dP(\psi)}{d\psi}-\mu_0^2F(\psi)\frac{dF(\psi)}{d\psi}. \qquad (14)$$

Note that on substitution of Eq.(12) into Eq.(14) we see the true power of the Grad-Shafranov equation. In particular, it is independent of the system of coordinates on a given flux surface.

Now Eq. (14) is a non-linear, second order elliptic partial differential equation for the equilibrium in terms of the flux. The general procedure for finding its solution is first to prescribe the pressure $P(\psi)$ and current function $F(\psi)$ as some physically reasonable distribution of the flux ψ.

Axisymmetric Toroidal Equilbria

Realistic boundary conditions (BC) are obviously required, and these come in essentially two forms.

1. A sufficient BC would be to define $\psi(R, Z)$ on a closed contour, i.e. by defining the shape of one flux surface, for instance. If a fixed outer surface is specified, then in essence the plasma-vacuum boundary is replaced by the surface of a perfect conductor (on which ψ is necessarily constant). This is a fixed boundary condition, which defines ψ in the entire plasma.
2. By specifying a flux surface in the vacuum region, one has a free boundary problem. Taking into account the currents in the coils leads to a somewhat different approach. One can use the known currents in the coils and an assumed plasma current distribution to compute ψ on a boundary which is convenient for the computations, a rectangle, say. With these Dirichlet boundary conditions one then solves the Grad-Shafranov equation in the interior. This leads to a different plasma current distribution than originally assumed, and one iterates the procedure. As an alternative, or in addition to considering the coil currents and computing $\boldsymbol{B}$ in the metal parts as well as the vacuum, poloidal field measurements can be available close to the coils or near the plasma. This makes the set of boundary conditions altogether more inhomogeneous and a very adaptable equilibrium solver is required. The system can even be over determined and to a certain extent the functions $P(\psi)$ and $F(\psi)$ can then be computed.

Flux Coordinates

Of great importance in equilibrium calculations, but also in the modelling of plasma transport and in stability analysis, are flux coordinates (r, θ, ϕ). Here ϕ is the usual toroidal angle. The radial coordinate $r(\psi)$ labels the flux surfaces. It can be the poloidal (or toroidal) flux itself, or the volume enclosed by each flux surface, or can be chosen to closely resemble the minor radius (distance to the magnetic axis). One possibility is the minor radius at Z = 0. Another definition takes the square root of the area of the cross section. The differences between such definitions are easy to account for and usually not very important. The various definitions used for the poloidal angle θ, however, are convenient in very specific applications: (i) the proper geometrical angle can be used when the geometry is fixed, for instance in tomographic diagnostic methods, (ii) an orthogonal coordinate system ($\nabla r \cdot \nabla \theta = 0$) is convenient in ballooning stability analysis and certain means of solving the Grad-Shafranov equation, (iii) and most universally applied, especially in stability studies, are coordinates in which the field lines appear straight. In these coordinates the local pitch of the magnetic field line trajectory

$$q_l = \frac{d\phi}{d\theta}$$

is a constant on each flux surface. Note that the standard definition of the safety factor q if the average of q_l over the poloidal angle,

$$q(\psi) = \frac{1}{2\pi} \int_0^{2\pi} q_l(\theta, \psi)\, d\theta \tag{15}$$

Hence q is invariant on the flux surface, i.e. $q = q(\psi)$. Moreover, for straight field line coordinates, $q_l = q$, so that $d\phi/d\theta$ is also a flux surface quantity (by definition). Finally, there is a modified version of type (iii), known as Boozer coordinates. Here, the toroidal angle and poloidal angles are modified in order to permit the field to be written in covariant form, and allow straight field lines even when the equilibrium is not axis-symmetric (e.g. stellarator). The covariant field description is essential for the development of drift orbit trajectory following formulation in canonical coordinates (rapid orbit following codes, e.g. VENUS at CRPP). A problem with straight field line coordinates is poor resolution on the low field side (LFS), especially for low aspect ratio, and high pressure (e.g. for modelling spherical tokamaks).

Flux Coordinates

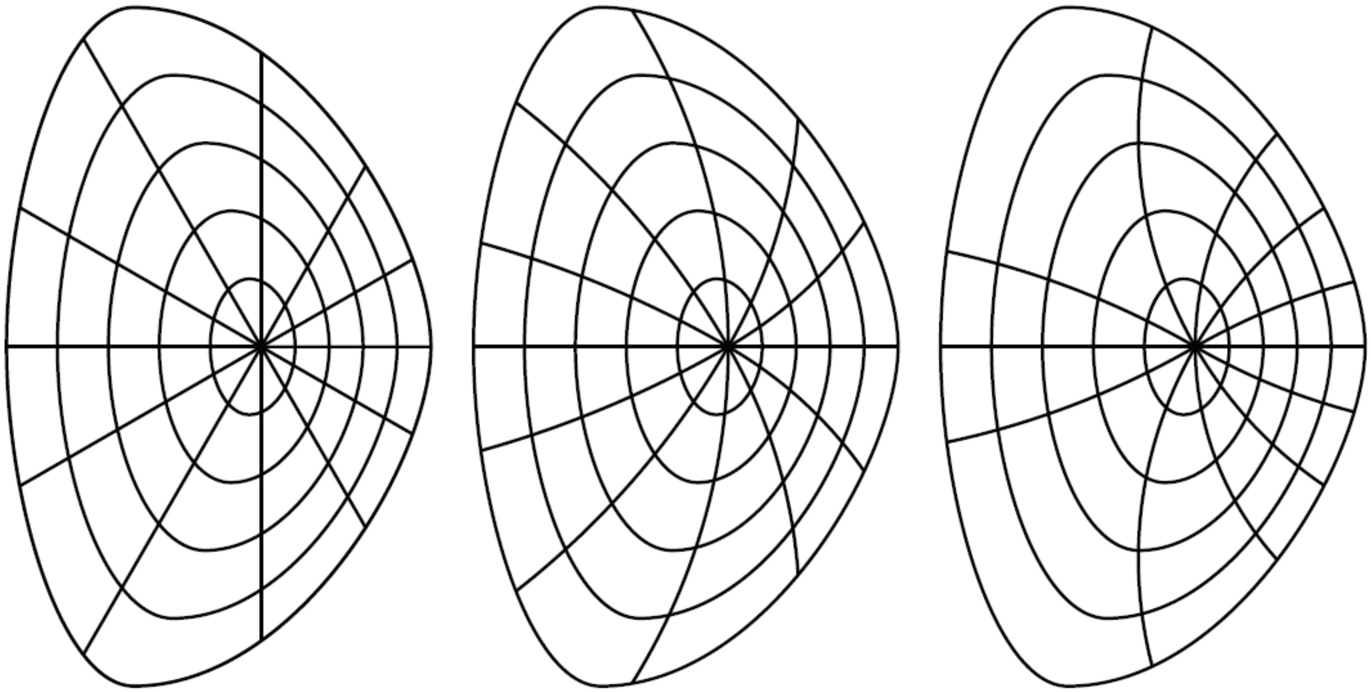

(i) Proper geometric angle (ii) Straight field line system (iv) Orthogonal system

In order to generate an analytic description of the equilibrium, we will develop a system with a simple Fourier decomposition (used e.g. in VMEC 3D code). It is neither type i), ii) or iii). The system is non-orthogonal ($\nabla r \cdot \nabla \theta \neq 0$), and so requires tensor calculus. There's no free lunch..

Flux Coordinates

Recall that the Jacobian $\mathcal{J}$ of any coordinate system (r, θ, ϕ) is such that the volume element is given by

$$dv^3 = dr\, d\theta\, d\phi\, \mathcal{J}$$

For general non-orthogonal flux coordinates, the Jacobian is written in its general form

$$\mathcal{J} = |\nabla r \times \nabla\theta \cdot \nabla\phi|^{-1}\,. \tag{16}$$

Meanwhile, the square of element of length dl along the magnetic field comprises the following sum the components of the metric tensor g_{ij}, with $\mathcal{J} = R\sqrt{\det(g_{i,j})}$:

$$dl^2 = g_{r,r}dr^2 + 2g_{r,\theta}dr\, d\theta + g_{\theta,\theta}d\theta^2 + g_{\phi,\phi}d\phi^2 \tag{17}$$

with

$$g_{r,r} = \frac{\mathcal{J}^2}{R^2}|\nabla\theta|^2, \;\; g_{r,\theta} = -\frac{\mathcal{J}^2}{R^2}\nabla\theta\cdot\nabla r, \;\; g_{\theta,\theta} = \frac{\mathcal{J}^2}{R^2}|\nabla r|^2 \text{ and } g_{\phi,\phi} = R^2. \tag{18}$$

We now employ these definitions in the Grad-Shafranov equation Eq.(14) (with Eq.(12)). The following general operator identity is required:

$$\nabla = \nabla r\frac{\partial}{\partial r} + \nabla\theta\frac{\partial}{\partial\theta} + \nabla\phi\frac{\partial}{\partial\phi} = \frac{1}{\mathcal{J}}\left\{\frac{\partial}{\partial r}\nabla r + \frac{\partial}{\partial\theta}\nabla\theta + \frac{\partial}{\partial\phi}\nabla\phi\right\}\mathcal{J} \tag{19}$$

and we have

$$\nabla\psi(r) = \psi'\nabla r, \quad where \;\; X' = \frac{dX}{dr} \tag{20}$$

With the above two equations, one finds that the Grad-Shafranov operator Eq.(12) is

$$\Delta^*\psi = \frac{R^2}{\mathcal{J}}\left[\frac{\partial}{\partial r}\left(\frac{\psi' g_{\theta,\theta}}{\mathcal{J}}\right) - \frac{\partial}{\partial\theta}\left(\frac{\psi' g_{r,\theta}}{\mathcal{J}}\right)\right] \tag{21}$$

Flux Coordinates

We note that the local pitch of the field lines is given by the

$$\frac{d\phi}{d\theta} = \frac{\boldsymbol{B}\cdot\boldsymbol{\nabla}\phi}{\boldsymbol{B}\cdot\boldsymbol{\nabla}\theta}.$$

Making use of the field definition Eq. (10) and Eq. (13), and neglecting to carry μ_0, gives

$$\boldsymbol{B} = F\boldsymbol{\nabla}\phi + \boldsymbol{\nabla}\psi \times \boldsymbol{\nabla}\phi, \tag{22}$$

and thus

$$q = \frac{1}{2\pi}\int_0^{2\pi} d\theta \left(\frac{d\phi}{d\theta}\right) \; = \; \frac{1}{2\pi}\int_0^{2\pi} d\theta \, \frac{F|\boldsymbol{\nabla}\phi|^2}{\boldsymbol{\nabla}\psi\times\boldsymbol{\nabla}\phi\cdot\boldsymbol{\nabla}\theta}$$

where, if we employ $|\boldsymbol{\nabla}\phi| = 1/R$, and the Jacobian definition Eq. (16) together with Eq. (20) we have the general expression,

$$q = \frac{F(\psi)}{2\pi\psi'}\int_0^{2\pi} d\theta \, \frac{\mathcal{J}}{R^2}, \tag{23}$$

where this definition will enable us write ψ' in terms q, and ψ'' in terms of the magnetic shear $s = rq'/q$.

Let us begin with the R, Z expansion (essentially as the axis-symmetric limit of VMEC):

$$R \quad = \quad R_0 + r\cos\theta - \Delta(r) + \sum_{m=2}^{\infty} S_m(r)\cos(m-1)\theta \tag{24}$$

$$Z \quad = \quad r\sin\theta - \sum_{m=2}^{\infty} S_m(r)\sin(m-1)\theta, \tag{25}$$

where R_0 is the major radius at the magnetic axis, r is a flux label, and Δ is the Shafranov shift.

Equilibrium in Large Aspect Ratio

Comparing this with another standard way of writing the equilibrium (e.g. as described in special CHEASE ad-hoc equilibrium),

$$R = \hat{R}_0 + \hat{r}\cos(\omega + \delta\sin\omega) \quad (26)$$

$$Z = \hat{r}\kappa\sin\omega, \quad (27)$$

where the squareness and higher harmonics are ignored, and $\hat{R}_0 = [R(\theta = 0) + R(\theta = \pi)]/2$ and $\hat{r} = [R(\theta = 0) - R(\theta = \pi)]/2$ are respectively the major and minor geometric radii. One can identify this equilibrium in terms of the parameters in Eqs. (24) and (25) with

$$\hat{R}_0 = R_0 - \Delta + S_3, \quad \hat{r} = r + S_2.$$

Also, upon choosing $R(\theta = \pi) = R(\omega = \pi)$ and $Z(\theta = \pi) = Z(\omega = \pi)$ we have

$$\kappa = \frac{r - S_2}{r + S_2}, \quad \text{and} \quad \delta = \frac{4S_3}{r}, \quad (28)$$

(thus the $S_2(r)$ profile defines the elongation profile, and $S_3(r)$ defines the triangularity profile) which together with $R(\omega) = R(\theta)$ gives,

$$\cos\theta - \frac{1+\kappa}{4}\sin^2\theta = \cos(\omega + \delta\sin\omega).$$

This latter condition will introduce a small difference in Z between the two coordinate systems, except at $\theta = 0, \pi, 2\pi$.

Problem: Derivation of Grad-Shafranov Equation in Flux Coordinates

Begin with the operator equation Eq. (19)

$$\nabla X = \frac{1}{\mathcal{J}}\left\{\frac{\partial}{\partial r}(X\mathcal{J}\nabla r) + \frac{\partial}{\partial \theta}(X\mathcal{J}\nabla\theta) + \frac{\partial}{\partial\phi}(X\mathcal{J}\nabla\phi)\right\},$$

or the more directly useful expression,

$$\nabla\cdot\boldsymbol{Y} = \frac{1}{\mathcal{J}}\left\{\frac{\partial}{\partial r}(\mathcal{J}\nabla r\cdot\boldsymbol{Y}) + \frac{\partial}{\partial\theta}(\mathcal{J}\nabla\theta\cdot\boldsymbol{Y}) + \frac{\partial}{\partial\phi}(\mathcal{J}\nabla\phi\cdot\boldsymbol{Y})\right\},$$

Now, we wish to obtain

$$\Delta^*\psi = R^2\nabla\cdot\left(\frac{1}{R^2}\nabla\right)\psi = R^2\nabla\cdot\left(\frac{1}{R^2}\nabla\psi\right),$$

so that in the above substitute,

$$\boldsymbol{Y} = \left(\frac{1}{R^2}\nabla\psi\right)$$

giving

$$\nabla\cdot\boldsymbol{Y} = \nabla\cdot\left(\frac{1}{R^2}\nabla\psi\right) = \frac{1}{\mathcal{J}}\left\{\frac{\partial}{\partial r}\left(\frac{\mathcal{J}}{R^2}\nabla r\cdot\nabla\psi\right) + \frac{\partial}{\partial\theta}\left(\frac{\mathcal{J}}{R^2}\nabla\theta\cdot\nabla\psi\right) + \frac{\partial}{\partial\phi}\left(\frac{\mathcal{J}}{R^2}\nabla\phi\cdot\nabla\psi\right)\right\}$$

Now, the poloidal plane is perpendicular to the ϕ direction, so that $\nabla\phi\cdot\nabla\psi = 0$. Using also Eq. (20), $\nabla\psi(r) = \psi'\nabla r$ where $X' = dX/dr$, and Eqs. (18), i.e. ($g_{r,\theta} = -(\mathcal{J}^2/R^2)\nabla\theta\cdot\nabla r$ and $g_{\theta,\theta} = (\mathcal{J}^2/R^2)|\nabla r|^2$) easily gives Eq. (21)

$$\Delta^*\psi = \frac{R^2}{\mathcal{J}}\left[\frac{\partial}{\partial r}\left(\frac{\psi' g_{\theta,\theta}}{\mathcal{J}}\right) - \psi'\frac{\partial}{\partial\theta}\left(\frac{g_{r,\theta}}{\mathcal{J}}\right)\right]$$

- Week 1: Derivation and limitations of the MHD model. Conservation of Flux, The Grad-Shafranov Equation. Coordinate systems in tokamak equilibrium.
- Week 2: Tokamak equilibrium. Analytical expansions. Shafranov Shift. Shaping, and shaping penetration into the torus.
- Week 3: Linearised ideal MHD stability, energy principle, stability boundaries, Internal ideal kink mode
- Week 4: External Kink modes, singular layer calculations (ideal, FLR, resistive), tearing modes
- Week 5: Toroidal effects: Interchange stability (Mercier) and ballooning. Infernal Modes
- Week 6: Parallel dynamics: compressibility in MHD, and analogous kinetic compressibility in hybrid kinetic MHD formulation.
- Week 7: Kinetic-MHD instabilities in tokamaks

Recap of Week 1

The Grad-Shafranov equation has been derived. It was shown that a tokamak equilibrium can be generated via:

(1) Given profiles in the pressure $P(\psi)$ and the 'current' function $F(\psi)$ with respect to the flux ψ.

(2) The flux ψ on a fixed boundary defined by $(R, Z)_{boundary}$.

With the introduction of flux coordinates, where $\psi = \psi(r)$, with r a minor radius with units of length, we are able to initialise the problem with

(1) $P(r)$, $q(r)$ (via Eq. (23), $q = \frac{F(\psi)}{2\pi\psi'}\int_0^{2\pi} d\theta\, \frac{\mathcal{J}}{R^2}$). Alternatively to $q(r)$ would be to define the toroidal current density J averaged over the flux surface defined by r, since from Eqs. (11) and (14) we have

$$\left\langle J_\phi \right\rangle(r) = \frac{\langle R \rangle}{\psi'} P' + \mu_0 \left\langle \frac{1}{R} \right\rangle \frac{F}{\psi'} F' \quad \text{where} \quad \langle X \rangle(r) = \frac{\int_0^{2\pi} d\theta\, X \mathcal{J}}{\int_0^{2\pi} d\theta\, \mathcal{J}}$$

(2) The flux ψ on a fixed boundary defined by $(R(r,\theta), Z(r,\theta))_{boundary}$

Typically, one would verify that the choice of ψ (with units Tesla m^2) at the boundary is consistent with the toroidal magnetic field (known experimentally). Also known, to some extent experimentally is the distribution of current $I_\phi(r)$, and certainly I_ϕ enclosed within the vessel. Note that $\left\langle J_\phi \right\rangle(r)$ is related to the toroidal current $I_\phi(r)$ enclosed within the surface defined by r:

From this, one will then obtain the surfaces in $R(r,\theta), Z(r,\theta)$ on which the field lines and current lines lie (the flux surfaces). Moreover, we can obtain $\boldsymbol{B}(r,\theta)$ and $\boldsymbol{J}(r,\theta)$ etc.

Recap of Week 1

Input

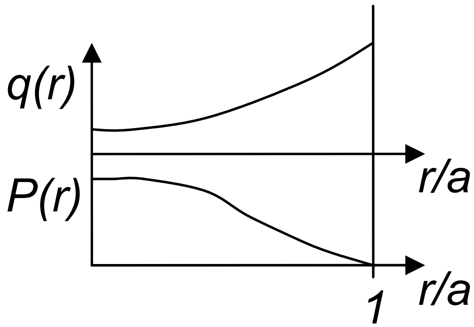

Output

$\Psi'(r)$
$\mathbf{B}(r,\theta)$
$\mathbf{J}(r,\theta)$
etc

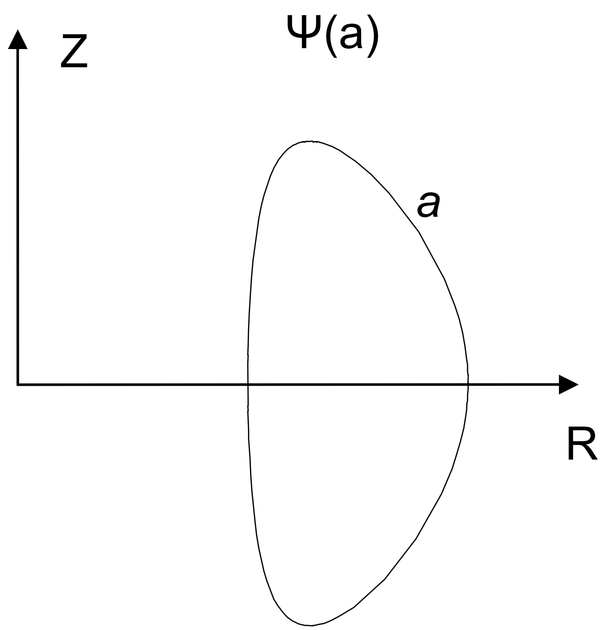

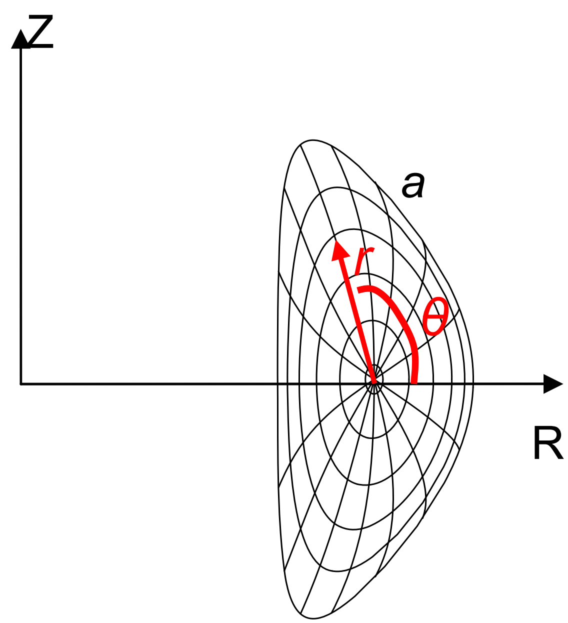

Boundary maps out $R(a,\theta)$, $Z(a,\theta)$,

Equilibrium in Large Aspect Ratio

In the following analysis, and analytical solution for the equilibrium, we will expand all quantities with respect to a small local inverse aspect ratio $\epsilon = r/R_0$. In each equation, we will carry an artificial tag, ε, which is used to denote the size of each term relative to the inverse aspect ratio. This approach is very useful for algebraic manipulation and minimisation, computational algebra or otherwise. For example:

$$
\begin{aligned}
R &= R_0\left(1+\varepsilon\,\epsilon\cos\theta-\varepsilon^2\frac{\Delta(r)}{R_0}+\varepsilon^2\sum_{m=2}^{\infty}\frac{S_m(r)}{R_0}\cos(m-1)\theta+O(\varepsilon^3)\right)\\
Z &= R_0\left(\varepsilon\,\epsilon\sin\theta-\varepsilon^2\sum_{m=2}^{\infty}\frac{S_m(r)}{R_0}\sin(m-1)\theta+O(\varepsilon^3)\right),
\end{aligned}
$$

where we assume that the Shafranov shift (to be calculated next) $\Delta \sim \epsilon^2 R_0$ and the non-circular shaping coefficients $S_m \sim \epsilon^2 R_0$ The quantities required for Δ^* are evidently and in general:

$$
\mathcal{J} = R\left(\frac{\partial R}{\partial\theta}\frac{\partial Z}{\partial r}-\frac{\partial R}{\partial r}\frac{\partial Z}{\partial\theta}\right), \quad g_{r,\theta}=\frac{\partial Z}{\partial r}\frac{\partial Z}{\partial\theta}+\frac{\partial R}{\partial r}\frac{\partial R}{\partial\theta}, \quad g_{\theta,\theta}=\left(\frac{\partial Z}{\partial\theta}\right)^2+\left(\frac{\partial R}{\partial\theta}\right)^2
$$

Employing Eqs. (29) and (30) one finds that

$$
\begin{aligned}
\mathcal{J} &= rR_0\,|\ldots|\\
g_{r,\theta} &= r\,\{\ldots\}\\
g_{\theta,\theta} &= r^2\,\{\ldots\}
\end{aligned}
$$

Equilibrium in Large Aspect Ratio

Depositing these ε expansion terms into the Grad-Shafranov equation of Eqs. (21) and (14) yields

$$\frac{\psi'^2}{r}\left\{1+\varepsilon\,(....)\cos\theta+\varepsilon\sum_{m=2}^{\infty}(....)\cos(m\theta)+O(\varepsilon^2)\right\}+$$

$$\psi'\,\psi''\,\{....\}+R_0^2\left(1+\varepsilon 2(....)+O(\varepsilon^2)\right)P'+FF'=0$$

So, gathering Fourier components, we have

$$\cos(0\theta):\qquad [......]\,[1+O(\varepsilon^2)]=0,$$

$$\cos(\theta):\qquad [.....]\,[1+O(\varepsilon)]=0,$$

$$\cos(m\theta):\qquad [....]\,[1+O(\varepsilon)]=0.$$

Equilibrium in Large Aspect Ratio

In the following analysis, and analytical solution for the equilibrium, we will expand all quantities with respect to a small local inverse aspect ratio $\epsilon = r/R_0$. In each equation, we will carry an artificial tag, ε, which is used to denote the size of each term relative to the inverse aspect ratio. This approach is very useful for algebraic manipulation and minimisation, computational algebra or otherwise. For example:

$$R = R_0\left(1 + \varepsilon\,\epsilon\cos\theta - \varepsilon^2\frac{\Delta(r)}{R_0} + \varepsilon^2\sum_{m=2}^{\infty}\frac{S_m(r)}{R_0}\cos(m-1)\theta + O(\varepsilon^3)\right) \tag{29}$$

$$Z = R_0\left(\varepsilon\,\epsilon\sin\theta - \varepsilon^2\sum_{m=2}^{\infty}\frac{S_m(r)}{R_0}\sin(m-1)\theta + O(\varepsilon^3)\right), \tag{30}$$

where we assume that the Shafranov shift (to be calculated next) $\Delta \sim \epsilon^2 R_0$ and the non-circular shaping coefficients $S_m \sim \epsilon^2 R_0$ The quantities required for Δ^* are evidently and in general:

$$\mathcal{J} = R\left(\frac{\partial R}{\partial\theta}\frac{\partial Z}{\partial r} - \frac{\partial R}{\partial r}\frac{\partial Z}{\partial\theta}\right), \quad g_{r,\theta} = \frac{\partial Z}{\partial r}\frac{\partial Z}{\partial\theta} + \frac{\partial R}{\partial r}\frac{\partial R}{\partial\theta}, \quad g_{\theta,\theta} = \left(\frac{\partial Z}{\partial\theta}\right)^2 + \left(\frac{\partial R}{\partial\theta}\right)^2$$

Employing Eqs. (29) and (30) one finds that

$$\mathcal{J} = rR_0\left|1 + \varepsilon(\epsilon - \Delta')\cos\theta + \varepsilon\sum_{m=2}^{\infty}\left(S'_m - (m-1)\frac{S_m}{r}\right)\cos(m\theta) + O(\varepsilon^2)\right| \tag{31}$$

$$g_{r,\theta} = r\left\{\varepsilon\Delta'\sin\theta - \varepsilon\sum_{m=2}^{\infty}\left(S'_m + (m-1)\frac{S_m}{r}\right)\sin(m\theta) + O(\varepsilon^2)\right\} \tag{32}$$

$$g_{\theta,\theta} = r^2\left\{1 - \varepsilon 2\sum_{m=2}^{\infty}(m-1)\frac{S_m}{r}\cos(m\theta) + O(\varepsilon^2)\right\} \tag{33}$$

Equilibrium in Large Aspect Ratio

Depositing these ε expansion terms into the Grad-Shafranov equation of Eqs. (21) and (14) yields

$$\frac{\psi'^2}{r}\left\{1+\varepsilon\left(r\Delta''+\Delta'-\frac{r}{R_0}\right)\cos\theta-\varepsilon\sum_{m=2}^{\infty}\left(rS_m''+S_m'+(1-m^2)\frac{S_m}{r}\right)\cos(m\theta)+O(\varepsilon^2)\right\}+$$

$$\psi'\,\psi''\left\{1+\varepsilon 2\Delta'\cos\theta-\varepsilon 2\sum_{m=2}^{\infty}S_m'\cos(m\theta)+O(\varepsilon^2)\right\}+R_0^2\left(1+\varepsilon 2\frac{r}{R_0}\cos\theta+O(\varepsilon^2)\right)P'+FF'=0 \quad (34)$$

So, gathering Fourier components, we clearly have

$$\cos(0\theta):\qquad \left[\frac{1}{2r^2}\left(r^2\psi'^2\right)'+R_0^2P'+FF'\right][1+O(\varepsilon^2)]=0, \quad (35)$$

$$\cos(\theta):\qquad \left[\Delta''+\left(2\frac{\psi''}{\psi'}+\frac{1}{r}\right)\Delta'-\frac{1}{R_0}+2\frac{rR_0P'}{(\psi')^2}\right][1+O(\varepsilon)]=0, \quad (36)$$

$$\cos(m\theta):\qquad \left[S_m''+\left(2\frac{\psi''}{\psi'}+\frac{1}{r}\right)S_m'+\frac{1-m^2}{r^2}S_m\right][1+O(\varepsilon)]=0. \quad (37)$$

Eq. (35) describes the balances of forces by the plasma pressure (∇P) and the magnetic pressure ($\nabla B^2/2$), and describes how the poloidal and toroidal fields prevent the plasma from expanding in the ∇r direction.

Eq. (36) yields the radial equation for the Shafranov shift, and expresses how the poloidal field prevents the plasma pressure from expanding the plasma in the ∇R direction.

Eq. (37) yields the radial equation for the shaping. The shaping profiles depend only on the shaping at the boundary, and (we will see) on the q-profile. It has no dependence on the pressure at this order.

Consequences of equilibrium ∇r equation

Now, referring to Eq. (23) and Eq. (31) we have,

$$\psi' = \frac{rF}{qR_0}[1+O(\varepsilon^2)], \quad \psi'' = \frac{F}{qR_0}\left[1+\frac{rF'}{F}-s+O(\varepsilon^2)\right] \quad \text{and thus} \tag{38}$$

$$\frac{\left(r^2\psi'^2\right)'}{2r^2} = \left(\frac{F}{qR_0}\right)^2 r\left[2+\frac{rF'}{F}-s+O(\varepsilon^2)\right] \quad \text{with} \quad s=\frac{r}{q}\frac{dq}{dr}. \tag{39}$$

Now what is F? From Eq. (13), and assuming that B_ϕ , $\propto$ $(1/R)[1+O(\varepsilon^2)]$ we have

$$F = R_0B_0[1+\varepsilon^2F_2(r)+O(\varepsilon^3)], \tag{40}$$

where $B_0 = B_\phi(r=0) = B(r=0)$ and $R_0 = R(r=0)$, i.e. R and B at the magnetic axis $r=0$. Hence, substituting F and Eq. (39) into Eq. (35) we have

$$\frac{1}{q^2}\left(1+\varepsilon^2F_2\right)^2(2-s)+\left(\varepsilon^{-1}\frac{R_0}{r}\right)^2\varepsilon^2\frac{rP'}{B_0^2}+\left(\varepsilon^{-1}\frac{R_0}{r}\right)^2\left[1+\left(\varepsilon\frac{r}{R_0q}\right)^2\right]\left(1+\varepsilon^2F_2\right)\varepsilon^2rF_2'=0,$$

So that we finally have,

$$F_2 = -\varepsilon^2\frac{P}{B_0^2}-\varepsilon^2\int_0^r\frac{dr\ r}{R_0^2}\left(\frac{2-s}{q^2}\right)+O(\varepsilon^4) \tag{41}$$

Note that the orders above assume that $P/B_0^2 \sim \varepsilon^2$, which is conventional ordering. However Eqs. (40) and (41) are valid even when $P/B_0^2 \sim \varepsilon$, although F_2 would be renamed F_1 and the ε tags would have to be modified.

Consequences of equilibrium ∇r equation

The toroidal field $B_\phi \boldsymbol{e}_\phi = F\boldsymbol{e}_\phi/R$ has now been fully described. Need still to obtain the poloidal field, and thus the total field, and field strength. Now from Eq. (10) the poloidal field

$$\boldsymbol{B}_p = \psi' \boldsymbol{\nabla} r \times \boldsymbol{\nabla}\phi = \psi' |\boldsymbol{\nabla} r||\boldsymbol{\nabla}\phi| \boldsymbol{e}_p \quad \text{where} \quad \boldsymbol{e}_p = \frac{\boldsymbol{\nabla} r \times \boldsymbol{\nabla}\phi}{|\boldsymbol{\nabla} r||\boldsymbol{\nabla}\phi|}$$

Here, clearly, $\boldsymbol{e}_p$ is the unit vector pointing in the poloidal direction. From Eqs.(18) and (38), and noting that $|\boldsymbol{\nabla}\phi|^2 = 1/R^2$ and $g_{r,r} = (\partial R/\partial r)^2 + (\partial Z/\partial r)^2$, we have:

$$\boldsymbol{B}_p = \psi' \frac{\sqrt{g_{\theta,\theta}}\boldsymbol{e}_p}{\mathcal{J}} = B_0 \left[\left(\frac{\varepsilon r}{R_0 q} \right) \frac{1}{1 + \varepsilon(\ldots..)} + O(\varepsilon^3) \right] \boldsymbol{e}_p$$

For many applications, it of great interest to evaluate the magnetic field strength $|\boldsymbol{B}|$, or indeed $\boldsymbol{B}^2$. Since $\boldsymbol{e}_p$ is perpendicular to $\boldsymbol{e}_\phi$ we have $B^2 = B_\phi^2 + \boldsymbol{B_p}^2$:

$$B^2 = B_0^2 \left[\left(\frac{1 + F_2}{1 + \epsilon\cos\theta - \Delta/R_0 + \sum_{m=2}^{\infty}(S_m/R_0)\cos(m-1)\theta} \right)^2 + \right.$$

$$\left. \frac{\epsilon^2}{q^2} \left(\frac{1}{1 + (\epsilon - \Delta')\cos\theta + \sum_{m=2}^{\infty} S'_m \cos m\theta} \right)^2 + O(\varepsilon^4) \right]$$

We now see that the field strength is affected by the plasma pressure in two ways.

(1) Pressure reduces the toroidal field through F_2. This is known as the diamagnetic effect of the plasma pressure.

(2) Furthermore, we will see that Δ' is governed by the plasma pressure, and this in turn strongly influences the poloidal field. It is clear that this effect enters through the $1/\mathcal{J}$ dependence of B_p, which in turn enters through the local field line pitch $d\phi/d\theta = F\mathcal{J}/(R^2\psi')$; i.e. the poloidal field is determined by the toroidal field, and the local field line pitch. It is also seen that shaping effects also determine this effect too.

Consequences of equilibrium ∇r equation

The toroidal field $B_\phi \boldsymbol{e}_\phi = F\boldsymbol{e}_\phi/R$ has now been fully described. Need still to obtain the poloidal field, and thus the total field, and field strength. Now from Eq. (10) the poloidal field

$$\boldsymbol{B}_p = \psi' \nabla r \times \nabla \phi = \psi' |\nabla r||\nabla \phi| \boldsymbol{e}_p \quad \text{where} \quad \boldsymbol{e}_p = \frac{\nabla r \times \nabla \phi}{|\nabla r||\nabla \phi|}$$

Here, clearly, $\boldsymbol{e}_p$ is the unit vector pointing in the poloidal direction. From Eqs.(18) and (38), and noting that $|\nabla \phi|^2 = 1/R^2$ and $g_{r,r} = (\partial R/\partial r)^2 + (\partial Z/\partial r)^2$, we have:

$$\boldsymbol{B}_p = \psi' \frac{\sqrt{g_{\theta,\theta}}\boldsymbol{e}_p}{\mathcal{J}} = B_0 \left[\left(\frac{\varepsilon r}{R_0 q} \right) \frac{1}{1 + \varepsilon(\epsilon - \Delta') \cos\theta + \varepsilon \sum_{m=2}^{\infty} S'_m \cos m\theta} + O(\varepsilon^3) \right] \boldsymbol{e}_p \qquad (42)$$

For many applications, it of great interest to evaluate the magnetic field strength $|\boldsymbol{B}|$, or indeed $\boldsymbol{B}^2$. Since $\boldsymbol{e}_p$ is perpendicular to $\boldsymbol{e}_\phi$ we have $B^2 = B_\phi^2 + \boldsymbol{B_p}^2$:

$$B^2 = B_0^2 \left[\left(\frac{1 + F_2}{1 + \epsilon\cos\theta - \Delta/R_0 + \sum_{m=2}^{\infty}(S_m/R_0)\cos(m-1)\theta} \right)^2 + \frac{\epsilon^2}{q^2} \left(\frac{1}{1 + (\epsilon - \Delta')\cos\theta + \sum_{m=2}^{\infty} S'_m \cos m\theta} \right)^2 + O(\varepsilon^4) \right] \qquad (43)$$

We now see that the field strength is affected by the plasma pressure in two ways.

(1) Pressure reduces the toroidal field through F_2. This is known as the diamagnetic effect of the plasma pressure.

(2) Furthermore, we will see that Δ' is governed by the plasma pressure, and this in turn strongly influences the poloidal field. It is clear that this effect enters through the $1/\mathcal{J}$ dependence of B_p, which in turn enters through the local field line pitch $d\phi/d\theta = F\mathcal{J}/(R^2\psi')$; i.e. the poloidal field is determined by the toroidal field, and the local field line pitch. It is also seen that shaping effects also determine this effect too.

Application: Particle Trapping

A single particle in a tokamak is considered to be trapped if it cannot circulate around the entire poloidal cross section. The standard definition of a point in phase space where the particle is trapped is given by

$$v_{||} = 0.$$

Now from elementary theory, we assume that the kinetic energy $E = v_{||}^2 + v_{\perp}^2$ is conserved over the trajectory of the particle (constant E assumes there is no time varying electric field). Moreover, the magnetic moment $\mu = v_{\perp}^2/(2B)$ is an (adiabatic) invariant. Consequently the poloidal variation of $v_{||}$ is given by,

$$v_{||}(r,\theta) = 2\sqrt{E - \mu B(r,\theta)} \tag{44}$$

For a low energy particle, which is strongly tied to a flux surface r (so that the banana width is small), the trapping angle θ_t, if it exists, is defined simply by

$$B(r,\theta_t) = E/\mu.$$

The condition for whether a particle is trapped or passing is determined by the location of θ where the field is at a maximum. A trapped particle requires:

$$B_{\text{max}} = B(r,\theta_{\text{max}}) > E/\mu$$

If this state exists, then particles will 'roll around' in a magnetic well.

Ignoring the effects of shaping and pressure in the poloidal field, one simply finds that $B \propto 1/R$, and hence B increases monotonically with θ up to $\theta_{\text{max}} = \pi$. However, in spherical tokamaks, the poloidal field is large (ϵ isn't small), and moreover, pressure gradients are large. Consequently, B is not generally a monotonic function of θ, and resultingly, special (tear-drop) trapped particles are generated.

Application: Particle Trapping

Plot the field strength as a function of θ at constant r $(= 0.7)$. Assume spherical tokamak $B_0 = 1$T, $R_0 = 1$, $a = 0.7$, with circular cross section ($\kappa(a) = 1$, or $S_2(a) = 0$ and $\delta(a) = 0$, or $S_3(a) = 0$). Chosen monotonic q-profile, and monotonic pressure profile reveal large Shafranov shift through internal inductance (see later). The plasma pressure was taken to be zero.

It is seen that the well in the magnetic field is conventional, meaning that the minimum in B is at $\theta = 0$, and rises monotonically with respect to $\pm\theta$. Consequently, conventional banana trapped particles are to be expected (as well as circulating particles).

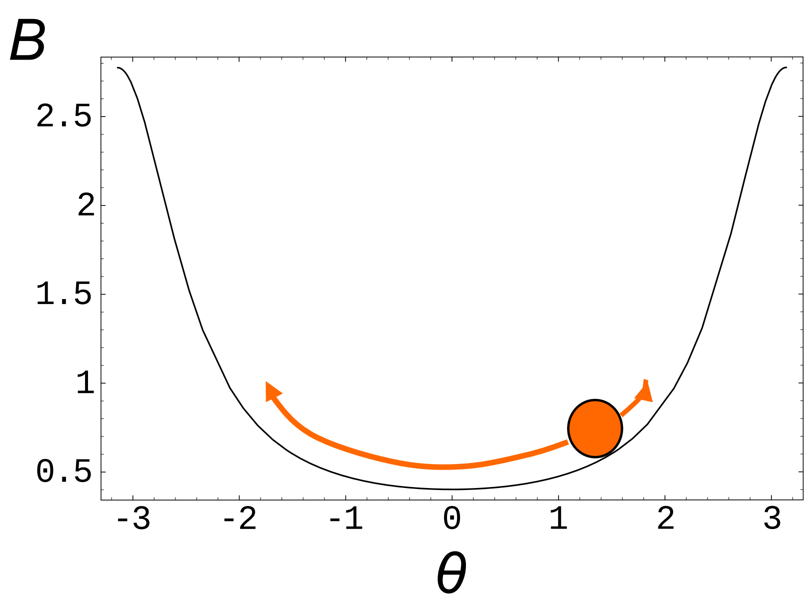

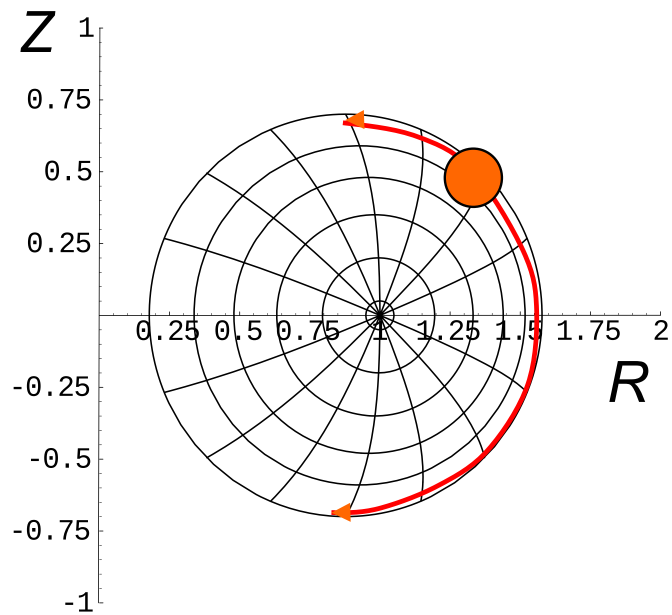

Application: Particle Trapping

Again plot field strength as a function of θ at constant r $(= 0.7)$. Assume spherical tokamak $B_0 = 1$T, $R_0 = 1$, $a = 0.7$, with typical shaped cross section ($\kappa(a) = 1.9$, or $S_2(a) = -0.22$ and $\delta(a) = 0.2$, or $S_3(a) = 0.035$). Monotonic q-profile, and poloidal beta $\beta_p(a) = 0.4$.

The dependence of Magnetic field with θ is unconventional. However, such a dependence is a normal occurrence in a spherical tokamak. There are two minima in the field, each located between $\pi/4 < |\theta| < \pi/2$. Given sufficiently small initial parallel velocity, particles can be trapped in this region. Conventional banana orbits also exist, but the bounce tips of such particles cannot reside on the local magnetic hill!

The local magnetic wells occur because the toroidal field is reduced globally by the pressure (through the diamagnetic effect F_2, and because the poloidal field is generally enhanced because of large ϵ near the edge of a spherical tokamak. The poloidal field can be locally enhanced due to the local shear $q_l = d\phi/d\theta$ i.e. the denominator of B_p is strongly reduced via Δ' at $|\theta| = \pi/2$, and through S_2' at $|\theta| = \pi/4$.

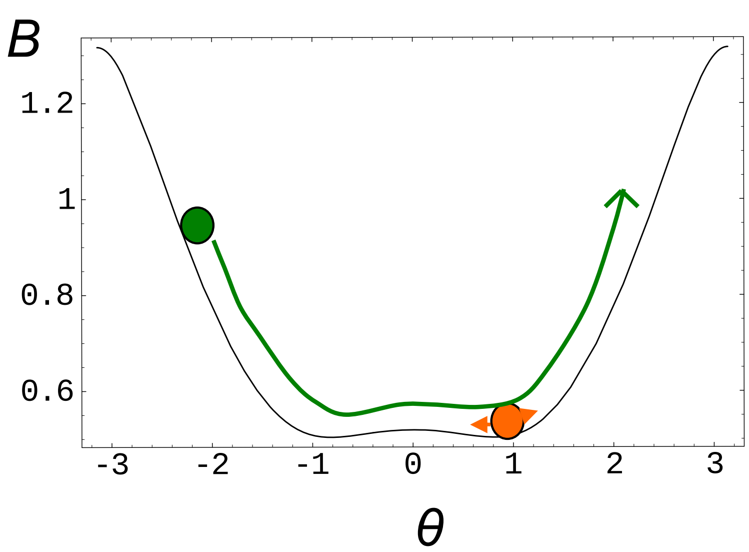

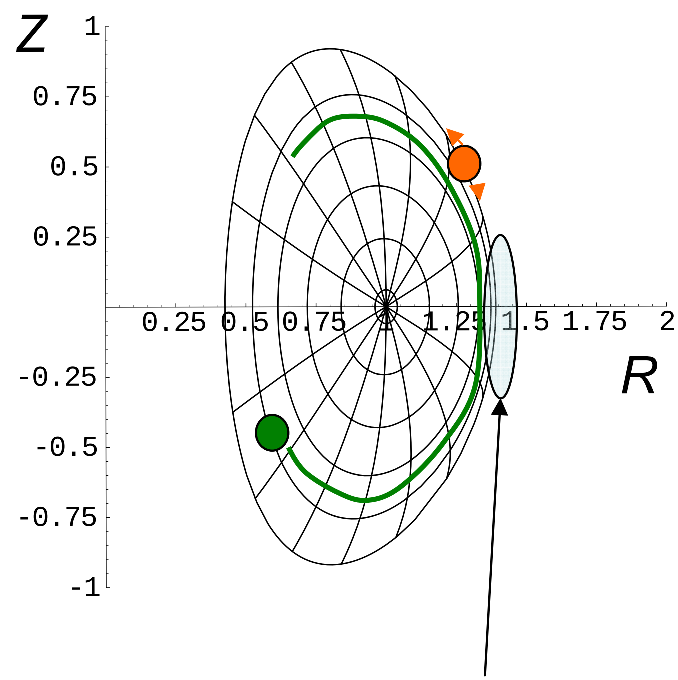

Conventional deeply trapped particles cannot entirely reside in this region

Advanced Topic: Tear-Drop Orbits in Spherical Tokamaks

The radial excursion of a trapped (or passing) particle can be accurately determined in terms of the equilibrium parameters that we have derived. In the drift formulation, one finds exactly:

$$\frac{d\psi}{dt} = \frac{m}{Ze} F \frac{d}{dt}\left(\frac{v_{||}}{B}\right).$$

From Eq. (38) we have,

$$\frac{dr}{dt} = \frac{d\psi}{dt}\frac{dr}{d\psi} = \frac{qR_0}{r}\frac{m}{Ze} F \frac{d}{dt}\left(\frac{v_{||}}{B}\right)$$

Now integrate directly, and note that temporal variation occurs most quickly in $\theta(t)$ coordinate ($d\theta/dt = v_{||}/(qR)$ is the bounce frequency), so that

$$r(t) - r(t_0) \approx \frac{q(t_0)R_0}{r(t_0)}\frac{m}{Ze}\left(\frac{v_{||}[\theta(t)]}{B[\theta(t)]} - \frac{v_{||}[\theta(t_0)]}{B[\theta(t_0)]}\right)$$

which is an equation for $r(\theta)$. From Eq. (44) recall that $v_{||}$ can be written in terms of $B(\theta)$ and the constants of motion.

For the conventional banana orbit, we choose a 350keV proton, with $\mu/E = 1/B_0 = T^{-1}$ with $r(t_0) = 0.4$ giving trapping angle $\theta_t = \theta(t_0) = \pm 2.26$ rads.

For the tear drop orbits, we choose a 3.5MeV proton, with $\mu/E = 1/B_{\text{min}} - 0.005 = 1.94/B_0 = 1.94T^{-1}$ with $r(t_0) = 0.67$ and giving trapping angles $|\theta_t| = |\theta(t_0)| = 0.54$ rads and $|\theta_t| = |\theta(t_0)| = 0.84$ rads.

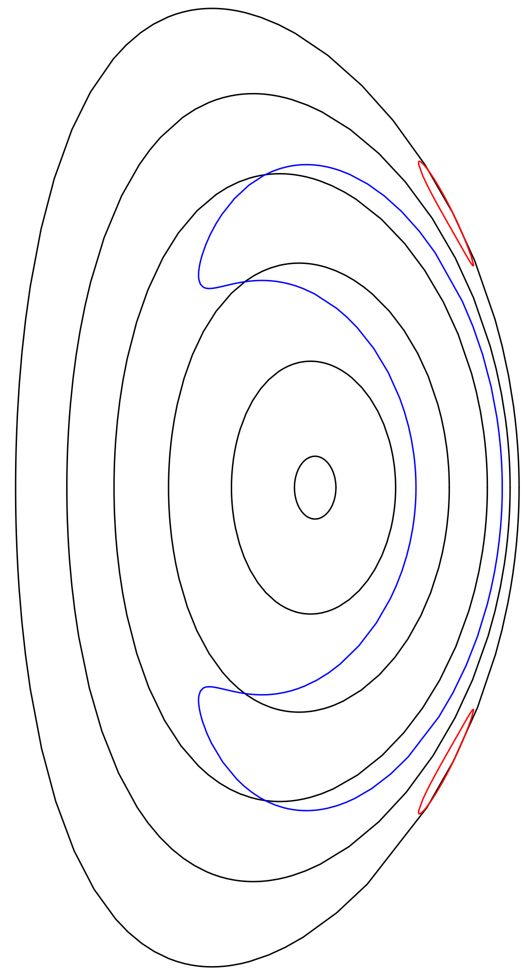

The ∇R equation: Shafranov Shift

So, here we consider the force balance equation with $\cos\theta$ dependence, i.e. Eq. (36). This equation can be integrated once, to obtain

$$\Delta' = \frac{1}{R_0 r \psi'^2}\left[-2R_0^2\int_0^r dr\, r^2 P' + \int_0^r dr\, r\psi'^2\right]$$

Now, recalling that $\psi' = rF/(qR_0)$ we obtain the convenient expression

$$\Delta'(r) = \frac{r}{R_0}\left[\beta_p(r) + \frac{l_i(r)}{2}\right] \tag{45}$$

where β_p is the local poloidal beta

$$\beta_p(r) = -2\frac{R_0^4 q^2}{F^2 r^4}\int_0^r dr\, r^2 P' \approx \frac{2}{\left\langle B_p^2\right\rangle}\left[\langle P\rangle - P(r)\right] \quad \text{with} \quad F \approx R_0 B_0 \tag{46}$$

where $\langle X\rangle = V(r)^{-1}\int_0^{V(r)} dV X$ is average of X within the volume defined by r. Also, l_i is the local internal inductance

$$l_i(r) = 2\frac{q^2}{F^2 r^4}\int_0^r dr\, \frac{r^3 F^2}{q^2} \approx 2\frac{q^2}{r^4}\int_0^r dr\, \frac{r^3}{q^2} \approx \frac{4}{I_p(r)^2 R_0}\int_0^{V(r)} \frac{1}{2}B_p^2\, dV. \tag{47}$$

where I_p is the plasma current.

Equation (45) describes $\boldsymbol{J}\times\boldsymbol{B}$ force balance in the $\boldsymbol{\nabla}R$ direction. The first term on the right attempts to increase the plasma volume. Since $V \approx 2\pi^2 r^2 R$, the volume of a torus can of course can be increased by increasing R. This force is known as the Tyre Tube Force, since the air pressure in a toroidal inner tube similarly expands the major radius of the tyre.

Problem: verify that Eq. (45), (46) and (47) satisfy the $\cos\theta$ component of the Grad-Shafranov equation of Eq. (34).

The ∇R equation: Shafranov Shift

The second term on the right of Eq. (45) is due to the toroidal current. It turns out the origin for this outward force, known as the Hoop Force, in the $\boldsymbol{\nabla} R$ direction, is analogous to the Tyre Tube Force, but where the plasma pressure is replaced by minus the poloidal magnetic pressure. To see this, one has to consider the two relevant quantities ψ and P, both of which are constants on the flux surface, and thus have the same value on the inboard or outboard side. Since ψ passes a smaller area on the inboard side than the outboard side, then the $B_p(in) > B_p(out)$ (this is clear from the $1/R$ dependence in B_p, though effect reduced for increased Shafranov shift). The outward Hoop Force is

$$F_{Hoop} \sim [B_p(in)^2 S_{in} - B_p(out)^2 S_{out}]\boldsymbol{e}_R,$$

where the quadratic dependence of B_p wins over the inverse dependence of S. Similarly, the Tyre Tube Force can be written

$$F_{Tyre} = -P(S_{in} - S_{out})\boldsymbol{e}_R,$$

whereby, as mentioned earlier, the force occurs because $S_{in} < S_{out}$.

The balancing of the force on the left hand side of (45), i.e. Δ', is caused by the compression of the flux surfaces, i.e. the compression of the poloidal flux on the LFS of the torus. Clearly the compression is measured by the Shafranov shift displacement Δ.

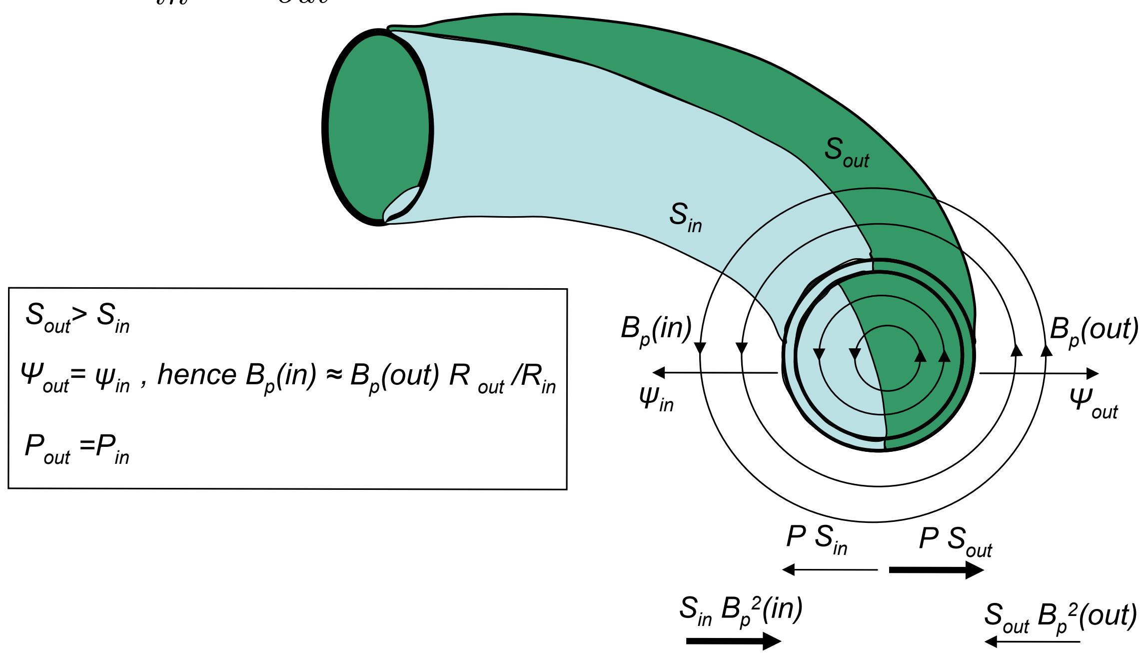

Importance of Poloidal and Toroidal Fields

TORUS WITH PURE TOROIDAL B

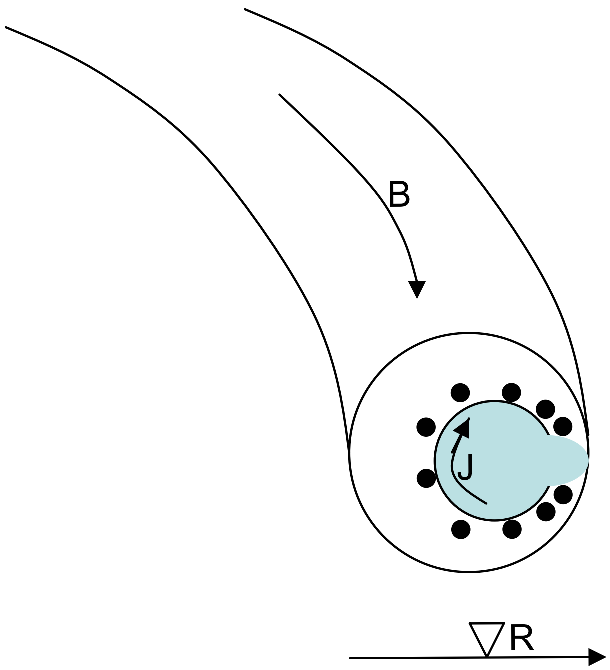

Field lines just slip around flux surface in response to a R-force due to imperfect conductor at wall. Flux cannot be trapped. Applied external field cannot generate J^B in R direction.

TORUS WITH PURE POLOIDAL B

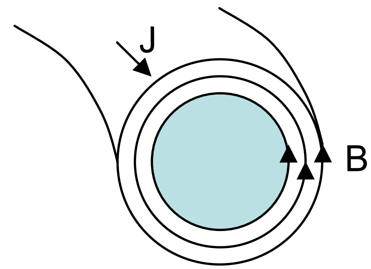

An idealised equilibrium can be generated,
Since poloidal flux can be compressed, and
Field lines do not displace. Can also use vertical
field to create Radial force. But any displacement
Of perfect equilibrium, and we have disaster, i.e.
very poor MHD stability properties (e.g. sausage).

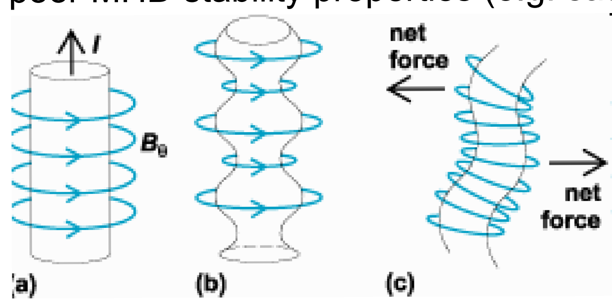

The Necessity of Vertical Field Coils

Within the plasma, the compression of the magnetic field compensates the Tyre Tube Force and the Hoop Force. However, the magnetic flux must also be compressed in the vacuum region, and this will occur right up to the vessel wall. In practice, a conducting vessel wall will not be a perfect conductor, and as such, the poloidal flux can only remain compressed for a skin time, which is typically short compared to experimental times of interest.

External coils generating a vertical field $\boldsymbol{B}_{vert}$ can generate a compensating inward force, in the $\boldsymbol{e}_R$ direction, via the cross product with the toroidal plasma current, $F_R\boldsymbol{e}_R = \boldsymbol{J}_\phi \times \boldsymbol{B}_{vert}$.

One can equivalently view the externally generated vertical field as being that required in order to the sustain the vertical component of the poloidal field, derived in Eq. (42):

$$\boldsymbol{B}_p = B_0\left[\left(\frac{\varepsilon r}{R_0 q}\right)\frac{1-\varepsilon\sum_{m=2}^{\infty}(m-1)(S_m/r)\cos m\theta}{1+\varepsilon(\epsilon-\Delta')\cos\theta+\varepsilon\sum_{m=2}^{\infty}[S_m'-(m-1)(S_m/r)]\cos m\theta}+O(\varepsilon^3)\right]\boldsymbol{e}_p, \qquad (48)$$

extended out to the vacuum region. The vacuum field satisfies $\boldsymbol{\nabla}\times\boldsymbol{B}=0$, i.e. $\Delta^*\psi=0$, and it is possible to integrate the vacuum equation outward from the initial values given by Eq. (48). The dominant contribution in Eq. (48), the poloidal field generated by the plasma current, vanishes for $R\to\infty$. One is left with the $\Delta'\cos\theta$ term, which does not vanish at infinity. Moreover, since the term depends on $\cos\theta$, projected in the poloidal direction, this field points in the vertical direction. This surface poloidal field cannot be generated by the toroidal current alone, but must instead be supplied by the vertical field coils.

The Shafranov Shift

By inspection of β_p and l_i is is clear that Δ' and Δ are monotonically increasing functions of r. Our definition of the Shafranov shift, Δ, is the shift relative to the magnetic axis B_0, which is located at $R = R_0$. Beware! This is not the definition understood by experimentalists!

For an experimentalist, the real world starts at the vessel wall, or the plasma edge. So any shift, due to toroidal effects, would be relative to the plasma edge. Defining $R_{out}(a)$ as the plasma edge (a) on the LFS, and $R_{in}(a)$ as the plasma edge on the HFS, the shafranov shift at a particular flux surface r is typically defined as the difference between the 'centres' of these surfaces:

$$\Delta_{exp}(r) = [R_{out}(r) + R_{in}(r)]/2 - [R_{out}(a) + R_{in}(a)]/2$$

Hence Δ_{exp} is maximum at the magnetic axis, i.e. the opposite of the definition of the theoretician. Nevertheless, experimentalists should also beware. Since $R_{out} = R(r, \theta = 0)$ and $R_{in} = R(r, \theta = \pi)$, the referring to Eqs. (24) and (28) we have:

$$\Delta_{exp}(r) = \Delta(a) - \Delta(r) + \frac{r\delta(r)}{4} - \frac{a\delta(a)}{4} \quad \text{and especially} \quad \Delta_{exp}(0) = \Delta(a) - \frac{a\delta(a)}{4}$$

A measurement of enhanced Δ_{exp} might lead one to believe that the configuration might be more resistant to instability, since e.g. it is known that pressure gradients drive various instabilities as well as the Shafranov shift. So, a large Shafranov shift would indicate that large pressure gradients have been estabilished, and the very existance of large pressure gradients would imply that MHD instabilities must have been tamed. However, one can also enhance $\Delta_{exp}(r)$ via e.g. negative triangularity and lower pressure gradients.

Hence, to summarise, the Shafranov shift is a very important quantity. It describes the primary effect of toroidicity in a tokamak. Many of the stability properties derived in the straight cylindrical approximation of a torus are entirely cancelled by toroidal effects. For such instabilities, the remaining stability criteria are due to toroidicity (and shaping), and sometimes the criteria can be written explicitly in terms of the Shafranov shift.

Shafranov shift with negative and positive triangularity

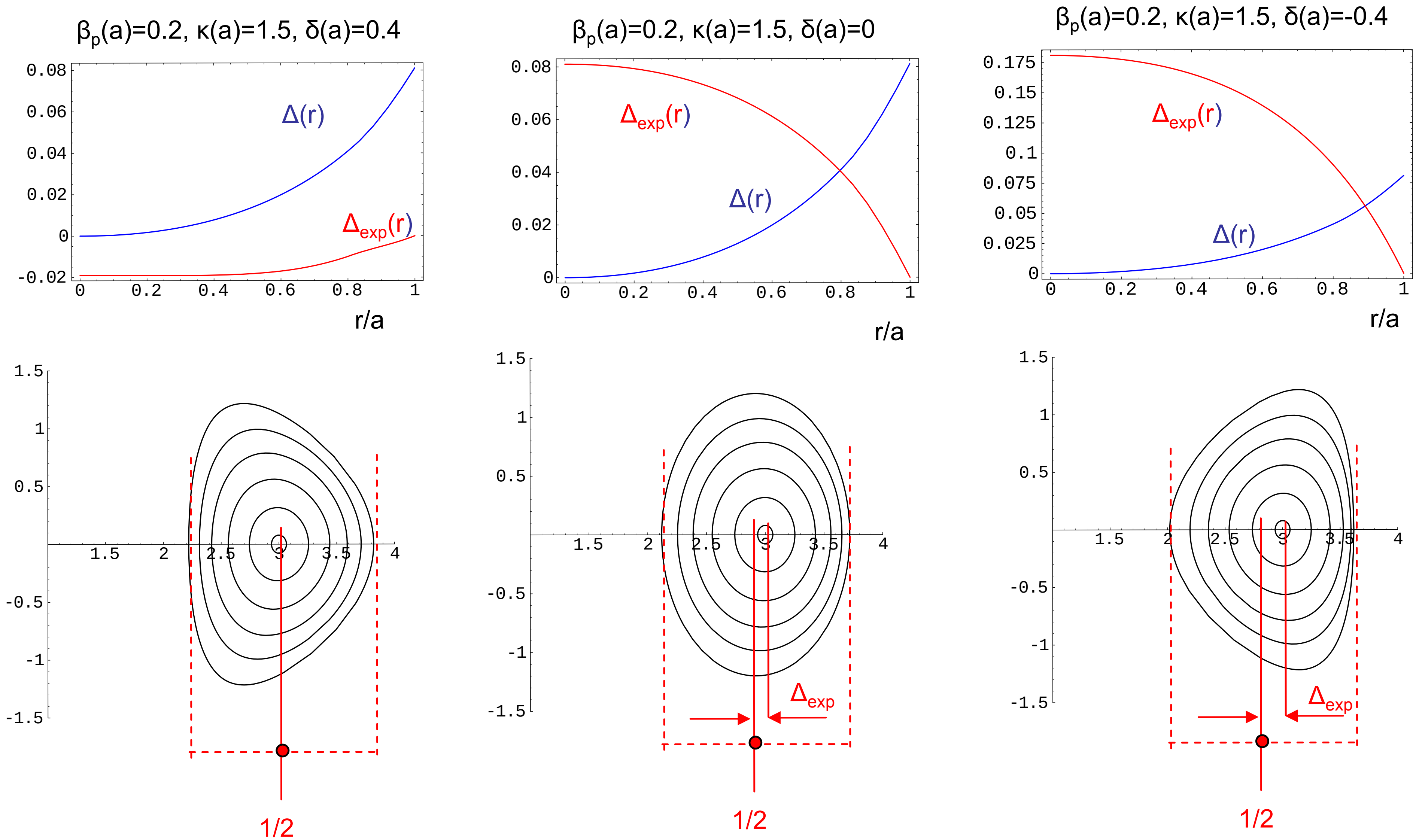

Shaped Plasma Cross Section

The shaping coefficients are given by the solution of the $\cos(m\theta)$ terms in the Grad-Shafranov equation, i.e. Eq. (37). Substituting Eq. (38), and ignoring small corrections in F_2', we have,

$$r^2 S_m'' + [3 - 2s(r)]rS_m' + (1 - m^2)S_m, \tag{49}$$

so we see that the penetration of the shaping into the core, from the defined shaping at the boundary, depends only on the magnetic shear (to leading order). If the magnetic shear is vanishingly small, one simply has obtains

$$S_m(r) = S_m(a)\left(\frac{r}{a}\right)^{m-1}$$

So that, from Eq. (28), one has for a flat q-profile:

$$\kappa(r) = \kappa(a) \quad \text{and} \quad \delta(r) = \delta(a)\frac{r}{a},$$

i.e. elongation remains constant from the edge to the magnetic axis, while the triangularity drops off linearly towards the core, and thus vanishes at the magnetic axis.

Magnetic shear modifies the penetration of the shaping into the core. An increase in the magnetic shear reduces the shaping in the core, while a decrease in shear increases the shaping. For an advanced scenario, the negative magnetic shear actually increases κ and δ inside a region of negative shear. This can be seen by taking

$$q(r) = 1 - \Delta q\left[1 - \left(\frac{r}{r_1}\right)^2\right] \quad \text{and thus} \quad s(r) = 2\frac{\Delta q}{q(r)}\left(\frac{r}{r_1}\right)^2.$$

Shaped Plasma Cross Section

Giving exactly,

$$S_m(r) = S_m(a)\left(\frac{r}{a}\right)^{m-1}\frac{q(r)s(r)+2(1-\Delta q)(1+m)/(m-1)}{q(a)s(a)+2(1-\Delta q)(1+m)/(m-1)}$$

For $\Delta q \ll 1$ one then obtains the useful expressions,

$$\kappa(r) = \kappa(a) - \frac{[\kappa(a)^2-1][q(a)s(a)-q(r)s(r)]}{12+[1+\kappa(a)]q(a)s(a)-[\kappa(a)-1]q(r)s(r)} \quad \text{and} \quad \delta(r) = \delta(a)\left(\frac{r}{a}\right)\frac{4+q(r)s(r)}{4+q(a)s(a)}$$

These expressions are almost exact for a q-profile with a quadratic dependence in r. However, since these expressions are written in terms of $q(r)$ and $s(r)$, they might be used with some confidence for wider classes of safety factor. Certainly, these expressions describe the penetration the shape of an arbitrary surface, a (not necessarily the plasma edge) into a surface inside, denoted by r, where the q-profile in the region $\{r, a\}$ is, ideally, locally quadratic.

The penetration of the shaping into the core region, from the boundary, is important from the stability point of view. Linear MHD stability in tokamaks is sensitive to the shaping (and Shafranov shift) in the region where the particular instability exists, and especially on rational surfaces. Rational surfaces and MHD instabilities will be considered in the remainder of this course.

Shaped Plasma Cross Section

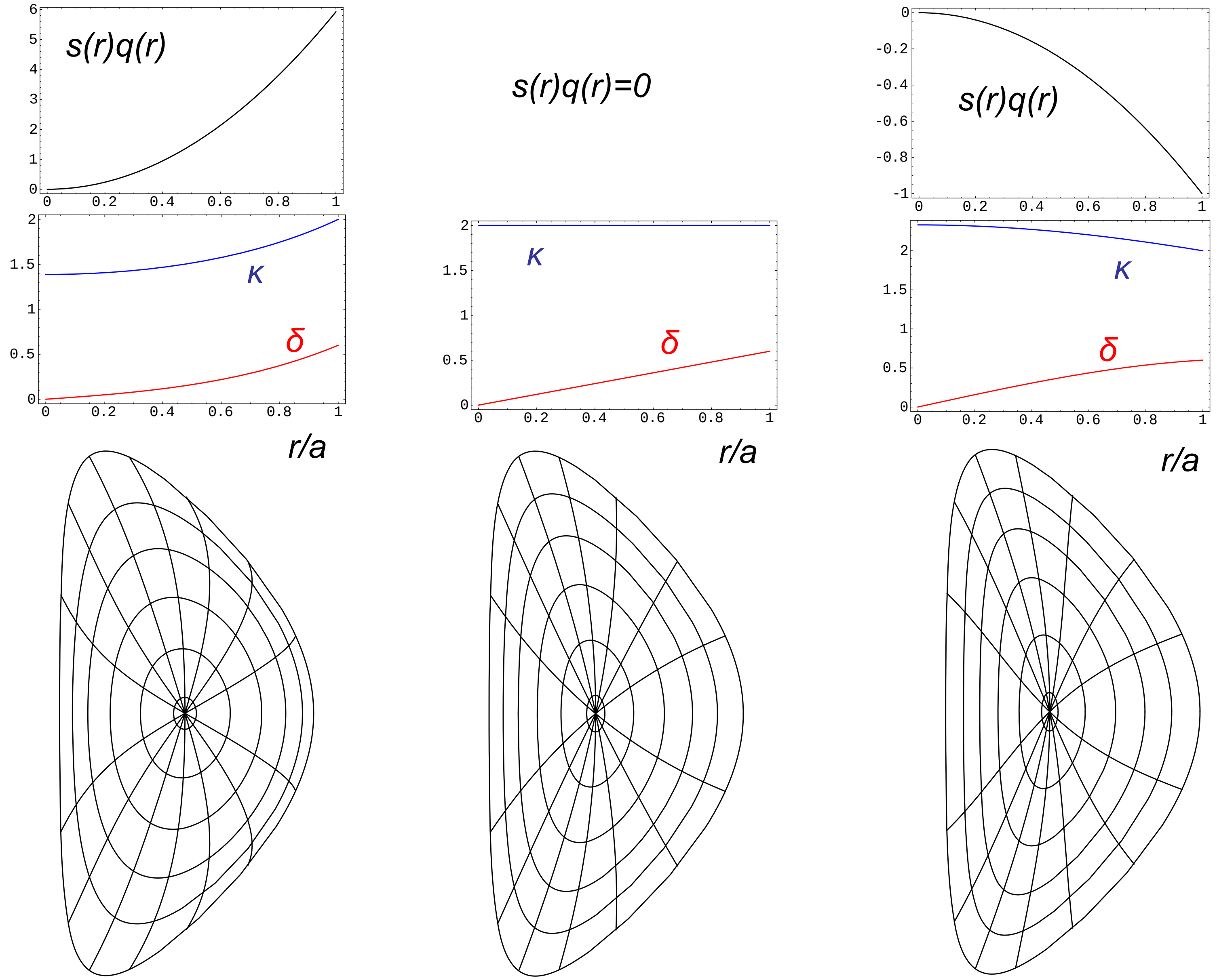

Appendix: components of B_p

We know that the poloidal field is perpendicular to the toroidal field,. Moreover, since the θ direction is not the poloidal direction, then if we attempt to write the poloidal field in terms of the θ direction, there has to be a correction factor pointing in the r (outwards from the flux surface) direction. However, we exploit the fact that we know that the true poloidal direction is perpendicular to r. Let,

$$\boldsymbol{e}_p \equiv \frac{\boldsymbol{\nabla} r \times \boldsymbol{\nabla}\phi}{|\boldsymbol{\nabla} r||\boldsymbol{\nabla}\phi|} = A\boldsymbol{\nabla}\theta + B\boldsymbol{\nabla} r$$

Dotting this with $\boldsymbol{\nabla} r$, we note that the LHS vanishes, hence we may rearrange to obtain

$$B = -A\frac{\boldsymbol{\nabla} r\cdot\boldsymbol{\nabla}\theta}{|\boldsymbol{\nabla} r|^2} = A\frac{g_{r,\theta}}{g_{\theta,\theta}}.$$

We still need to obtain A. However, since $\boldsymbol{e}_p$ is a unit vector, we must have

$$\boldsymbol{e}_p = \frac{\boldsymbol{\nabla}\theta + \frac{g_{r,\theta}}{g_{\theta,\theta}}\boldsymbol{\nabla} r}{\sqrt{\boldsymbol{\nabla}\theta^2 + 2\frac{g_{r,\theta}}{g_{\theta,\theta}}\boldsymbol{\nabla}\theta\cdot\boldsymbol{\nabla} r + \left(\frac{g_{r,\theta}}{g_{\theta,\theta}}\right)^2\boldsymbol{\nabla} r^2}}.$$

Noting that $\boldsymbol{\nabla}\theta = |\boldsymbol{\nabla}\theta|\boldsymbol{e}_\theta$ and $\boldsymbol{\nabla} r = |\boldsymbol{\nabla} r|\boldsymbol{e}_r$, then from Eq. (18) we can rearrange to obtain

$$\boldsymbol{e}_p = \frac{\boldsymbol{e}_\theta + \left(\frac{g_{r,\theta}^2}{g_{\theta,\theta}g_{r,r}}\right)^{1/2}\boldsymbol{e}_r}{\left(1 - \frac{g_{r,\theta}^2}{g_{\theta,\theta}g_{r,r}}\right)^{1/2}}$$

Appendix: components of B_p

Now, $|\nabla\theta|$ which appears in $g_{r,r}$ has yet to be evaluated. One finds that

$$g_{r,r} = \left(\frac{\partial Z}{\partial r}\right)^2 + \left(\frac{\partial R}{\partial r}\right)^2 = 1 + O(\varepsilon^2) = 1 - \varepsilon\left(2\Delta' \cos\theta + 2\sum_{m=2}^{\infty} S'_m \cos m\theta\right) + O(\varepsilon^2)$$

which gives,

$$\sqrt{\frac{g_{r,\theta}^2}{g_{\theta,\theta}g_{r,r}}} = \varepsilon\Delta' \sin\theta - \varepsilon\sum_{m=2}^{\infty}\left(S'_m + (m-1)\frac{S_m}{r}\right)\sin m\theta + O(\varepsilon^2),$$

and thus,

$$\boldsymbol{e}_p = \frac{\boldsymbol{e}_\theta + \left[\Delta' \sin\theta - \sum_{m=2}^{\infty}\left(S'_m + (m-1)\frac{S_m}{r}\right)\sin m\theta\right]\boldsymbol{e}_r}{\left(1 - \left[\Delta' \sin\theta - \sum_{m=2}^{\infty}\left(S'_m + (m-1)\frac{S_m}{r}\right)\sin m\theta\right]^2\right)^{1/2}} + O(\varepsilon^2).$$

But, noting that the denominator should be replaced by unity at this order, because $\sqrt{1-\varepsilon^2} = \varepsilon^2/2 + ..$, so that

$$\boldsymbol{e}_p = \boldsymbol{e}_\theta + \left[\Delta' \sin\theta - \sum_{m=2}^{\infty}\left(S'_m + (m-1)\frac{S_m}{r}\right)\sin m\theta\right]\boldsymbol{e}_r + O(\varepsilon^2).$$

That the magnetic field appears to point partially in the radial direction seems, on first thought to be wrong, since we know that r is a flux coordinate describing the surface of constant P. In fact, there is not a net radial field. Indeed, $\boldsymbol{e}_\theta$ is not aligned tangentially to $\boldsymbol{e}_p$, which itself is tangent to the poloidal boundary. This means that relative to $\boldsymbol{e}_p$ it turns out that $\boldsymbol{e}_\theta$ has a small component in the $\boldsymbol{e}_r$ direction (recall that the coordinates are not orthogonal). The role of the radial field $\boldsymbol{B}_p \cdot \boldsymbol{e}_r$ is to cancel this out.

- Week 1: Derivation and limitations of the MHD model. Conservation of Flux, The Grad-Shafranov Equation. Coordinate systems in tokamak equilibrium.
- Week 2: Tokamak equilibrium. Analytical expansions. Shafranov Shift. Shaping, and shaping penetration into the torus
- Week 3: Linearised ideal MHD stability, energy principle, stability boundaries, ideal internal kink mode
- Week 4: External Kink modes, singular layer calculations (ideal, FLR, resistive), tearing modes
- Week 5: Toroidal effects: Interchange stability (Mercier) and ballooning.
- Week 6: Examination of toroidal coupling: interchange, quasi-interchange and infernal modes
- Week 7: Parallel dynamics: compressibility in MHD, and analogous kinetic compressibility in hybrid kinetic MHD formulation. Introduction to kinetic-MHD instabilities in tokamaks

Linear MHD Equations

Allow all the MHD quantities to comprise the sum of an equilibrium component and a perturbation which is small in comparison:

$$\boldsymbol{Q} \to \boldsymbol{Q} + \boldsymbol{\delta Q}.$$

For example, employing the normal mode approach, the perturbations acquire the form $\boldsymbol{\delta Q}(\boldsymbol{x}, t) = \boldsymbol{\delta Q}(\boldsymbol{x}) \exp(-i\omega t)$, representing disturbances that have always existed and do not require initial conditions.

In MHD it is usually assumed that the equilibrium velocity $\boldsymbol{u}$ is negligible. This approximation is valid providing the centrifugal forces associated with a circulating fluid is small. It is convenient to define the perturbed fluid velocity in terms of the fluid displacement $\boldsymbol{\xi}$ such that

$$\boldsymbol{\delta u} = \frac{\partial \boldsymbol{\xi}}{\partial t}.$$

Here we have used the fact that there is no initial displacement at $t = 0$. Let us start by assuming the standard ideal MHD momentum equation, and then linearise in perturbations:

$$\rho \frac{\partial^2 \boldsymbol{\xi}}{\partial t^2} = \boldsymbol{\delta F}, \tag{50}$$

where

$$\boldsymbol{\delta F} = \boldsymbol{\delta J} \times \boldsymbol{B} + \boldsymbol{J} \times \boldsymbol{\delta B} - \boldsymbol{\nabla} \delta P.$$

Again, we have assumed that the equilibrium $\boldsymbol{u}$ is zero (i.e. no equilibrium plasma flows or momenta). The perturbed pressure can be written in terms of the fluid displacement as follows,

$$\delta P = -\gamma P \boldsymbol{\nabla} \cdot \boldsymbol{\xi} - \boldsymbol{\xi} \cdot \boldsymbol{\nabla} P. \tag{51}$$

Linear MHD Equations

This was obtained by taking the adiabatic equation of state $(d/dt)(P\rho^{-\gamma}) = 0$ and linearising to give:

$$\frac{\partial \delta P}{\delta t} + \frac{\partial \boldsymbol{\xi}}{\partial t} \cdot \boldsymbol{\nabla} P = \frac{P\gamma}{\rho}\left(\frac{\partial \delta \rho}{\delta t} + \frac{\partial \boldsymbol{\xi}}{\partial t} \cdot \boldsymbol{\nabla}\rho\right),$$

which must be combined with an equation for the rate of change of the perturbed mass density, i.e. the mass density equation $d\rho/dt + \rho\boldsymbol{\nabla}\cdot\boldsymbol{u} = 0$, so that $\partial\delta\rho/\partial t + \boldsymbol{\nabla}\cdot(\rho\partial\boldsymbol{\xi}/\partial t) = 0$, to give the result (by integration).

We see that the perturbed pressure contains the adiabatic effect of $-\boldsymbol{\xi}\cdot\boldsymbol{\nabla}P$ which is caused by the displacement of the fluid orientated in the direction of the equilibrium pressure gradient. Recalling that the equilibrium pressure is always perpendicular to the equilibrium field lines, then $-\boldsymbol{\xi}\cdot\boldsymbol{\nabla}P = -\boldsymbol{\xi}_\perp\cdot\boldsymbol{\nabla}P$. Meanwhile, $-\gamma P\boldsymbol{\nabla}\cdot\boldsymbol{\xi}$ is the effect of compressibility, and the effect necessarily involves $\boldsymbol{\xi}_\parallel$. Incompressibility requires $d\delta\rho/dt = 0$ which in turn requires

$$\boldsymbol{\nabla}\cdot\boldsymbol{\delta u} = \boldsymbol{\nabla}\cdot\boldsymbol{\xi} = 0.$$

The linearised magnetic field $\boldsymbol{\delta B}$ can be calculated by combining Faraday's Law with Ohm's law, which integrates to give

$$\boldsymbol{\delta B} = \boldsymbol{\nabla}\times(\boldsymbol{\xi}\times\boldsymbol{B}), \tag{52}$$

and consequently, from Amperes law, the perturbed current is

$$\boldsymbol{\delta J} = \frac{1}{\mu_0}\boldsymbol{\nabla}\times\boldsymbol{\delta B} = \frac{1}{\mu_0}\boldsymbol{\nabla}\times[\boldsymbol{\nabla}\times(\boldsymbol{\xi}\times\boldsymbol{B})]$$

thus giving the linearised perturbed force

$$\boldsymbol{\delta F}(\boldsymbol{\xi}) = \boldsymbol{\nabla}(\gamma P\boldsymbol{\nabla}\cdot\boldsymbol{\xi} + \boldsymbol{\xi}\cdot\boldsymbol{\nabla}P) + \frac{1}{\mu_0}[(\boldsymbol{\nabla}\times\boldsymbol{\nabla}\times(\boldsymbol{\xi}\times\boldsymbol{B}))\times\boldsymbol{B} + (\boldsymbol{\nabla}\times\boldsymbol{B})\times(\boldsymbol{\nabla}\times(\boldsymbol{\xi}\ \times\boldsymbol{B}))]. \tag{53}$$

Linear MHD Equations

The equation of motion Eq. (50) and Eq. (53) is now entirely in terms of the fluid displacement vector $\boldsymbol{\xi}$ and the equilibrium magnetic field. There are at least four ways of deploying Eq. (50) and Eq. (53) in order to analyse MHD stability, and these are listed in order of their complexity (from most difficult to least difficult)

- (1) The Initial Value Problem
- (2) The Normal Mode Method
- (3) Variation of the total Energy
- (4) Energy Principle

The Initial Value Problem

Eqs. (50) and (53) are solved as an initial value problem. The complexity of the MHD force operator usually means that this approach must be tackled computationally. Whilst it yields a detailed description of the evolution of a perturbation, it is often the case that this information is in excess of what is required to characterise an instability. Hence the method lacks the overall power of the other techniques. Nevertheless an advantage is that nothing is assumed about the form of the time dependence of the perturbations (i.e. not necessarily normal modes), so that the method provides a framework consistent with a non-linear treatment.

Conservation of Energy

Before the normal mode, variational energy, and energy principle methods are considered, it is useful to demonstrate that linear MHD perturbations conform to the conservation of energy. The proof requires the definition of important and compact energy related quantities.

First, apply $\int d^3x\, \dot{\boldsymbol{\xi}}^* \cdot$ to the RHS and LHS of Eq. (50), where the volume integral is over all the plasma volume so that

$$\int d^3x\, \rho\, \dot{\boldsymbol{\xi}}^* \cdot \ddot{\boldsymbol{\xi}} = \int d^3x\, \dot{\boldsymbol{\xi}}^* \cdot \boldsymbol{\delta F}(\boldsymbol{\xi}), \tag{54}$$

and since $\partial/\partial t(\dot{\boldsymbol{\xi}}^* \cdot \dot{\boldsymbol{\xi}}) = \dot{\boldsymbol{\xi}}^* \cdot \ddot{\boldsymbol{\xi}} + \ddot{\boldsymbol{\xi}}^* \cdot \dot{\boldsymbol{\xi}} = 2\dot{\boldsymbol{\xi}}^* \cdot \ddot{\boldsymbol{\xi}}$, then,

$$\frac{1}{2}\frac{\partial}{\partial t}\left(\int d^3x\, \rho\, \left|\dot{\boldsymbol{\xi}}\right|^2\right) = \int d^3x\, \dot{\boldsymbol{\xi}}^* \cdot \boldsymbol{\delta F}(\boldsymbol{\xi}). \tag{55}$$

This is almost in the form of an energy conservation equation. A little bit more work is required for this. Now,

$$\frac{1}{2}\frac{\partial}{\partial t}\left[\int d^3x \boldsymbol{\xi}^* \cdot \boldsymbol{\delta F}(\boldsymbol{\xi})\right] = \frac{1}{2}\int d^3x\, \dot{\boldsymbol{\xi}}^* \cdot \boldsymbol{\delta F}(\boldsymbol{\xi}) + \frac{1}{2}\int dx^3\, \boldsymbol{\xi}^* \cdot \boldsymbol{\delta}\dot{\boldsymbol{F}}(\boldsymbol{\xi})$$

A VERY IMPORTANT PROPERTY IS NOW REQUIRED. We will not prove it (see Freidberg for details). We require the self adjointness property

$$\int d^3x\, \boldsymbol{\xi_1} \cdot \boldsymbol{\delta F}(\boldsymbol{\xi_2}) = \int d^3x\, \boldsymbol{\xi_2} \cdot \boldsymbol{\delta F}(\boldsymbol{\xi_1}), \tag{56}$$

Now, since $\boldsymbol{\delta F}(\boldsymbol{\xi})$ is linear in $\boldsymbol{\xi}$, and since the time dependence in $\boldsymbol{\delta F}$ resides entirely in $\boldsymbol{\xi}$ then $\boldsymbol{\delta}\dot{\boldsymbol{F}}(\boldsymbol{\xi}) = \boldsymbol{\delta F}(\dot{\boldsymbol{\xi}})$. Thus together with the self-adjointness property we have,

$$\frac{1}{2}\int dx^3\, \boldsymbol{\xi}^* \cdot \boldsymbol{\delta}\dot{\boldsymbol{F}}(\boldsymbol{\xi}) = \frac{1}{2}\int dx^3\, \dot{\boldsymbol{\xi}} \cdot \boldsymbol{\delta F}(\boldsymbol{\xi}^*) \quad \text{and therefore} \quad \int d^3x\, \dot{\boldsymbol{\xi}}^* \cdot \boldsymbol{\delta F}(\boldsymbol{\xi}) = \frac{1}{2}\frac{\partial}{\partial t}\left[\int d^3x\, \boldsymbol{\xi}^* \cdot \boldsymbol{\delta F}(\boldsymbol{\xi})\right].$$

Normal Mode Method

Therefore, Eq. (55) can be written as the following energy conservation equation:

$$\frac{\partial}{\partial t}\left[\delta K + \delta W\right] = 0 \qquad (57)$$

where

$$\delta K = \frac{1}{2}\int d^3x\,\rho\,\left|\dot{\boldsymbol{\xi}}\right|^2 \quad \text{and} \quad \delta W = -\frac{1}{2}\int d^3x\,\boldsymbol{\xi}^* \cdot \boldsymbol{\delta F}(\boldsymbol{\xi}). \qquad (58)$$

Here, δK is the kinetic energy, and δW is the potential energy. One then clearly has

$$\delta K + \delta W = \text{constant}.$$

Conservation of Energy

For the study of spontaneously occurring instabilities, one assumes that the perturbations are normal modes of the form

$$\boldsymbol{\xi} \sim \exp(-i\omega t) \quad (\text{and therefore } \boldsymbol{\xi}^* \sim \exp(i\omega t)).$$

With the normal mode method one then solves (from Eq. (50))

$$-\,\omega^2\rho\boldsymbol{\xi} = \boldsymbol{\delta F}(\boldsymbol{\xi}), \qquad (59)$$

for the eigenvalue ω and each component of the eigenvector, where $\boldsymbol{\delta F}$ is given by (53).

Normal Mode Method

In general, the eigenvalues can only be found by obtaining the solutions of three coupled partial differential equations. Nevertheless, if the system contains a degree of symmetry (slab or axis-symmetric cylinder) the complexity is reduced.

Before embarking on applications, another very important property is required. Substituting the normal mode assumption into Eq. (54) one obtains

$$i\omega^3 \int d^3x\, \rho\, |\boldsymbol{\xi}|^2 = i\omega \int d^3x\, \boldsymbol{\xi}^* \cdot \boldsymbol{\delta F}(\boldsymbol{\xi})$$

and this directly ensures that for normal modes, the constant in the energy conservation equation (Eq. 57) is zero

$$\delta K + \delta W = 0 \tag{60}$$

so that

$$\omega^2 = \frac{\delta W}{K} \quad \text{with} \quad K = \frac{1}{2}\int d^3x\, \rho\, |\boldsymbol{\xi}|^2 \tag{61}$$

where

$$\delta K = -\omega^2 K$$

It is therefore clear that ω^2 is real. Normal modes therefore conform to either.
1) Two stationary modes, with one growing and the other decaying (i.e. $\omega^2 < 0$), so that $\xi \sim \exp(\pm|\omega|t)$
2) Two modes neither growing or decaying but both propagate with equal speeds and in the opposite sense (i.e. $\omega^2 > 0$), so that $\xi \sim \exp(\pm i|\omega|t)$

Thus, $\omega = 0$ marks the transition between purely growing (or decaying) modes, and purely propagating modes. Finally we note that Eqs. (60) and (61) are very important for the variation energy method and energy principle method, as we will see later.

Energy Method for analysing Stability

It turns out that there are an infinite number of oscillations, or modes that conform to Eq. (60) or equivalently Eq. (61). However, most of these modes will not satisfy the normal mode equation of Eq. (59). Conceptually, it is clear that we are interested in the most unstable modes, thus giving the largest growth rates. In the following, we will show that the maxima or minima of

$$\frac{\delta W}{K},$$

with respect to variation over $\boldsymbol{\xi}$, conforms to the equation of motion (i.e. the normal mode equation Eq. (59)), and moreover, since $\omega^2 = \frac{\delta W}{K}$, the minima (or maxima in $-\omega^2$) clearly identifies the most unstable mode.

We start by perturbing the "eigenvector" and "eigenvalue":

$$\omega^2 \to \omega^2 + \delta\omega^2, \quad \boldsymbol{\xi} \to \boldsymbol{\xi} + \boldsymbol{\delta\xi}, \quad \boldsymbol{\xi}^* \to \boldsymbol{\xi}^* + \boldsymbol{\delta\xi}^*,$$

so that Eq. (61) becomes

$$\omega^2 + \delta\omega^2 = \frac{\delta W(\boldsymbol{\xi}^*, \boldsymbol{\xi}) + \delta W(\boldsymbol{\delta\xi}^*, \boldsymbol{\xi}) + \delta W(\boldsymbol{\xi}^*, \boldsymbol{\delta\xi}) + \delta W(\boldsymbol{\delta\xi}^*, \boldsymbol{\delta\xi})}{K(\boldsymbol{\xi}^*, \boldsymbol{\xi}) + K(\boldsymbol{\delta\xi}^*, \boldsymbol{\xi}) + K(\boldsymbol{\xi}^*, \boldsymbol{\delta\xi}) + K(\boldsymbol{\delta\xi}^*, \boldsymbol{\delta\xi})}$$

Energy Method for analysing Stability

It turns out that there are an infinite number of oscillations, or modes that conform to Eq. (60) or equivalently Eq. (61). However, most of these modes will not satisfy the normal mode equation of Eq. (59). Conceptually, it is clear that we are interested in the most unstable modes, thus giving the largest growth rates. In the following, we will show that the maxima or minima of

$$\frac{\delta W}{K},$$

with respect to variation over $\boldsymbol{\xi}$, conforms to the equation of motion (i.e. the normal mode equation Eq. (59)), and moreover, since $\omega^2 = \frac{\delta W}{K}$, the minima (or maxima in $-\omega^2$) clearly identifies the most unstable mode.

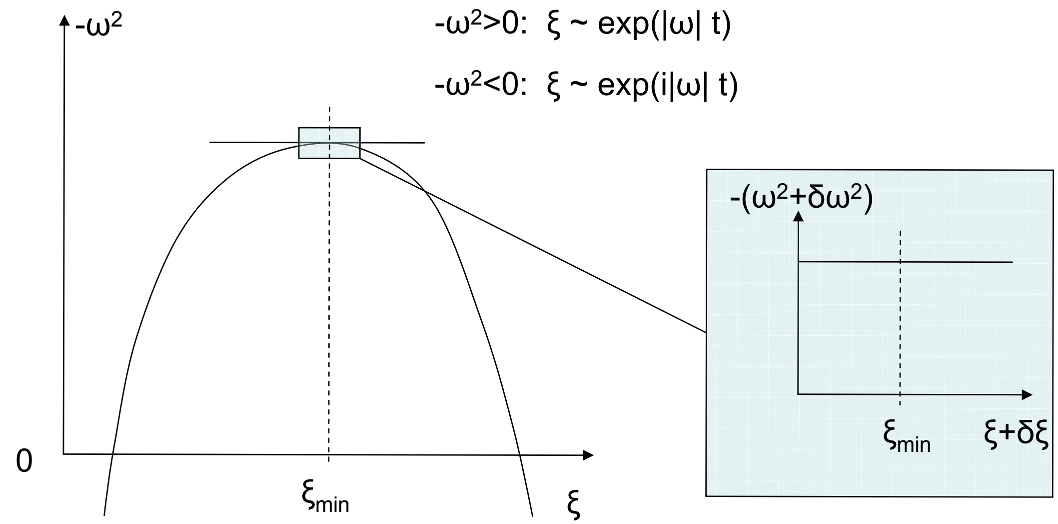

We start by perturbing the "eigenvector" and "eigenvalue":

$$\omega^2 \to \omega^2 + \delta\omega^2, \quad \boldsymbol{\xi} \to \boldsymbol{\xi} + \boldsymbol{\delta\xi}, \quad \boldsymbol{\xi}^* \to \boldsymbol{\xi}^* + \boldsymbol{\delta\xi}^*,$$

We note that we want to find the extrema of the above wrt $\boldsymbol{\xi}$, which clearly requires $\delta\omega^2 = 0$.

$$\omega^2 = \frac{\delta W(\boldsymbol{\xi}^*, \boldsymbol{\xi}) + \delta W(\boldsymbol{\delta\xi}^*, \boldsymbol{\xi}) + \delta W(\boldsymbol{\xi}^*, \boldsymbol{\delta\xi}) + \delta W(\boldsymbol{\delta\xi}^*, \boldsymbol{\delta\xi})}{K(\boldsymbol{\xi}^*, \boldsymbol{\xi}) + K(\boldsymbol{\delta\xi}^*, \boldsymbol{\xi}) + K(\boldsymbol{\xi}^*, \boldsymbol{\delta\xi}) + K(\boldsymbol{\delta\xi}^*, \boldsymbol{\delta\xi})}\Bigg|_{\boldsymbol{\delta\xi}\to 0, \boldsymbol{\xi}\to\boldsymbol{\xi}_{\text{min}}}$$

Energy Method for analysing Stability

Retaining $\delta\omega^2$ for now, and Taylor expanding the denominator, we have

$$\omega^2+\delta\omega^2 = \frac{\delta W(\boldsymbol{\xi}^*,\boldsymbol{\xi})+\delta W(\boldsymbol{\delta\xi}^*,\boldsymbol{\xi})+\delta W(\boldsymbol{\xi}^*,\boldsymbol{\delta\xi})+\delta W(\boldsymbol{\delta\xi}^*,\boldsymbol{\delta\xi})}{K(\boldsymbol{\xi}^*,\boldsymbol{\xi})}\left[1-\frac{K(\boldsymbol{\delta\xi}^*,\boldsymbol{\xi})}{K(\boldsymbol{\xi}^*,\boldsymbol{\xi})}-\frac{K(\boldsymbol{\xi}^*,\boldsymbol{\delta\xi})}{K(\boldsymbol{\xi}^*,\boldsymbol{\xi})}-O(\frac{K(\delta^2)}{K})\right]$$

Continuing by linearising in small δ we have

$$\omega^2+\delta\omega^2 = \frac{\delta W(\boldsymbol{\xi}^*,\boldsymbol{\xi})}{K(\boldsymbol{\xi}^*,\boldsymbol{\xi})}+\frac{\delta W(\boldsymbol{\delta\xi}^*,\boldsymbol{\xi})+\delta W(\boldsymbol{\xi}^*,\boldsymbol{\delta\xi})}{K(\boldsymbol{\xi}^*,\boldsymbol{\xi})}-\frac{\delta W(\boldsymbol{\xi}^*,\boldsymbol{\xi})}{K(\boldsymbol{\xi}^*,\boldsymbol{\xi})}\left[\frac{K(\boldsymbol{\delta\xi}^*,\boldsymbol{\xi})}{K(\boldsymbol{\xi}^*,\boldsymbol{\xi})}+\frac{K(\boldsymbol{\xi}^*,\boldsymbol{\delta\xi})}{K(\boldsymbol{\xi}^*,\boldsymbol{\xi})}\right]$$

Now substituting $\omega^2 = \delta W(\boldsymbol{\xi}^*,\boldsymbol{\xi})/K(\boldsymbol{\xi}^*,\boldsymbol{\xi})$ we have,

$$\delta\omega^2 K(\boldsymbol{\xi}^*,\boldsymbol{\xi}) = \delta W(\boldsymbol{\delta\xi}^*,\boldsymbol{\xi})+\delta W(\boldsymbol{\xi}^*,\boldsymbol{\delta\xi})-\omega^2\left(K(\boldsymbol{\delta\xi}^*,\boldsymbol{\xi})+K(\boldsymbol{\xi}^*,\boldsymbol{\delta\xi})\right).$$

or, since $\delta K = -\omega^2 K$,

$$-\frac{\delta\omega^2}{\omega^2}\delta K(\boldsymbol{\xi}^*,\boldsymbol{\xi}) = 0 = \delta W(\boldsymbol{\delta\xi}^*,\boldsymbol{\xi})+\delta W(\boldsymbol{\xi}^*,\boldsymbol{\delta\xi})+\delta K(\boldsymbol{\delta\xi}^*,\boldsymbol{\xi})+\delta K(\boldsymbol{\xi}^*,\boldsymbol{\delta\xi}). \qquad (62)$$

Thus, the extremum in ω^2, for which $\delta\omega^2 = 0$, conforms to an extremum (or stationary point) of

$$\delta K(\omega^2,\boldsymbol{\xi}^*,\boldsymbol{\xi})+\delta W(\boldsymbol{\xi}^*,\boldsymbol{\xi})$$

over variation with respect to $\boldsymbol{\xi}$ for constant ω. We now have to demonstrate that the stationary point of $\delta K+\delta W$ conforms to the normal mode equation.

Energy Method for analysing Stability

Examining Eq. (62) we have: $0 = \int d^3x \left\{ \boldsymbol{\delta\xi}^* \cdot \delta F(\boldsymbol{\xi}) + \boldsymbol{\xi}^* \cdot \delta F(\boldsymbol{\delta\xi}) + \omega^2 \rho \boldsymbol{\delta\xi}^* \cdot \boldsymbol{\xi} + \omega^2 \rho \boldsymbol{\xi}^* \cdot \boldsymbol{\delta\xi} \right\}$.

Now, applying the self adjoint property of Eq. (56),

$$\int d^3x \, \boldsymbol{\xi}^* \cdot \delta F(\boldsymbol{\delta\xi}) = \int d^3x \, \boldsymbol{\delta\xi} \cdot \delta F(\boldsymbol{\xi}^*)$$

we have

$$0 = \int d^3x \, \left\{ \boldsymbol{\delta\xi}^* \cdot \left[\omega^2 \rho \boldsymbol{\xi} + \delta F(\boldsymbol{\xi}) \right] + \boldsymbol{\delta\xi} \cdot \left[\omega^2 \rho \boldsymbol{\xi}^* + \delta F(\boldsymbol{\xi}^*) \right] \right\},$$

Because $\boldsymbol{\delta\xi}^*$ is arbitrary, it means that the stationary point of $\delta K + \delta W$ over a variation wrt $\boldsymbol{\xi}$ for constant ω^2, reproduces the equation of motion $\omega^2 \rho \boldsymbol{\xi} + \delta F(\boldsymbol{\xi}) = 0$.

In much of the remaining parts of this course, we will analyse linear stability by minimisation of $\delta K + \delta W$ via the Euler-Lagrange equations. Typically, much of the minimisation will be done algebraically, leaving the total energy to be minimised in terms of only the radial component of the displacement,

$$\delta K + \delta W = \int_0^{\text{edge}} dr \, I(\omega^2, r, \xi_r, \xi_r')$$

for some I to be identified, and $\xi_r' = d\xi_r/dr$. The extremum of $\delta K + \delta W$ with respect to variation over ξ_r for constant ω^2 is given by the Euler-Lagrange equation:

$$\frac{\partial I}{\partial \xi_r} - \frac{d}{dr} \left\{ \frac{\partial I}{\partial \xi_r'} \right\} = 0. \tag{63}$$

Energy Principle

The primary interest is to know simply whether a particular equilibrium is linearly unstable to a particular type of instability, or not. The exact eigenvalue and eigenvector might be surplus to requirements. If this is the case, the energy principle is far and away the easiest way to proceed with stability (or instability) analysis. From Eq. (61), and noting that $K(\boldsymbol{\xi}, \boldsymbol{\xi}^*)$ is positive definite, we have

$$\text{sign}\{\omega^2\} = \text{sign}\{\delta W\}$$

where we note that the RHS depends only on $\boldsymbol{\xi}$, and is independent of ω^2. One can then analyse whether a mode has the 'potential' to be unstable by applying all physically allowable trial functions in δW to see if any of them generate $\text{sign}\{\delta W\} = -1$, i.e. instability. Mathematically this is equivalent to finding the minimum of δW over variation in $\boldsymbol{\xi}$, and to see if this minimum δW is negative. This is exactly what is done when establishing marginal stability boundaries (where a marginal point is $\omega^2 = 0$).

We note that the extremum of δW does not in general conform to the normal mode equation, since the inertia δK has been neglected. Nevertheless, close to marginal stability, it *might* be expected that the ξ_{min}, which satisfies $\delta W(\xi_{min}) = \delta W_{min}$, could be employed to give

$$\omega^2 \approx \frac{\delta W_{min}}{K(\xi_{min})}.$$

However, the above relation completely breaks down for some modes, such as the internal kink mode. It turns out the minimisation of δW does correctly recover the stability threshold, but any information regarding ω^2 has to be obtained through variation of the total energy $\delta K + \delta W$.

This apparent anomaly remains true even as we approach the stability boundary, for which $\omega^2 \to 0$. For the internal kink mode, it turns out that minimisation of the total energy reveals $K \sim 1/|\omega|$, so that $\omega^2 \propto |\omega|\delta W$.

Convenient form for δW

First, insert Eq. (53), using Eq. (52) into Eq. (58) and integrate by parts (use divergence theorem) to give,

$$\delta W = \frac{1}{2}\int_P d^3x \left\{ |\boldsymbol{\delta B}|^2 - \boldsymbol{\xi}^* \cdot [\boldsymbol{J} \times B + \boldsymbol{\nabla}(\boldsymbol{\xi} \cdot \nabla P)] + \gamma P |\boldsymbol{\nabla} \cdot \boldsymbol{\xi}|^2 \right\} - \frac{1}{2}\int dS\, (\boldsymbol{n} \cdot \boldsymbol{\xi}^*)\, (\gamma P \boldsymbol{\nabla} \cdot \boldsymbol{\xi} - \boldsymbol{B} \cdot \boldsymbol{\delta B})$$

where μ_0 has been replaced by unity for convenience, $\boldsymbol{n}$ is a vector pointing normal to the plasma surface S, and dS is a surface element, separating the plasma-vacuum interface. Here subscript P denotes integration over the plasma volume.

One can show that $\boldsymbol{B} \cdot [\boldsymbol{J} \times B + \boldsymbol{\nabla}(\boldsymbol{\xi} \cdot \nabla P)] = 0$ so that only the perpendicular component of $\boldsymbol{\xi}^*$, i.e. $\boldsymbol{\xi}^*_\perp$, survives in $\boldsymbol{\xi}^* \cdot [\boldsymbol{J} \times B + \boldsymbol{\nabla}(\boldsymbol{\xi} \cdot \nabla P)]$. Further simplifications are made by integration by parts. If is is assumed that there are no currents on the plasma-vacuum interface, then the surface integral can be converted to a volume integral over the vacuum region (denoted V), to obtain

$$\delta W = \delta W_P + \delta W_V$$

where

$$\delta W_P = \frac{1}{2}\int_P d^3x \left\{ |\boldsymbol{\delta B}|^2 - \boldsymbol{\xi}^*_\perp \cdot (\boldsymbol{J} \times B) + (\boldsymbol{\xi}_\perp \cdot \nabla P) \boldsymbol{\nabla} \cdot \boldsymbol{\xi}^*_\perp + \gamma P |\boldsymbol{\nabla} \cdot \boldsymbol{\xi}|^2 \right\} \quad \text{and} \quad \delta W_V = \frac{1}{2}\int_V d^3x \left| \boldsymbol{\delta \hat{B}} \right|^2 \tag{64}$$

where $\boldsymbol{\delta \hat{B}}$ is the perturbed magnetic field in the vacuum region, which is coupled to plasma displacement by solving $\boldsymbol{\nabla} \cdot \boldsymbol{\delta \hat{B}} = \boldsymbol{\nabla} \times \boldsymbol{\delta \hat{B}} = 0$, subject to the conditions ($\boldsymbol{n}$ is normal to plasma interface, or conducting wall),

$$\boldsymbol{n} \cdot \boldsymbol{\delta \hat{B}}|_b = 0 \quad \text{and} \quad \boldsymbol{n} \cdot \boldsymbol{\delta \hat{B}}|_a = \boldsymbol{n} \cdot \boldsymbol{\nabla} \times (\boldsymbol{\xi}_\perp \times \boldsymbol{B})|_a \tag{65}$$

where b is the conducting wall 'radius' and a is the 'radius' of the plasma-vacuum interface, so that $a < b$.

Convenient form for δW

This nearly completes the derivation of the intuitive form of δW. What remains is to separate $|\delta B|$ and $\boldsymbol{J}$ into perpendicular and parallel components. Use is made of

$$\boldsymbol{J}_\perp = \frac{B \times \boldsymbol{\nabla} P}{B^2} \quad \text{and} \quad \delta B_{||} = -B\left(\boldsymbol{\nabla}\cdot\boldsymbol{\xi}_\perp + 2\boldsymbol{\xi}_\perp\cdot\boldsymbol{\kappa}\right) + \frac{\boldsymbol{\xi}_\perp\cdot\boldsymbol{\nabla} P}{B} \tag{66}$$

where (recall from equilibrium lectures) $\kappa = (\boldsymbol{e}_{||}\cdot\boldsymbol{\nabla}\boldsymbol{e}_{||})$, (where $\boldsymbol{e}_{||} = \boldsymbol{B}/B$) to give

$$\delta W_P(\boldsymbol{\xi},\boldsymbol{\xi}^*) = \delta W_\perp(\boldsymbol{\xi}_\perp,\boldsymbol{\xi}_\perp^*) + \overline{\delta W}(\boldsymbol{\xi},\boldsymbol{\xi}^*) \quad \text{where,} \tag{67}$$

$$\delta W_\perp(\boldsymbol{\xi}_\perp,\boldsymbol{\xi}_\perp^*) = \frac{1}{2}\int_P d^3x \left[\delta B_\perp^2 + B^2\left(\boldsymbol{\nabla}\cdot\boldsymbol{\xi}_\perp + 2\boldsymbol{\xi}_\perp\cdot\boldsymbol{\kappa}\right)^2 - 2(\boldsymbol{\xi}_\perp\cdot\boldsymbol{\nabla}P)(\boldsymbol{\kappa}\cdot\boldsymbol{\xi}_\perp^*) - J_{||}(\boldsymbol{\xi}_\perp^*\times\boldsymbol{e}_{||})\cdot\boldsymbol{\delta B}_\perp\right] \tag{68}$$

$$\overline{\delta W}(\boldsymbol{\xi},\boldsymbol{\xi}^*) = \frac{1}{2}\int_P d^3x\, \gamma P(\boldsymbol{\nabla}\cdot\boldsymbol{\xi})^2, \tag{69}$$

where $J_{||}$ is the parallel current density.

Since $\boldsymbol{\delta B} = \boldsymbol{\nabla}\times(\boldsymbol{\xi}_\perp\times\boldsymbol{B})$ then it is seen that $\delta W_\perp$ is independent of $\boldsymbol{\xi}_{||}$. Each of the terms in Eq. (68) has a simple physical interpretation. The first term in $\delta W_\perp$ is always stabilising and is the magnetic energy in the Alfvén wave associated with field line bending. The second term is also stabilising and corresponds to the energy necessary to compress the magnetic field and describes the major potential energy contribution to magnetosonic waves. The third term, proportional to the pressure gradient, is the potential energy for the ballooning and interchange instabilities. It is destabilising if $\boldsymbol{\nabla}P$ and $\boldsymbol{\kappa}$ are parallel (unfavourable curvature). The fourth term is the free energy arising from the current and is responsible for kink instabilities. Finally, $\overline{\delta W}$ is the energy required to compress the plasma. It is stabilising.

Incompressibility

Before using the energy method it is essential to attempt a reduction in the complexity of the analysis. Here we demonstrate that under certain conditions, the dimensions of the system can be reduced from three to two.

Equation (68) shows that $\delta W_\perp$ is independent of $\boldsymbol{\xi}_{\|}$. This means that δW can be minimised with respect to $\boldsymbol{\xi}_{\|}$ by only considering $\overline{\delta W}$. It is clear that $\overline{\delta W}$ is positive definite and minimises to zero when $\boldsymbol{\nabla}\cdot\boldsymbol{\xi} = 0$. This requires that the parallel flow satisfies

$$B\frac{\partial}{\partial l}\left(\frac{\boldsymbol{\xi}_{\|}}{B}\right) = -\boldsymbol{\nabla}\cdot\boldsymbol{\xi}_\perp. \tag{70}$$

Hence, the most unstable modes that exist in the vicinity of marginal stability are incompressible. This is the reason for many stability codes assuming incompressibility - i.e. it is a good approximation near marginal stability (so that $\delta K(\boldsymbol{\xi}_\perp, \boldsymbol{\xi}_{\|})$ variation can be ignored), and exact at marginal stability, and thus the problem is reduced by one dimension. We note that near marginal stability, $\boldsymbol{\xi}_{\|}$ will still appear in the total energy (to undergo variation). It will feature in the inertia δK. However, through Eq. (70), it can be written in terms of $\boldsymbol{\xi}_\perp$.

One should note that the parallel displacement does not satisfy Eq. (70) far from the stability boundary, i.e. normal modes are not incompressible when their rate of growth is large. Where the effects of compressibility are expected to be important, the adiabatic model, which generates $\overline{\delta W}(\boldsymbol{\xi}, \boldsymbol{\xi}^*)$ is lacking in rigour, and a more sophisticated model is required to account for the parallel dynamics.

For most of this course, the incompressible MHD model is investigated (i.e. we take variations of $\delta K + \delta W_\perp + \delta W_V$). At the end of the course, kinetic effects are included in order to account for 'kinetic compressibility,' i.e. the kinetic analogue of $\overline{\delta W}(\boldsymbol{\xi}, \boldsymbol{\xi}^*)$. We will now derive the general formulation.

Kinetic MHD

The aim is to avoid the adiabatic equation of state for the energy equation $\frac{d}{dt}\left(P\rho^{-\gamma}\right)$, which yields Eq. (51), i.e $\delta P = -\gamma P \boldsymbol{\nabla}\cdot\boldsymbol{\xi} - \boldsymbol{\xi}\cdot\boldsymbol{\nabla}P$, and replace this with a kinetic closure which ultimately yields

$$\underline{\underline{\delta P}} = \underline{\underline{I}}(\boldsymbol{\xi}_\perp \cdot \boldsymbol{\nabla}P) + \underline{\underline{\delta P}}_k \tag{71}$$

where the pressure tensor conforms to the diagonal tensor defined in Eq. (7). Also $\underline{\underline{\delta P}}_k$ will be defined later, but suffice to say at present that $\underline{\underline{\delta P}}_k$ depends explicitly on $\boldsymbol{\xi}_\perp$ and ω.

Rather than employing the full MHD equations, we choose the (more valid) perpendicular MHD equations defined by Eqs. (8), derived earlier. Ignoring equilibrium plasma flows, one then has the perpendicular normal mode equation,

$$-\omega^2\rho\boldsymbol{\xi}_\perp = \boldsymbol{\delta F}_\perp(\boldsymbol{\xi}_\perp), \tag{72}$$

with

$$\begin{aligned}\boldsymbol{\delta F}_\perp(\boldsymbol{\xi}_\perp) \quad = \quad & [\boldsymbol{\nabla} - \boldsymbol{e}_\parallel(\boldsymbol{e}_\parallel\cdot\boldsymbol{\nabla})](\boldsymbol{\xi}_\perp\cdot\boldsymbol{\nabla}P) - [\boldsymbol{\nabla} - \boldsymbol{e}_\parallel(\boldsymbol{e}_\parallel\cdot\boldsymbol{\nabla})]\delta P_{k\perp} - (\delta P_{k\parallel} - \delta P_{k\perp})\boldsymbol{\kappa} + \\ & [(\boldsymbol{\nabla}\times\boldsymbol{\nabla}\times(\boldsymbol{\xi}_\perp\times\boldsymbol{B}))\times\boldsymbol{B} + (\boldsymbol{\nabla}\times\boldsymbol{B})\times(\boldsymbol{\nabla}\times(\boldsymbol{\xi}_\perp \times\boldsymbol{B}))]_\perp .\end{aligned} \tag{73}$$

We now follow the energy method of ideal MHD, but this time, form the dot product of Eq. (72) with $\boldsymbol{\xi}^*_\perp$ and integrate over all space, giving

$$\delta K_\perp + \delta W_\perp + \delta W_V + \delta W_k = 0 \tag{74}$$

where

$$\delta K_\perp = -\omega^2\frac{1}{2}\int d^3x\,\rho\,|\boldsymbol{\xi}_\perp|^2 \quad \text{and} \quad \delta W_k = -\frac{1}{2}\int d^3x\,\left[\delta P_{k\perp}(\boldsymbol{\nabla}\cdot\boldsymbol{\xi}^*_\perp) - (\delta P_{k\parallel} - \delta P_{k\perp})\boldsymbol{\xi}^*_\perp\cdot\boldsymbol{\kappa}\right]$$

From inspection, it is clear that $\delta W_\perp$ is simply that defined in Eq. (68), and δW_V is simply that defined in Eq. (64).

Kinetic MHD

This is obvious because the sum of the δW contributions has to be identical if $\gamma \rightarrow 0$ and $\boldsymbol{\xi} \rightarrow \boldsymbol{\xi}_\perp$ in the MHD model, and $\delta P_k = 0$ in the kinetic model. Hence, δW_k has replaced the compressibility term, $\overline{\delta W}$, of the MHD model. One other subtle difference is that $\delta K_\perp$ has replaced δK. This modification to the inertia is currently being explored by a number of researchers, but it is out of the scope of this course (I can supply references for those interested)

We note that Eq. (74) forms a dispersion relation, and if δW_k is self-adjoint, one is permitted to apply variation to Eq. (74), and thereby recover the perpendicular equation of motion Eq. (72). We note that we have been able to avoid the MHD parallel equation of motion. Parallel dynamics will be controlled by the drift kinetic equation. In principle the latter obtains a kinetic equation analogous to Eq. (70). We note however that the parallel displacement is not required explicitly (though it is implicitly in the definition of δP_k in terms of $\boldsymbol{\xi}_\perp$).

The generalised dispersion relation of Eq. (74) is extremely powerful. It is capable of including the physics of wave-particle interaction, e.g. Landau damping. Modes frequently investigated include the internal kink mode, including the interaction of fast ions on sawteeth and fishbones. Also investigated are kinetic ballooning modes, interchange modes, infernal modes, resistive wall modes, and many others.

Low Order Macroscopic Stability

We will consider stability to large scale modes (long wave lengths). We will expand all quantities in inverse aspect ratio. At lowest order in ϵ, the results are identical in a torus and a cylinder. The derivations are a little different from those typically found in textbooks, which often start by assuming cylindrical geometry. I argue that there is never any virtue in strictly assuming cylindrical geometry. This is because, where the stability results are different in a cylinder and a torus, then the differences are catastrophic.

In an axisymmetric torus, a perturbation may be described by a Fourier decomposition in poloidal harmonics as

$$\boldsymbol{\xi}(r,\theta,\phi) = \sum_m \boldsymbol{\xi}^{(m)}(r) e^{i(m\theta - n\phi - \omega t)}$$

by virtue of the periodicity in the poloidal and toroidal directions. Since the equilibrium magnetic field strength $B \approx B_0(1 - \varepsilon\cos\theta)$ is a function of θ, a coupling in the different poloidal harmonics arises in $\boldsymbol{\xi}$. This coupling will not appear in the present lecture since only lowest order effects are considered at present, and as a consequence, we do not need to be careful about the definition of θ (orthogonal, straight field line etc).

We will minimise δW with respect to $\boldsymbol{\xi}$. We permit ourselves to introduce the inertia δK later, should growth rates be required, and we can order δK as required (depends on closeness to stability threshold). To aid the analysis the eigenvector is written as follows:

$$\boldsymbol{\xi} = \boldsymbol{\xi}_0 + \boldsymbol{\xi}_1 + \boldsymbol{\xi}_2,$$

where the subscript denotes the aspect ratio ordering of the term, e.g. $\boldsymbol{\xi}_2/\boldsymbol{\xi}_0 \sim O(\varepsilon^2)$. Subsequently, it is found that

$$\delta W = \delta W_0 + \delta W_2 + \delta W_4.$$

δW_0, δW_2 and δW_4 are minimised with respect to $\boldsymbol{\xi}_0$, $\boldsymbol{\xi}_1$ and $\boldsymbol{\xi}_2$ as shown in the following.

Minimisation of δW_0

We initially consider the plasma region, i.e. $\delta W_\perp$ defined in Eq. (68). In both δW_0 and δW_2 it is appropriate to write,

$$\begin{aligned}\boldsymbol{\xi}_\perp &= \xi_r \hat{\boldsymbol{e}}_r + \xi_\theta \hat{\boldsymbol{e}}_\theta \\ \boldsymbol{\delta B}_\perp &= \delta B_r \hat{\boldsymbol{e}}_r + \delta B_\theta \hat{\boldsymbol{e}}_\theta \\ J_\| &= J_\phi.\end{aligned}$$

We will later show that $\delta B_{\perp 0} \sim \varepsilon B_0 \boldsymbol{\nabla}\cdot\boldsymbol{\xi}_{\perp 0}$. The curvature vector $\boldsymbol{\kappa}$ is also not a leading order effect i.e. $\boldsymbol{\xi}_{\perp 0}\cdot\boldsymbol{\kappa}/\boldsymbol{\nabla}\cdot\boldsymbol{\xi}_{\perp 0} \sim \varepsilon$. Hence, from Eq. (68) it is clear that,

$$\delta W_0 = \frac{1}{2}\int d^3x \frac{B^2}{\mu_0}\left(\boldsymbol{\nabla}\cdot\boldsymbol{\xi}_{\perp 0}\right)^2. \tag{75}$$

Since this term is positive definite the minimisation of Eq. (75) corresponds to $\boldsymbol{\nabla}\cdot\boldsymbol{\xi}_{\perp 0} = 0$, which gives $\delta W_0 = 0$. The leading order displacement does not allow poloidal coupling; hence $\boldsymbol{\xi}_0 = \boldsymbol{\xi}_0(r)e^{i(m\theta - n\phi - \omega t)}$, which gives

$$\xi_{\theta 0} = \frac{i}{m}\frac{\partial}{\partial r}\left(r\xi_{r0}\right). \tag{76}$$

This equation states that the field line compression energy is zero, i.e. the plasma motion in the poloidal plane is incompressible at this lowest order.

Since the minimised zeroth order potential energy vanishes, the next order must be considered.

Minimisation of δW_2

All except the third term in Eq. (68) feature in δW_2. This term is neglected because the ordering of $\beta \sim O(\varepsilon^2)$ means that terms involving the equilibrium pressure first appear in δW_4. Referring to Eq. (68) it is now clear that

$$\delta W_2 = \frac{1}{2}\int d^3x \left(\frac{\delta B_{\perp 0}^2}{\mu_0} + \frac{B^2}{\mu_0}(\boldsymbol{\nabla}\cdot\boldsymbol{\xi}_{\perp 1} + 2\boldsymbol{\xi}_{\perp 0}\cdot\boldsymbol{\kappa})^2 - J_{\|}(\boldsymbol{\xi}_{\perp 0}^* \times \hat{\boldsymbol{e}}_{\|})\cdot\boldsymbol{\delta B}_{\perp 0}\right). \qquad (77)$$

the second term is minimised to zero by a constraint on $\boldsymbol{\xi}_{\perp 1}$ such that,

$$\boldsymbol{\nabla}\cdot\boldsymbol{\xi}_{\perp 1} + 2\boldsymbol{\xi}_{\perp 0}\cdot\boldsymbol{\kappa} = 0. \qquad (78)$$

This states that the plasma motion in the poloidal plane is compressible at the next order, and the effect is balanced by lowest order curvature of the magnetic field lines.

To minimise δW_2, both $\delta B_{\theta 0}$ and δB_{r0} are written in terms of ξ_{r0}. The perturbed field is defined in terms of the eigenfunction using Eq. (52). Recalling that $\boldsymbol{\nabla}\cdot\boldsymbol{\xi}_{\perp 0} = 0$ and using Eq. (42) for $q \approx rB_0/(R_0 B_\theta)$, together with Eq. (76) and $\boldsymbol{\nabla} = \hat{\boldsymbol{e}}_r \partial/\partial r + (\hat{\boldsymbol{e}}_\theta/r)\partial/\partial\theta + (\hat{\boldsymbol{e}}_\phi/R)\partial/\partial\phi$ gives,

$$\begin{aligned} \delta B_{r0} &= -\frac{imB_0}{R_0}\left(\frac{n}{m} - \frac{1}{q}\right)\xi_{r0} \\ \delta B_{\theta 0} &= \frac{B_0}{R_0}\frac{\partial}{\partial r}\left[\left(\frac{n}{m} - \frac{1}{q}\right) r\xi_{r0}\right]. \end{aligned} \qquad (79)$$

In addition, from Ampère's law:

$$\mu_0 J_\phi = \frac{1}{r}\frac{d}{dr}(rB_\theta) \approx \frac{B_0}{R_0}\frac{1}{r}\frac{d}{dr}\left(\frac{r^2}{q}\right). \qquad (80)$$

Minimisation of δW_2

Hence, using $\int d^3x \approx R_0 \int_0^{2\pi} d\phi \int_0^{2\pi} d\theta \int_0^a r\, dr$ (where a marks the plasma-vacuum interface) we have simply,

$$\delta W_2 = \frac{2\pi^2 B_0^2}{\mu_0 R_0} \int_0^a dr \left\{ r \left[m^2 \left(\frac{n}{m} - \frac{1}{q} \right)^2 \xi_{r0}^2 + \left(\frac{d}{dr} \left[\left(\frac{n}{m} - \frac{1}{q} \right) r|\xi_{r0}| \right] \right)^2 \right] + \left(\frac{d}{dr} \left[\frac{r^2}{q} \right] \right) \left[\left(\frac{n}{m} - \frac{1}{q} \right) |\xi_{r0}| \frac{d}{dr}(r|\xi_{r0}|) + |\xi_{r0}| \frac{d}{dr} \left[\left(\frac{n}{m} - \frac{1}{q} \right) r|\xi_{r0}| \right] \right] \right\}.$$

Dropping the modulus in $|\xi_{r0}|$, and after some integration by parts and cancellation, Eq. (77) becomes,

$$\delta W_2 = \frac{2\pi^2 B_0^2}{\mu_0 R_0} \left\{ \int_0^a dr\, r \left[\left(r \frac{d\xi_{r0}}{dr} \right)^2 + \left(m^2 - 1 \right) \xi_{r0}^2 \right] \left(\frac{n}{m} - \frac{1}{q} \right)^2 + a^2 \xi_{r0}(a)^2 \left[\frac{2}{q_a} \left(\frac{n}{m} - \frac{1}{q_a} \right) + \left(\frac{n}{m} - \frac{1}{q_a} \right)^2 \right] \right\} \tag{81}$$

where $q_a = q(a)$. Equation (81) shows that to second order in the inverse aspect ratio, ideal MHD does not allow unstable internal modes (where $\xi_{r0}(a) = 0$) since all the terms in the plasma region are positive definite.

We still have to treat the vacuum region, and we will do this when we examine external modes.

Internal Modes

Consider internal modes conforming to Eq. (81) for which we force $\delta B(a) = 0$. We will examine whether this a valid boundary condition. First, since the integrand of Eq. (81) is positive definite, meaning that entirely internal modes cannot be unstable at this order in δW. However, we see that marginal stability occurs when $q(r) = m/n$.

It turns out that for negligible magnetic shear the stabilisation associated with the bending of field lines, in response to a plasma displacement, vanishes when the pitch of the unperturbed magnetic field lines is perpendicular to the wave vector (see figure), i.e. when

$$|\delta B_\perp| \propto k_{\|} \cdot \boldsymbol{B} = 0 \approx (nq(r) - m)\frac{B_0}{R_0}$$

Recall the "frozen in theorem", which should help in understanding the figure. Bending field lines requires energy $(\int d^3x\, |\delta B_\perp|^2/2)$, and this strongly damps instabilities. Instabilities occur when field line bending is not strong (where $q(r) \approx m/n$).

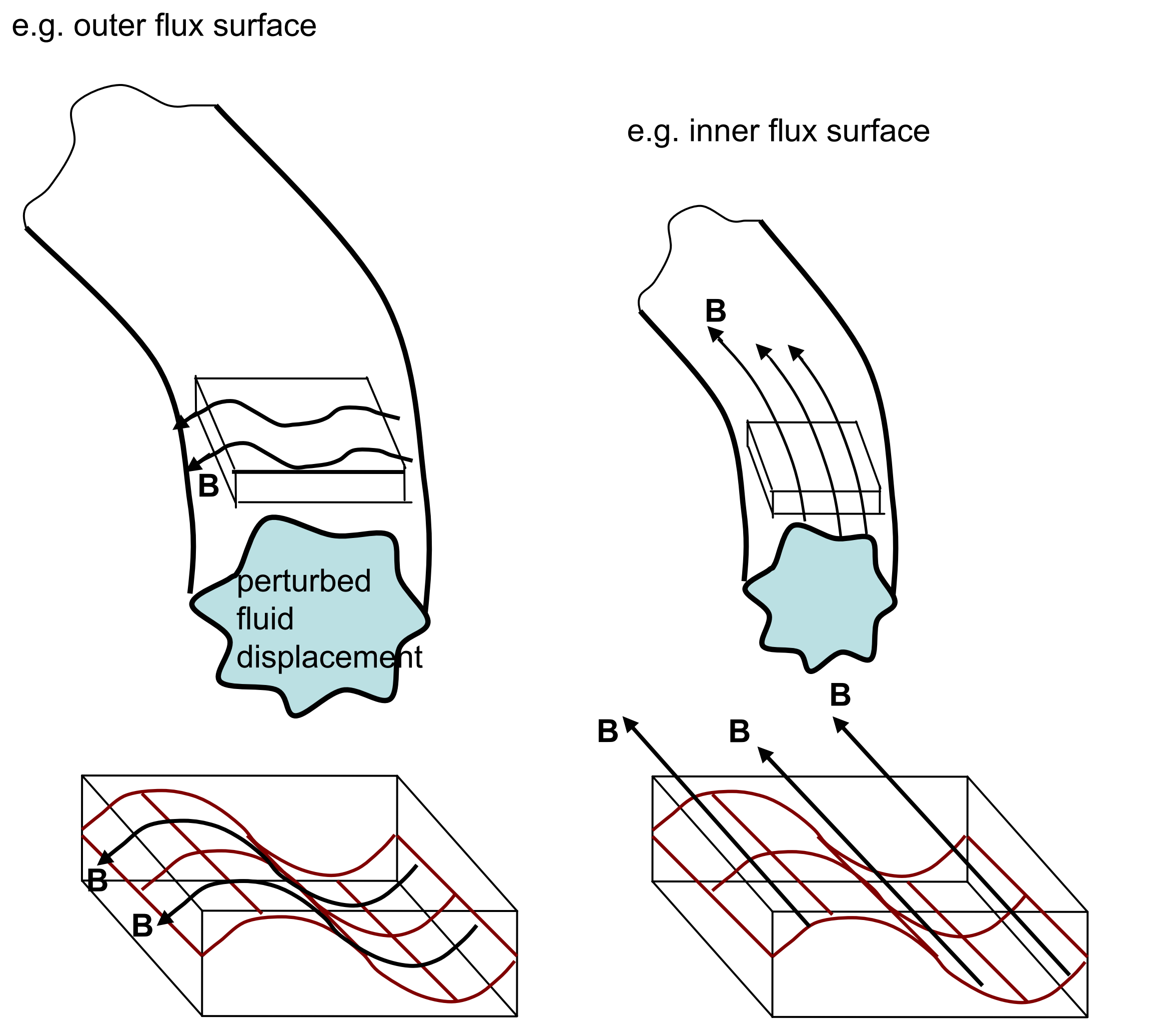

k is parallel to B, i.e. k_par is non-zero
Frozen in theorem means that field lines
have to bend with fluid motion

k is perpendicular to B, i.e. k_par =0.
Field lines move, due to frozen
In theorem, but they don't bend.

Internal Modes cont'd

We minimise the energy of Eq. (81) by applying the Euler-Lagrange minimisation, as defined in Eq. (63), giving

$$\frac{d}{dr}\left[\left(\frac{n}{m}-\frac{1}{q}\right)^2 r^3 \frac{d\xi_{r0}}{dr}\right] = (m^2-1)\left(\frac{n}{m}-\frac{1}{q}\right)^2 r\xi_{r0}. \quad (82)$$

We note that for $n = 0$ this turns out to be the same equation as Eq. (49) defining the equilibrium shaping terms S_m.

Equation (82) is singular for $q = m/n$. Near the magnetic axis q is approximately constant, so that the exact solution for small r is $\xi_{r0}(r) \sim r^{-1\pm m}$, where the regular solution at $r = 0$ is clearly:

$$\xi_{r0} \sim r^{m-1} \quad \text{and} \quad \xi_{\theta 0} \sim i\xi_{r0}.$$

For $m > 1$ the mode amplitude vanishes at the plasma centre. At the edge the $m > 1$ mode will in general couple to the vacuum region, and so these external kink modes will be considered later.

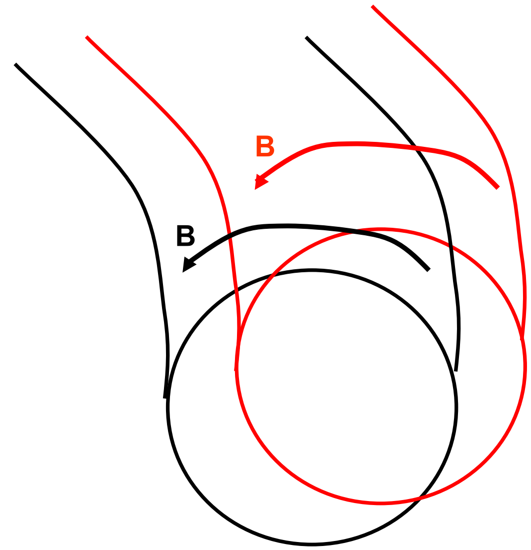

m=1 fluid displacement just shifts to an identical equilibrium in the poloidal plane. Field lines cannot bend In poloidal plane in response to m=1.

$m = 1$ is a special case: it reduces the effect of field line bending stabilisation (see figure for explanation). For $m = 1$, ξ_{r0} is constant in the plasma core. Regardless of magnetic shear, δW_2 entirely vanishes for $m = 1$ with $\xi'_{r0} = 0$, or ξ_{r0} constant at all radii. In order to satisfy the boundary condition $\xi_{r0}(a) = 0$, the displacement can reduce δW_2 to zero by being constant in the core region where $q < 1$ (assuming $n = 1$), and zero in the region where $q > 1$. There is a narrow transition region, or layer region, which requires consideration of the effect of inertia (later). Since δW_2 vanishes, we need to go to δW_4. At this order, toroidal effects, including the Shafranov shift, are crucial. The effects of inertia, and toroidal effects on the $m = n = 1$ internal kink mode will be considered in detail later.

$m = n = 1$ Internal Kink Mode

Both δW_0 and δW_2 have been minimised to zero. That is, the internal kink mode is marginally stable to order ε^2. The stability of the kink mode therefore depends on the fourth order correction, i.e. since both δW_0 and δW_2 have been minimised to zero one must consider fourth order terms. In calculating δW_4 the results for $\boldsymbol{\xi}_{\perp 0}$ and $\boldsymbol{\xi}_{\perp 1}$ given in the previous two sections must be used. The remaining component of $\boldsymbol{\xi}_{\perp 1}$ together with $\boldsymbol{\xi}_{\perp 2}$ are still to be identified.

A cylindrical calculation accurate to fourth order in the aspect ratio was first published by Rosenbluth (1973). However, for the all important $n = 1$ case Bussac *et al* (1976) demonstrated that the fourth order cylindrical calculation is irrelevant. By including the toroidal effects of Shafranov shifted circular flux surfaces, Bussac showed that the fourth order solution has the form

$$\delta \hat{W}_4 = \left(1 - \frac{1}{n^2}\right) \delta \hat{W}_4^C + \delta \hat{W}_4^T \tag{83}$$

$$\text{with } \delta W = \delta \hat{W} (2\pi^2 R_0 B_0^2 \xi_{r0}^2 \varepsilon^4 / \mu_0)\Big|_{r_1 - \delta}$$

where $\delta \hat{W}_4^C$ is the cylindrical potential energy [Rosenbluth] and $\delta \hat{W}_4^T$ is a toroidal contribution.

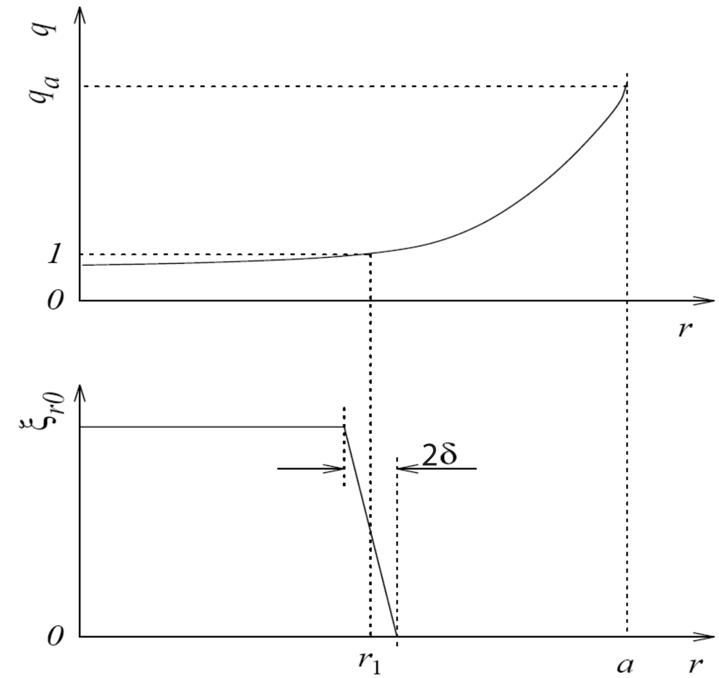

$m = n = 1$ Internal Kink Mode

It is seen that the cylindrical term is entirely cancelled (for $n = 1$) by the inclusion of toroidal effects!! This was probably a massive surprise, and made the community realise that inclusion of full toroidal effects are not simply important, but that cylindrical results are in some cases, meaningless. The cancelation is due to toroidal curvature, and it's matching with the $n = 1$ bending of the field lines. This is therefore analogous to the $m = 1$ cancellation already described.

Such is its complexity, the calculation for δW_4 has only been performed analytically by a few researchers worldwide, and is beyond the scope for this course. The algebra is apparently horrendous. Nevertheless, the prevailing features will be uncovered in the physics of Mercier modes, quasi-interchange modes and infernal modes (week 5 - these modes are much easier to treat). In particular, there are stabilising effects due to toroidal coupling with $m = 0$ and $m = 2$ modes. The net effect is only destabilising at high plasma $beta$, since for a simple quadratic q profile:

$$\delta \hat{W}_4^T \approx 3(1 - q_0)\left((\beta_p^c)^2 - \beta_p^2\right), \qquad (84)$$

where $\beta_p = \beta_p(r_1 - \delta)$ and typically $0.1 < \beta_p^c < 0.3$ So it is seen that the internal kink mode is an ideal mode, with instability governed by both the current profile, and pressure profile.

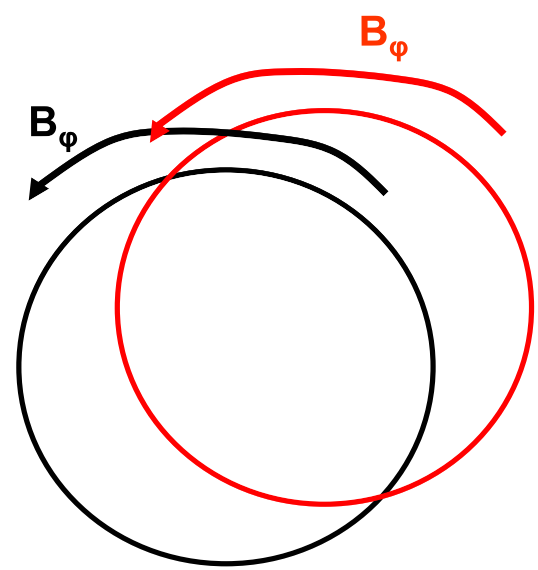

Looking down on torus from above. n=1 fluid displacement just shifts to an identical equilibrium in the toroidal plane. Field lines cannot bend in toroidal plane in response to n=1.

Problems

(1) Prove that the extremum in ω^2, for which $\delta\omega^2 = 0$, conforms to an extremum (or stationary point) of

$$\delta K(\omega^2, \boldsymbol{\xi}^*, \boldsymbol{\xi}) + \delta W(\boldsymbol{\xi}^*, \boldsymbol{\xi})$$

over variation with respect to $\boldsymbol{\xi}$ for constant ω.

Also, use the self-adjoint property to show that the stationary point of $\delta K + \delta W$ over a variation wrt $\boldsymbol{\xi}$ for constant ω^2, reproduces the equation of motion $\omega^2 \rho \boldsymbol{\xi} + \delta F(\boldsymbol{\xi}) = 0$.

(2) Examine Eq. (70)

$$B\frac{\partial}{\partial l}\left(\frac{\boldsymbol{\xi}_\parallel}{B}\right) = -\boldsymbol{\nabla}\cdot\boldsymbol{\xi}_\perp .$$

in order to derive the Glasser-Green-Johnson inertial enhancement

$$\delta K = \delta K_\perp (1 + 2q^2)$$

This result shows that growth rates are strongly reduced by the parallel inertial (parallel displacement), while, as we have seen, the threshold for stability is not affected by the parallel displacement.

Hints, use

$$\frac{\partial}{\partial l} = \frac{1}{R_0 q}\left[\frac{\partial}{\partial \theta} - inq\right],$$

$$\boldsymbol{\xi}_\perp(r,\theta,\phi,t) = \hat{\boldsymbol{\xi}}_\perp(r)\exp(im\theta - in\phi - i\omega t),$$

$$m/n \approx q,$$

$$\boldsymbol{\nabla}\cdot\boldsymbol{\xi}_\perp \approx -2\frac{\boldsymbol{\xi}_\perp\cdot\nabla B}{B},$$

Problems continued

$$B = B_0[1 - (r/R_0)\cos\theta],$$

$$\boldsymbol{\xi}_\perp \approx \xi_\theta \boldsymbol{e}_\theta + \xi_r \boldsymbol{e}_r,$$

to obtain the intermediate result showing that the parallel displacement is the sum of poloidal sidebands:

$$\xi_{||} \approx -2q(\xi_r \sin\theta + \xi_\theta \cos\theta) \equiv -q[\xi_\theta(r,\theta)(\exp(i\theta) + \exp(-i\theta)) - i\xi_r(r,\theta)(\exp(i\theta) - \exp(-i\theta))].$$

(3) Prove Eq. (79) for the lowest order components of the perpendicular perturbed magnetic field. Calculate the field line bending energy $\delta B_{\perp 0}^2$, and examine the energy on a rational surface $m = nq$. Speculate why tokamaks usually operate with monotonically increasing q profile (with respect to flux label r), and where non-monotonic q-profiles (e.g. advanced scenarios) are employed, speculate on what value's of q_{min} should avoided.

- Week 1: Derivation and limitations of the MHD model. Conservation of Flux, The Grad-Shafranov Equation. Coordinate systems in tokamak equilibrium.
- Week 2: Tokamak equilibrium. Analytical expansions. Shafranov Shift. Shaping, and shaping penetration into the torus.
- Week 3: Linearised ideal MHD stability, energy principle, stability boundaries, ideal internal kink mode
- Week 4: External Kink modes, linear tearing modes
- week 5: Ideal singular layer calculations, magnetic islands, non-linear resistive MHD, NTMs
- Week 6: Toroidal effects: Interchange stability (Mercier) and ballooning.
- Week 7: Ballooning continued. Introduction to kinetic MHD and long mean free path parallel dynamics.

External Kink Modes

Now that we have learned that internal modes are stable (except for the possibility of $m = 1$), we now need to look more carefully at the vacuum-plasma interface, and the vacuum region itself. We will see that, under certain conditions, modes that extend up to and beyond the plasma edge can be unstable. Moreover, since $\xi \sim r^{m-1}$, this means that all modes with $m > 1$ could be potentially ideal unstable.

To treat external modes, we have to consider the plasma surface terms in δW_p, i.e. the second term of Eq. (81)

$$\frac{2\pi^2 B_0^2}{\mu_0 R_0}\left\{a^2\xi_{r0}(a)^2\left[\frac{2}{q_a}\left(\frac{n}{m}-\frac{1}{q_a}\right)+\left(\frac{n}{m}-\frac{1}{q_a}\right)^2\right]\right\},$$

as well as the vacuum term, defined in Eq. (64) given by

$$\delta W_V = \frac{1}{2}\int_V d^3x\left|\boldsymbol{\delta}\hat{\boldsymbol{B}}\right|^2.$$

The internal plasma δW_P expression given by the first term of Eq. (81) remains valid for the portion of the displacement which is entirely inside the plasma. Moreover, the minimisation of the displacement in the plasma region remains valid, so that Eq. (82) holds for the displacement. Indeed, variation of δW_P with respect to ξ_{r0} is necessarily a variation of just the first term of Eq. (81), since the second term of Eq. (81) is independent of the displacement (after normalising the total δW with $\xi_{r0}(a)$.

It remains to obtain δW_V by solving for the vacuum perturbed fields, subject to boundary conditions matching the internal minimised solution given by Eq. (65). (Clearly, in the vacuum region there is no plasma, so the displacement is zero. Thus, δW_V has to be defined in terms of the perturbed field.)

External Kink Modes-Vacuum Region

Let us begin by looking at the perturbed parallel field in the plasma region (which must be continuous across the interface). It can be shown that (Eq. (66)):

$$\delta B_{\|} = \frac{\boldsymbol{\xi}_{\perp} \cdot \boldsymbol{\nabla} P}{B} - B(\boldsymbol{\nabla} \cdot \boldsymbol{\xi}_{\perp} + 2\boldsymbol{\xi}_{\perp} \cdot \boldsymbol{\kappa}).$$

We note that $(\boldsymbol{\nabla} \cdot \boldsymbol{\xi}_{\perp} + 2\boldsymbol{\xi}_{\perp} \cdot \boldsymbol{\kappa})$ has been minimised to zero, and moreover, $P/B^2 \sim \epsilon^2$, and near the edge, the pressure is vanishingly small. Hence, $\delta B_{\|} = 0$ at this order in the plasma region, and thus, due to the boundary condition of Eq. (65), it is zero in the vacuum region. Note that $\delta B_{\|}$ is associated with magnetosonic (sonic-magnetic) waves, which would be expected to be zero in vacuum. Since $\delta B_{\|} \approx \delta B_{\phi}$, we are left once again with δB_r and δB_θ.

The analysis is greatly simplified by defining a perturbed poloidal flux $\delta\psi$ for which

$$\delta B_\theta = \frac{\partial \delta\psi}{\partial r} \tag{85}$$

(see the similar definition of the equilibrium poloidal flux of Eq. (10)). Applying $\boldsymbol{\nabla} \cdot \boldsymbol{\delta \hat{B}} = 0$ we have

$$\frac{1}{r}\frac{\partial}{\partial r}(r\,\delta B_r) + \frac{1}{r}\frac{\partial\,\delta B_\theta}{\partial\theta} = 0$$

and upon applying Eq. (85) this becomes

$$\frac{1}{r}\frac{\partial}{\partial r}(r\,\delta B_r) = -\frac{1}{r}\frac{\partial}{\partial\theta}\left(\frac{\partial\delta\psi}{\partial r}\right)$$

and thus, since $\partial/\partial\theta = im$, then in the vacuum:

$$\delta B_r = -im\frac{\delta\psi}{r} \quad \text{giving} \quad |\delta B|^2 = |\delta B_\theta|^2 + |\delta B_r|^2 = \frac{m^2}{r^2}\delta\psi^2 + \left(\frac{d\delta\psi}{dr}\right)^2. \tag{86}$$

External Kink Modes

Moreover, equating δB_r in the vacuum and the plasma (Eq. (79)), at $r = a$ we have the BC (at $r = a$):

$$\delta\psi_a = \frac{B_0}{R_0}\left(\frac{n}{m} - \frac{1}{q_a}\right) a\,\xi_a \tag{87}$$

Let us now consider $\boldsymbol{\nabla} \times \boldsymbol{\delta\hat{B}} = 0$ (no currents in the vacuum), which in the ϕ direction gives

$$\frac{1}{r}\frac{\partial}{\partial r}(r\,\delta B_\theta) - \frac{1}{r}\frac{\partial\,\delta B_r}{\partial\theta} = 0$$

So, that, $\delta\psi$ satisfies Laplace's equation

$$\frac{1}{r}\frac{d}{dr}\left(r\frac{d\delta\psi}{dr}\right) - \frac{m^2}{r^2}\delta\psi = 0, \tag{88}$$

which has solution

$$\delta\psi = \alpha r^m + \beta r^{-m} \tag{89}$$

Now substituting the BC at $r = a$ given by Eq. (87), and the BC $\delta\psi_b = 0$ at $r = b$ ($\delta B_r = 0$ at b as defined in Eq. (65)), eventually gives

$$\delta\psi = \frac{B_0}{R_0}\left(\frac{n}{m} - \frac{1}{q_a}\right)\frac{\left(\frac{r}{b}\right)^m - \left(\frac{b}{r}\right)^m}{\left(\frac{a}{b}\right)^m - \left(\frac{b}{a}\right)^m}\,\xi_a$$

Now returning to δW_V, and inserting Eq. (86), and integrating by parts,

$$\delta W_V = 2\pi^2 R_0\left\{\int_a^b dr\,r\left[\frac{m^2}{r^2}\delta\psi^2 - \delta\psi\frac{1}{r}\frac{d}{dr}\left(r\frac{d\delta\psi}{dr}\right)\right] + \left(r\delta\psi\frac{d\delta\psi}{dr}\right)\Bigg|_a^b\right\}.$$

External Kink Modes

The first term is zero due to Laplace's equation (Eq. (88)), and inserting Eq. (89) into the second term we have simply

$$\delta W_V = \frac{2\pi^2 B_0^2}{R_0} m\lambda a^2 \xi_{r0}(a)^2 \left(\frac{n}{m} - \frac{1}{q_a}\right)^2, \quad \text{with} \quad \lambda = \frac{1+(a/b)^{2m}}{1-(a/b)^{2m}}$$

which, combining with Eq. (81) we have the total contribution including the internal plasma, the plasma-vacuum interface, and the vacuum terms:

$$\begin{aligned}\delta W_2 \quad = \quad & \frac{2\pi^2 B_0^2}{\mu_0 R_0} \left\{ \int_0^a dr\, r \left[\left(r\frac{d\xi_{r0}}{dr}\right)^2 + \left(m^2 - 1\right)^2 \xi_{r0}^2 \right] \left(\frac{n}{m} - \frac{1}{q}\right)^2 + \right. \\ & \left. a^2 \xi_{r0}(a)^2 \left[\frac{2}{q_a}\left(\frac{n}{m} - \frac{1}{q_a}\right) + (1+m\lambda)\left(\frac{n}{m} - \frac{1}{q_a}\right)^2 \right] \right\}, \end{aligned} \qquad (90)$$

where the most unstable mode is determined by the minimised δW in the plasma region, i.e. by Eq (82), which can be written in the convenient form

$$r^2 \frac{d^2\xi_{r0}}{dr^2} + r\frac{d\xi_{r0}}{dr}\left[3 - \frac{2s(r)}{1 - \frac{nq(r)}{m}}\right] - (m^2 - 1)\xi_{r0} = 0. \qquad (91)$$

The procedure is insert the solution of Eq. (91) back into Eq. (90), and then determine the magnitude of the corresponding first term in δW_2, which is a measure of field line bending stabilisation intergrated over the plasma volume. We will therefore determine whether this gross field line bending stabilisation is sufficient to compensate destabilising effects resulting from the external region. It is clear that the external contribution (the second term in Eq. (90) is destabilising for $q_a < m/n$, i.e. it is unstable, when the the rational $q = m/n$ is not inside the plasma region.

External Kink Modes

We will see that, strongest instability occurs when q_a is very close to, but less than m/n. Under these conditions field line bending stabilisation at the edge of the plasma region is almost zero. This effect is worsened if the shear over the plasma volume is small (measured by $q_a/q_0 = 1 + \nu$ in Wesson diagram), because this will enhance the volume over which $\delta B_\perp^2$ (in the plasma region) is small. These comments essentially explain Wesson's famous external kink stability diagram.

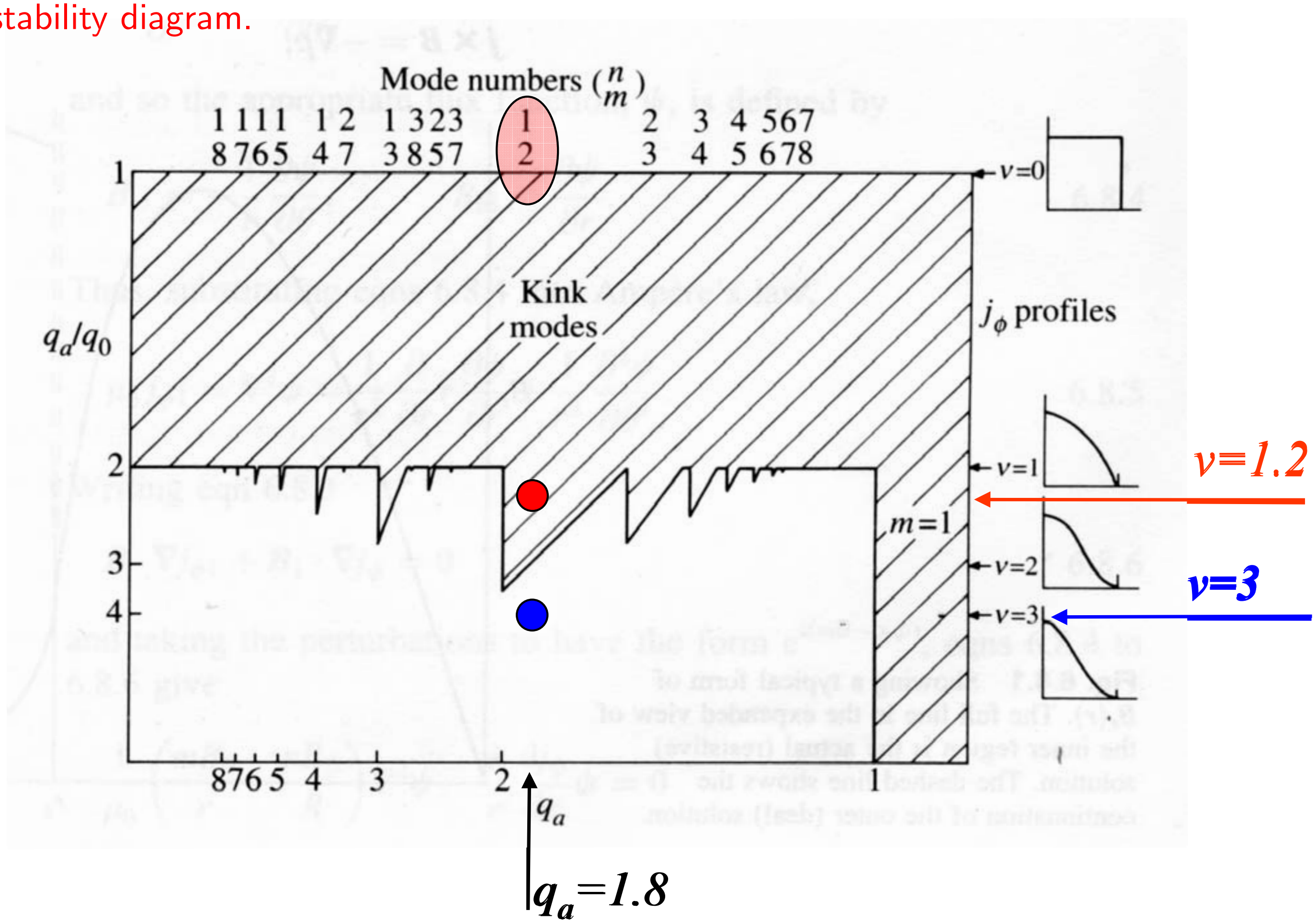

We investigate the red dot (unstable), and the blue dot (stable). Figure from Wesson, Tokamaks

Example: $n = 1$, $m = 2$ external kink stability with two different equilibria

We see that Wesson's diagram is in terms of
(1) mode numbers m and n
(2) Edge value of safety factor q_a
(3) Peakedness of the current profile (ν or q_a/q_0).

Let us examine the most obvious and unstable (except for $m = n = 1$ external kink requiring $q_a < 1$) which is $m = 2$ and $n = 1$. As we have mentioned, instability requires $q_a < m/n$ Choose $q_a = 1.8$. Finally, examine, numerically, two cases from the stability diagram $\nu = 1.2$ (unstable) and $\nu = 3$ (stable).

Wesson's current profile iso of the form $J = J_0[1-(r/a)^2]^\nu$, which, from Eq. (80) is

$$q = \frac{R_0}{B_0}\frac{1}{r^2}\int_0^r dr\, r\mu_0 J_\phi = \frac{q_0(1+\nu)(r/a)^2}{1-[1-(r/a)2]^{1+\nu}},$$

and from this it is seen that

$$\frac{q_a}{q_0} = 1+\nu \quad \text{and} \quad q = \frac{q_a(r/a)^2}{1-[1-(r/a)^2]^{1+\nu}}.$$

We then insert the chosen values for ν, q_a and m and n and solve for the most unstable mode in the plasma region (solve Eq. 91). Then substitute the solution for $\xi_{r0}(r)/\xi_{r0}(a)$ into δW_2 (Eq. 90) and evaluate the stabilising plasma contribution, and the destabilising external contributions (choose also $b/a \to \infty$)

$$\delta\hat{W}_2 = \frac{\mu_0 R_0 \delta W_2}{2\pi^2 a^2 \xi_{r0}(a)^2 B_0^2} = \frac{1}{a^2}\int_0^a dr\, r\left[\left\{r\frac{d}{dr}\left(\frac{\xi_{r0}(r)}{\xi_{r0}(a)}\right)\right\}^2 + \left(m^2-1\right)^2\left(\frac{\xi_{r0}(r)}{\xi_{r0}(a)}\right)^2\right]\left(\frac{n}{m}-\frac{1}{q}\right)^2 + (1+m\lambda)\left[\frac{2}{q_a}\left(\frac{n}{m}-\frac{1}{q_a}\right)+\left(\frac{n}{m}-\frac{1}{q_a}\right)^2\right]. \qquad (92)$$

Example $n = 1$, $m = 2$ External Kink Mode

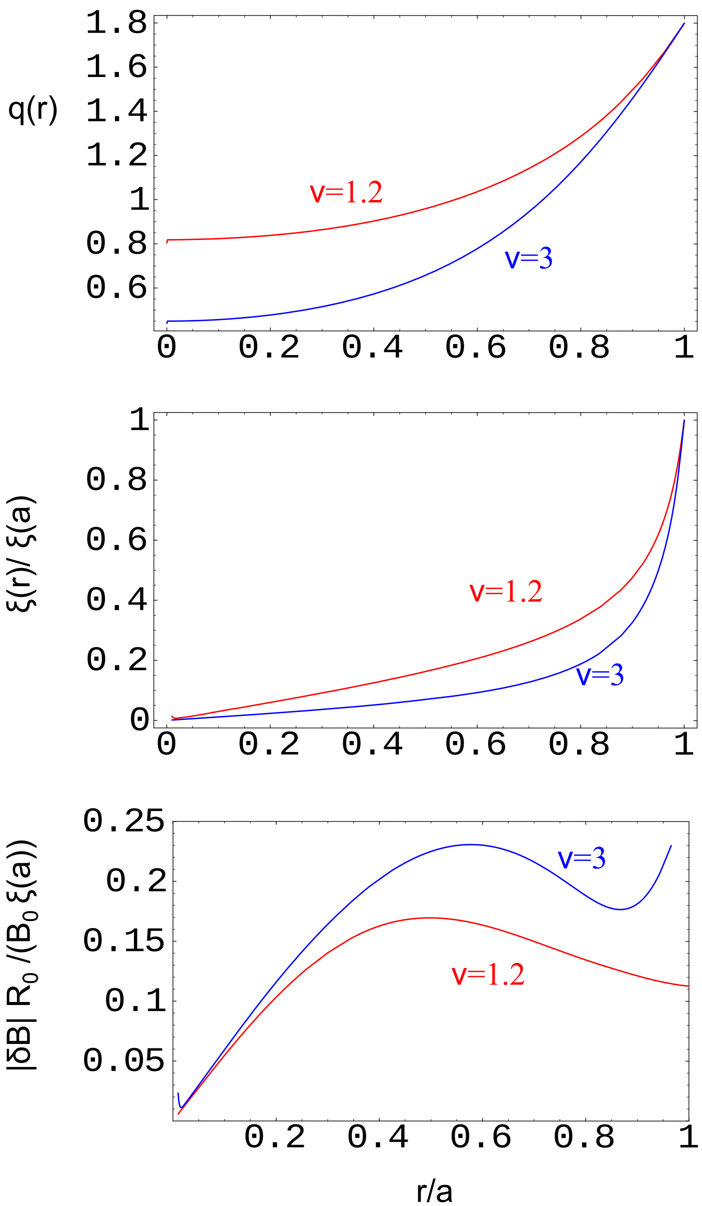

For $\nu = 3$, the enhanced global magnetic shear (q_a/q_0) leads to enhanced field line bending stabilisation $|\delta B_\perp|$.

$\nu = 1.2$: we have $\delta\hat{W}_2(plasma) = 0.0447$ and $\delta\hat{W}_2(external) = -0.0516461$. Hence $\delta W_2 < 0$.

$\nu = 3$: we have $\delta\hat{W}_2(plasma) = 0.059671$ and $\delta\hat{W}_2(external) = -0.0516461$. Hence $\delta W_2 > 0$.

It is straightforward to evaluate the perturbed radial magnetic field in both regions

$$\frac{\delta B_r R_0}{B_0 \xi_{r0}(a)} = \begin{cases} \left(n - \frac{m}{q(r)}\right) \frac{\xi_{r0}(r)}{\xi_{r0}(a)} & \text{for } r \leq a \\ \left(n - \frac{m}{qa}\right) \frac{\left(\frac{r}{b}\right)^m - \left(\frac{b}{r}\right)^m}{\left(\frac{a}{b}\right)^m - \left(\frac{b}{a}\right)^m} & \text{for } a \leq r \leq b. \end{cases}$$

and $\delta B_\theta = m^{-1} (r\delta B_r)'$

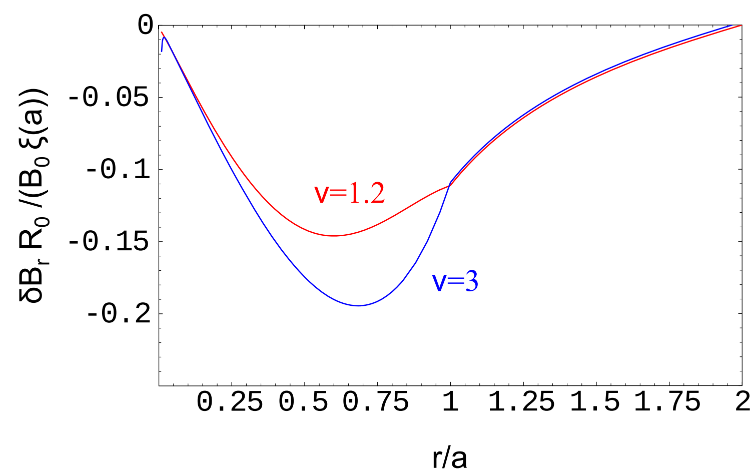

Example $n = 1$, $m = 2$ External Kink Mode

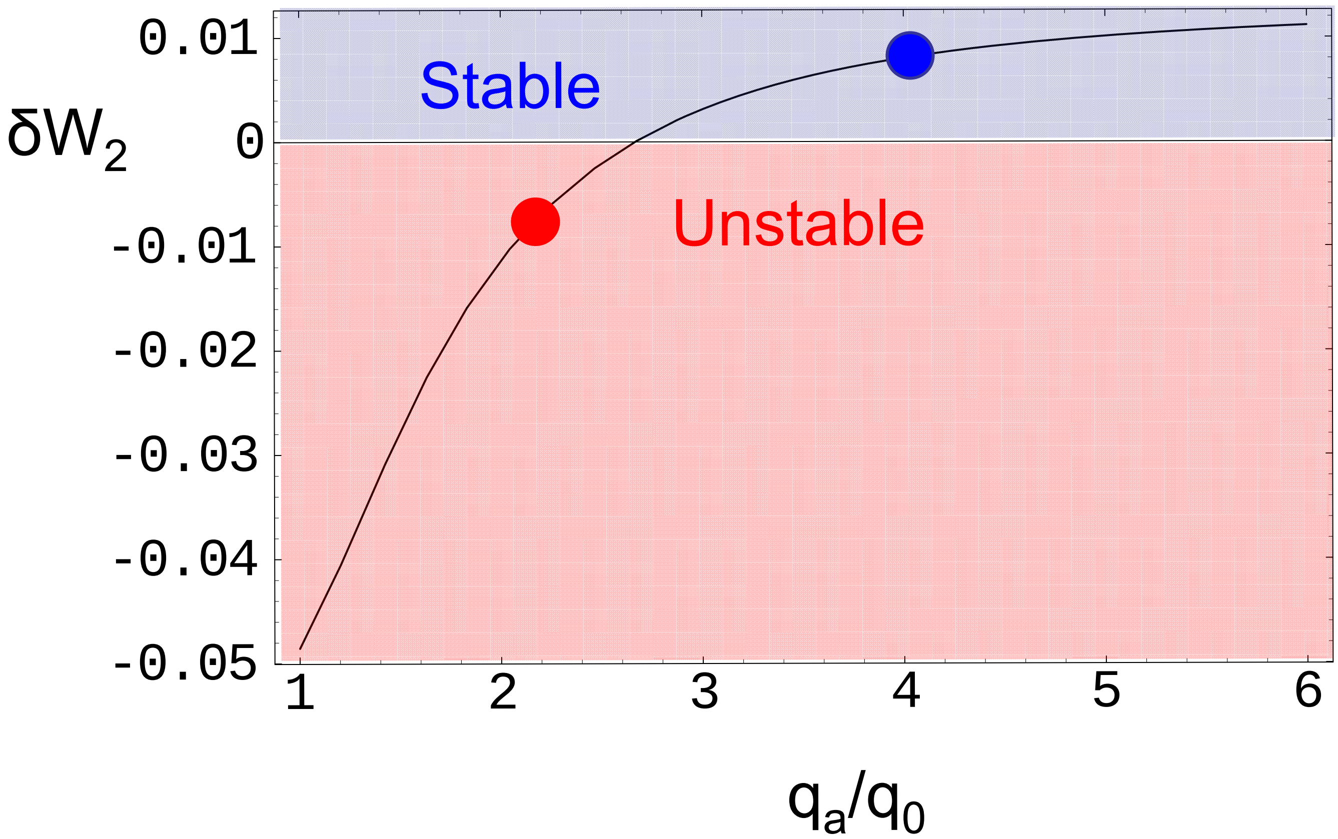

Introduction to Inertia and Resistivity

It has been shown that large scale purely ideal modes, with $m \neq 1$ are stable for a rational surface that is inside the plasma region (not external kink).

However, it has also been mentioned that in the region where magnetic field line bending is nullified, the ideal euler equation for the plasma displacement, i.e. Eq. (82), is singular. This means that more physics is needed in the region of $q = m/n$, and without this physics, the stability analysis cannot be relied on.

The new physics comes in two forms, those of plasma inertia and resistivity. We note that inertia can be small, indeed vanishing small if sufficiently close to stability boundary (recall that $\delta K = -(\omega^2/2)\int |\boldsymbol{\xi}| d^3x$ measures inertia), and moreover, resistive timescales (defined in a few pages) are very slow compared to ideal timescales. Nevertheless, in the region of the rational surface, the inertia and resistivity contains all the dynamics that remains.

It turns out that inertia in the absence of resistivity is sufficient to resolve the singularity. But, as evident from the derivation of the energy principle, ideal inertia alone does not affect the threshold for instability. For the case of the $m = n = 1$ internal kink mode, which we know can be ideal-unstable, the addition of inertia enables removal of the singularity at $q = 1$, and for the ideal growth rate to be established. However, $m \neq 1$ kink modes with rational surface inside the plasma will remain marginally stable unless resistivity is included.

The problem of finite inertia and resistivity is difficult. However, the problem becomes analytically tractable if the inertia and resistivity is treated only in the region where it has an impact, i.e. in a narrow region, known as the layer region around $q = m/n$.

Inertia and Resistivity

We start by defining the inertia $\delta K = -(\omega^2/2)\int |\boldsymbol{\xi}|^2 d^3x$. For simplicity, and since it is more accurate in collisionless plasmas, we define the perpendicular inertia, defined in Eq. (74) so that we can eventually recover the perpendicular momentum equation of Eq. (8). This we have

$$\delta K_\perp = -\frac{\omega^2}{2}\int d^3x\,\rho\left(|\xi_r|^2 + |\xi_\theta|^2\right),$$

(where $\rho = m_i n_i$ is the mass density) and then substitute Eq. (76), i.e. $\xi_{\theta 0} = (i/m)\partial\xi_{r0}/\partial r$ so that $|\xi_\theta|^2 = (1/m^2)(d|r\xi_{r0}|/dr)^2$, giving approximately,

$$\delta K_\perp = -2\pi^2\omega^2\int_0^a \rho dr\, r\left[|\xi_{r0}|^2\left(1+\frac{1}{m^2}\right) + \frac{2r|\xi_{r0}||\xi'_{r0}|}{m^2} + \frac{r^2}{m^2}|\xi'_{r0}|^2\right]$$

Defining the Alfven toroidal frequency

$$\omega_A = \frac{v_A}{R_0} \quad \text{with} \quad v_A = \left(\frac{B_0^2}{\rho\mu_0}\right)^{1/2} \tag{93}$$

then, $\delta K_\perp$ can be added to the first term of Eq. (81) for the ϵ^2 contribution to δW for internal plasma modes, to give (by integration by parts) the compact expression

$$\delta W_2 + \delta K_\perp = \frac{2\pi^2 B_0^2}{\mu_0 R_0}\int_0^a dr\, r\left[\left(r\frac{d\xi_{r0}}{dr}\right)^2 + \left(m^2-1\right)\xi_{r0}^2\right]\left[\left(\frac{n}{m}-\frac{1}{q}\right)^2 + \frac{1}{m^2}\left(\frac{\gamma}{\omega_A}\right)^2\right] \tag{94}$$

where for an unstable mode we have

$$\gamma^2 \equiv -\omega^2 > 0.$$

ÉCOLE POLYTECHNIQUE
FÉDÉRALE DE LAUSANNE

Inertia and Resistivity

We now attempt to obtain the eigenvalue equation for this system by minisation of the total energy (recall Eq. (63), By solving the Euler-Lagrange equations (Eq. 63)) by identification of the integrand I of Eq. (94). Now, taking ω_A to be constant, or at least slowly varying with r compared to the other radially dependent terms in Eq. (94), we have,

$$\frac{d}{dr}\left[r^3\frac{d\xi_{r0}}{dr}\left\{\left(\frac{n}{m}-\frac{1}{q}\right)^2+\frac{1}{m^2}\left(\frac{\gamma}{\omega_A}\right)^2\right\}\right]+(1-m^2)\left[\left(\frac{n}{m}-\frac{1}{q}\right)^2+\frac{1}{m^2}\left(\frac{\gamma}{\omega_A}\right)^2\right]r\xi_{r0}=0, \quad (95)$$

which generalises Eq. (82) in order to account for perpendicular inertia.

The above compact expression conforms to the momentum equation, and normal-mode equation, subject to the ideal MHD model and in particular ideal OHMs law. If we wish to include resistivity, it is convenient to re-arrange Eq. (95) to:

$$\left(\frac{\gamma}{\omega_A}\right)^2\left[\frac{d}{dr}(r^3\xi'_{r0})+r\xi_{r0}(1-m^2)\right]=-m^2\left\{\frac{d}{dr}\left[r^3\xi'_{r0}\left(\frac{n}{m}-\frac{1}{q}\right)^2\right]+r\xi_{r0}(1-m^2)\left(\frac{n}{m}-\frac{1}{q}\right)^2\right\}. \quad (96)$$

This equation is clearly in the form

$$\partial^2\boldsymbol{\xi}/\partial t^2=\rho^{-1}(\boldsymbol{\delta J}\times\boldsymbol{B}+\boldsymbol{J}\times\boldsymbol{\delta B}-\boldsymbol{\nabla}\delta P)$$

where, at this order, δP does not enter. The RHS of Eq. (96) has been written in terms of the fluid displacement through the use of ideal Ohms law. We can remove the restriction of Ohms law simply by inverting its employment, and writing the RHS of Eq. (96) in terms of δB_r via Eq. (79)

$$\delta B_{r0}=-\frac{imB_0}{R_0}\left(\frac{n}{m}-\frac{1}{q}\right)\xi_{r0}.$$

Inertia and Resistivity

Giving
$$\left(\frac{\gamma}{\omega_A}\right)^2 \left[\frac{d}{dr}\left(r^3\frac{d\xi_{r0}}{dr}\right) + r\xi_{r0}(1-m^2)\right] =$$
$$-im\frac{R_0}{B_0}\left\{r\left(\frac{n}{m}-\frac{1}{q}\right)\left(\frac{d}{dr}\left[r\frac{d}{dr}|r\,\delta B_r|\right] - m^2|\delta B_r|\right) + r^2|\delta B_r|\frac{R_0}{B_0}\frac{dJ_\phi}{dr}\right\} \qquad (97)$$

where it has been convenient to deploy (from Eq. (80)):

$$\frac{d}{dr}\left[r^3\frac{d}{dr}\left(\frac{1}{q}\right)\right] = r^2\frac{R_0}{B_0}\frac{dJ_\phi}{dr}.$$

The power of Eq. (97) is evident; it is an eigenvalue equation that obeys the equation of motion at lowest order in ξ and δB, but is not subject to the assumption of ideal Ohm's law. i.e. we can now attempt to model the affect of resistivity on internal modes. Nevertheless, in order to examine resistive modes, we require an equation relating ξ_r and δB_r, this time subject to resistive Ohm's law. Make progress by taking the curl of linearised Ohm's law $\boldsymbol{\delta E} + \boldsymbol{\delta u}\times\boldsymbol{B} = \eta\boldsymbol{J}$ and apply Amperes law on the right hand side,

$$-\frac{\partial\delta B}{\delta t} + \boldsymbol{\nabla}\times(\boldsymbol{\delta u}_\perp\times\boldsymbol{B}) = \frac{\eta}{\mu_0}\boldsymbol{\nabla}\times(\boldsymbol{\nabla}\times\boldsymbol{B})$$

Employing $\boldsymbol{\nabla}\times(\boldsymbol{\delta u}_\perp\times\boldsymbol{B}) = \boldsymbol{\delta u}_\perp(\boldsymbol{\nabla}\cdot\boldsymbol{B}) - \boldsymbol{B}(\boldsymbol{\nabla}\cdot\boldsymbol{\delta u}_\perp) + (\boldsymbol{B}\cdot\boldsymbol{\nabla})\boldsymbol{\delta u}_\perp - (\boldsymbol{\delta u}_\perp\cdot\boldsymbol{\nabla})\boldsymbol{B}$, and noting that $\boldsymbol{\nabla}\cdot\boldsymbol{B} = 0$ and, from Eq. (75) or (76) the leading order displacement, or velocity conforms to $\boldsymbol{\nabla}\cdot\boldsymbol{\delta u}_\perp = 0$, then choosing the radial component, and employing $\boldsymbol{\nabla}\times(\boldsymbol{\nabla}\times\boldsymbol{\delta B}) \equiv \boldsymbol{\nabla}(\boldsymbol{\nabla}\cdot\boldsymbol{\delta B}) - \boldsymbol{\nabla}^2\boldsymbol{\delta B}$ then

$$\delta B_r + \boldsymbol{B}\cdot\boldsymbol{\nabla}\delta u_r \approx -\frac{\eta}{\mu_0}\boldsymbol{\nabla}^2\delta B_r$$

Layer Theory: Inertia and Resistivity

Now employing the definition of perturbed flux, given in Eq. (86), and the identities given in that section of these notes, it is straightforward to show that

$$\left(\frac{\gamma}{\omega_A}\right)^2\left[\frac{d}{dr}\left(r^3\frac{d|\xi_{r0}|}{dr}\right)+r|\xi_{r0}|(1-m^2)\right]=$$

$$-m^2\frac{R_0}{B_0}\left\{r\left(\frac{n}{m}-\frac{1}{q}\right)\left(\frac{d}{dr}\left[r\frac{d}{dr}|\delta\psi|\right]-m^2|\delta\psi|\right)+r|\delta\psi|\frac{R_0}{B_0}\frac{dJ_\phi}{dr}\right\}\quad \text{with} \qquad (98)$$

$$\xi_{r0}=\frac{R_0}{B_0 r}\left(\frac{n}{m}-\frac{1}{q}\right)^{-1}\left[\delta\psi-\frac{r\eta}{\gamma\mu_0}\nabla^2\left(\frac{\delta\psi}{r}\right)\right], \qquad (99)$$

Equations (98) and (99) form a complete eigenvalue equation for $|\delta\psi|$ that is extremely complicated, at least if analytical solutions are sought. Fortunately, there is a means of making progress. Inertia, on the left hand side of Eq. (98) is only important very close to the rational surface, i.e where $q \approx m/n$. Assuming that growth rates are small, such that $\gamma/\omega_A \sim \epsilon^2$, then it is clear from Eqs. (98) and (99) that the inertial needs to be considered only when $|q-m/n| \sim \epsilon^2$ or less. In the outer region, where this is not the case, one simply solves Eq. (98) with the left hand side equal to zero,

$$r\frac{d}{dr}\left(r\frac{d\delta\psi}{dr}\right)+\left(\frac{R_0}{B_0}\right)\frac{rqm\delta\psi}{nq-m}\frac{dJ_\phi}{dr}-m^2\delta\psi=0. \qquad (100)$$

This equation is identical to Eq. (82) for the displacement ξ_{r0}. But, in Eq. (100) for the flux, or perturbed radial field, it is directly seen that ignoring the inertia in the region of the rational surface leads to an un-physical singularity, thus confirming that both Eq. (82) and Eq. (100) are only valid in the outer region.

Layer Theory: Inertia and Resistivity

Equation (100) is solved for a particular m, n and $J_\phi(r)$ etc from the inner boundary $r = 0$, with BC's $\delta\psi(r = 0) = 0$ and $\delta\psi'(r = 0) = C_1$, and separately from an outer boundary, e.g. $r = a$ with BC's $\delta\psi(r = a) = 0$ and $\delta\psi'(r = a) = C_2$. In the first case, $\delta\psi$ is solved from $r = 0$ up to just within the rational surface $r_s - \delta$, while in the second case, $\delta\psi$ is solved from $r = a$ up to just on the other side of the rational surface $r_s + \delta$. We are permitted to assume an infinitely thin inner region, so that C_1 and C_2 are chosen such that $\delta\psi(r_s - \delta) = \delta\psi(r_s + \delta)$. But the two outer solutions approach r_s differently, such that $\delta\psi'(r_s - \delta) \neq \delta\psi'(r_s + \delta)$. The role of the inner region is to resolve this singularity. Thus we define

$$\Delta' = \left.\frac{\delta\psi'}{\delta\psi}\right|_{r_s-\delta}^{r_s+\delta} \qquad \delta \to 0 \qquad (101)$$

for the outer region, and this is matched to the corresponding quantity evaluated in the inner region.

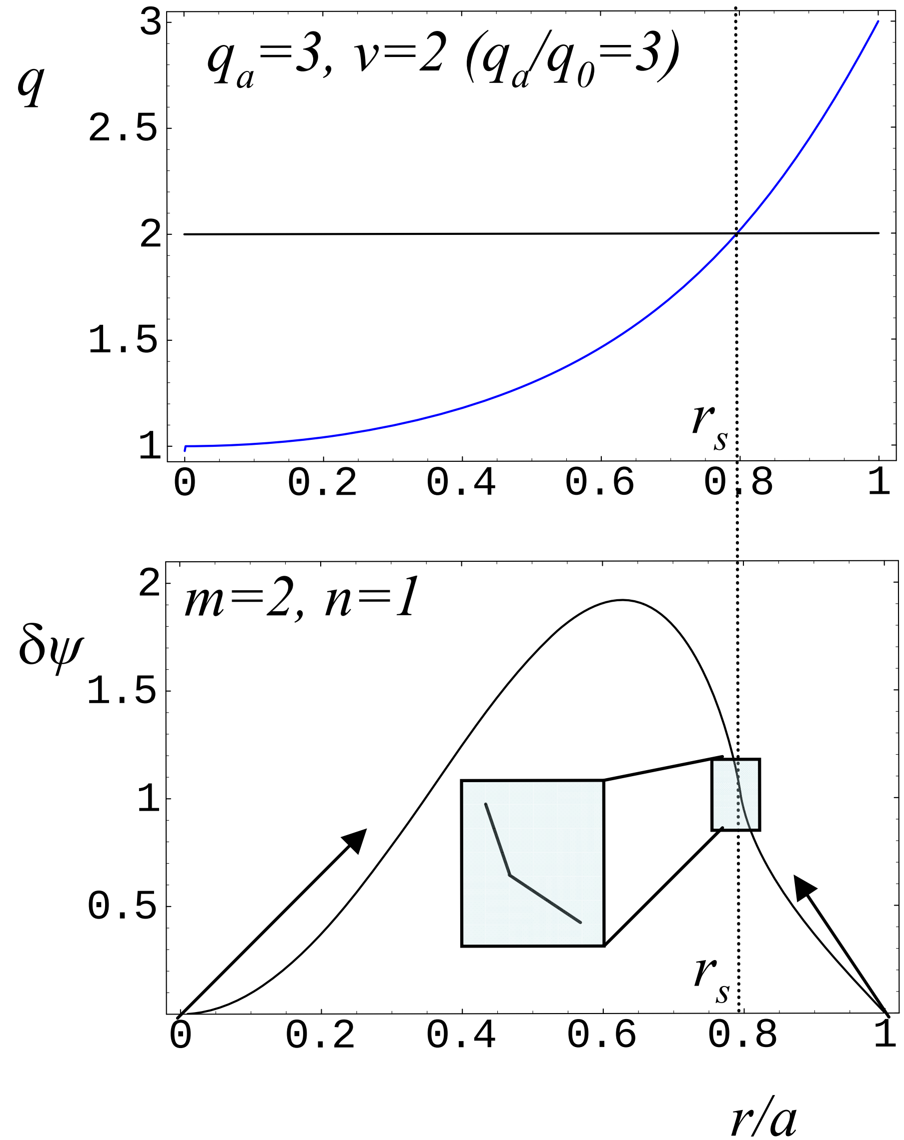

Layer Theory: Inertia and Resistivity

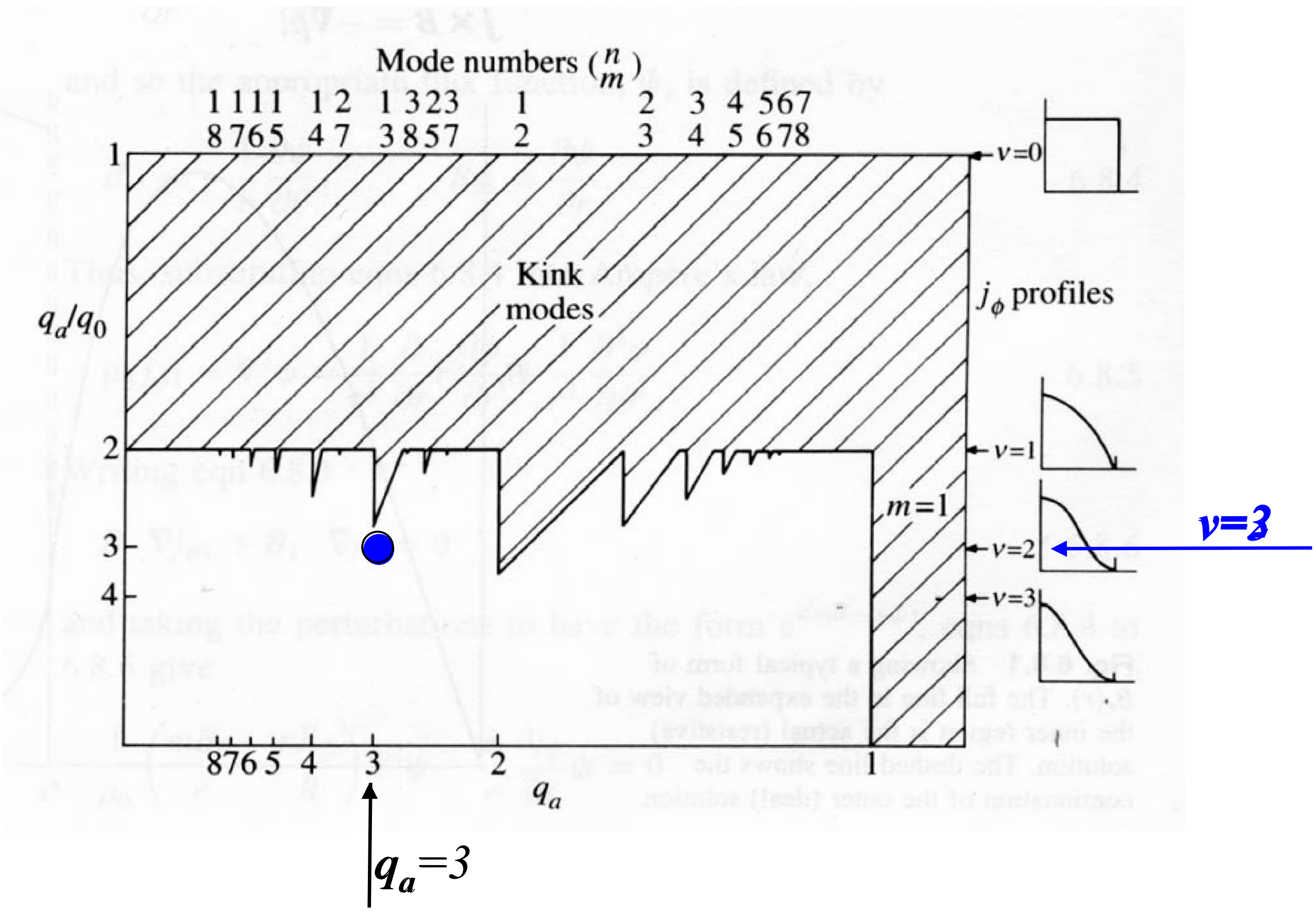

This case is stable to Ideal External Kink modes (even m=3, n=1 mode).
We can investigate stability of Internal Resistive Tearing Mode (n=1, m=2). It is UNSTABLE .

Layer Theory: Tearing Modes

We can define Δ' in the layer directly from Eq.(99), upon re-organisation, and noting that radial derivatives of $\delta\psi$ and ξ_r dominate all other derivatives in all other quantities in the resonance region (e.g. $\nabla^2(\delta\psi/r) \approx r^{-1}\partial^2\delta\psi/\partial r^2$) so that

$$\frac{d^2|\delta\psi|}{dr^2} = \frac{\gamma\mu_0}{\eta}\left[\delta\psi - |\xi_{r0}|\frac{rB_0}{R_0}\left(\frac{n}{m} - \frac{1}{q}\right)\right] \tag{102}$$

Integrating gives

$$\frac{d|\delta\psi|}{dr} = \int dr\,\delta\psi\frac{\gamma\mu_0}{\eta}\left[1 - \frac{\xi_{r0}}{\delta\psi}\left(\frac{rB_0}{R_0}\right)\left(\frac{n}{m} - \frac{1}{q}\right)\right]$$

As we have seen, $\delta\psi$ is approximately constant over the thin layer (but its derivatives are not, and moreover neither is $\xi_r 0$), so that we may obtain a quantity in the form of Δ':

$$\frac{\delta\psi'}{\delta\psi} = \int dr\,\frac{\gamma\mu_0}{\eta}\left[1 - \frac{\xi_{r0}}{\delta\psi}\left(\frac{rB_0}{R_0}\right)\left(\frac{n}{m} - \frac{1}{q}\right)\right].$$

where the modulus has been dropped. We now expand around the rational surface, $q = (m/n)[1 + q'(r_s)(r - r_s)/q(r_s)]$ so that

$$\frac{n}{m} - \frac{1}{q} \approx \frac{n}{m}s(r_s)x \quad \text{with} \quad x = \frac{r - r_s}{r_s} \quad \text{and} \quad s = \frac{r}{q}\frac{dq}{dr}, \quad \text{giving}$$

$$\frac{\delta\psi'}{\delta\psi} = \int dx\,r_s\frac{\gamma\mu_0}{\eta}\left[1 - \frac{\xi_{r0}}{\delta\psi}\left(\frac{rB_0}{R_0}\right)\frac{n}{m}s(r_s)x\right]. \tag{103}$$

It now remains to obtain $\xi_{r0}/\delta\psi$, and this is done by solving Eq. (98) in the layer region, where, of course, inertia must be included (the LHS of Eq. (98) non-zero).

Layer Theory: Tearing Modes

Due to the large radial derivatives in $\delta\psi$ and ξ_{r0} in the inertial region, we keep only the terms in Eq. (98) with largest order derivatives. Also need to keep the $\delta\psi J_\phi$ term because is also competes because it is not proportional to $1/q - n/m$. Therefore, in the layer we have,

$$\left(\frac{\gamma}{\omega_A}\right)^2 r^3 \frac{d^2\xi_{r0}}{dr^2} = -m^2 \frac{R_0}{B_0}\left\{r^2\left(\frac{n}{m}-\frac{1}{q}\right)\frac{d^2\delta\psi}{dr^2} + r\delta\psi\frac{R_0}{B_0}\frac{dJ_\phi}{dr}\right\} \tag{104}$$

We now, substitute Eq. (102) for $\delta\psi''$, and expanding once again around the rational surface, we have

$$\frac{d^2\xi_{r0}}{dx^2} = -\left(\frac{\gamma}{\omega_A}\right)^{-2} m^2 \frac{R_0}{r_s B_0}\left\{\frac{n}{m}s(r_s)x\frac{r_s^2\gamma\mu_0}{\eta}\left[\delta\psi - |\xi_{r0}|\frac{r_s B_0}{R_0}\frac{n}{m}s(r_s)x\right] + \delta\psi\frac{R_0}{B_0}\frac{dJ_\phi}{dx}\right\}$$

Now, let,

$$z = xd \quad \text{with} \quad d = \left(\frac{\omega_A^2 n^2 r_s^2 s^2 \mu_0}{\eta\gamma}\right)^{1/4}$$

to give

$$\left(\frac{d^2\xi_{r0}}{dz^2} - z^2\xi_{r0}\right)\left(\frac{d^2 B_0\eta\gamma}{\omega_A^2 nmR_0 r_s s\mu_0}\right) = -\frac{z\delta\psi}{d} - \delta\psi J'_\phi\frac{R_0\eta}{\mu_0 B_0\gamma r_s^2}$$

Again, assuming that $\delta\psi$ can be taken as a constant, we have

$$\frac{d^2y}{dz^2} - z^2 y = -z - J'_\phi\frac{R_0\eta d}{\mu_0 B_0\gamma r_s^2} \quad \text{with} \quad y = \frac{d^3 B_0\eta\gamma}{\omega_A^2 nmR_0 r_s s\mu_0}\left(\frac{\xi_{r0}}{\delta\psi}\right). \tag{105}$$

Now, the inhomogeneity on the RHS of the differential equation (for $y(z)$) comprises the sum of odd and even contributions in z. As a consequence, the solution $y(z)$ comprises the corresponding sum in odd and even contributions in z. It is clear that the even component of y vanishes in the integral of Eq. (103), when integrated with respect to dz across the rational surface, so for this reason, we are permitted to drop the even term proportional to J'_ϕ, and thus we solve $d^2y/dz^2 = -z(1-zy)$.

Layer Theory: Tearing Modes

Now Rutherford and Furth, 1971, showed that

$$y = \frac{z}{2}\int_0^1 d\mu \frac{\exp(-z^2\mu/2)}{(1-\mu^2)^{1/4}} \quad \text{satisfies} \quad \frac{d^2y}{dz^2} = -z(1-zy) \tag{106}$$

which can easily be verified by substitution. One now substitutes this solution (odd in z) into Eq. (103), which can be written in terms of y and z as follows:

$$\frac{\delta\psi'}{\delta\psi} = \int_{-\infty}^{\infty} dz \frac{r_s}{d}\frac{\gamma\mu_0}{\eta}\left[1 - \frac{\xi_{r0}}{\delta\psi}\left(\frac{r_sB_0}{R_0}\right)\frac{n}{m}s(r_s)\frac{z}{d}\right],$$

where the limits of integration can be taken as infinite on the scale of the layer (wrt dz), and the asymptotic behaviour of the integrand will be checked a posteriori. Substituting for $\xi_{r0}/\delta\psi$ in terms of y, as defined in Eq. (105) gives the compact expression

$$\frac{\delta\psi'}{\delta\psi} = \frac{\gamma\tau_R}{dr_s}\int_{-\infty}^{\infty} dz(1-yz) \quad \text{where} \quad \tau_R = \frac{\mu_0 r_s^2}{\eta},$$

where it is now clearly seen that it was legitimate to drop the even z component of y. In the above τ_R is the 'resistive time'. Moreover, it is convenient to define d in terms of the ratio of the resistive time and the Alfven time:

$$S = \frac{\tau_R}{\tau_A} \equiv \tau_R\omega_A \quad \sim 10^8 \quad \text{in large tokamaks}$$

Giving d^4 proportional to the products of the ratios of mode timescale $(1/\gamma)$ and the Alfven time, and the resistive time and the Alfven time:

$$d^4 = n^2s^2S\frac{\omega_A}{\gamma}$$

Layer Theory: Tearing Modes

Since $\Delta' = \delta\psi'/\delta\psi$, where we match with Eq. (101), we have

$$r_s\Delta' = \frac{\gamma\tau_R}{d}\int_{-\infty}^{\infty} dz\left[1 - \frac{z^2}{2}\int_0^1 d\mu\frac{\exp(-z^2\mu/2)}{(1-\mu^2)^{1/4}}\right] = \frac{\gamma\tau_R}{d}\left(\frac{\pi\Gamma(3/4)}{\Gamma(1/4)}\right)$$

So, that, inserting d and using the definition of S , we have

$$r_s\Delta'(r_s) = \left(\frac{\pi\Gamma(3/4)}{\Gamma(1/4)}\right)\frac{(\gamma/\omega_A)^{5/4}S^{3/4}}{(ns)^{1/2}},$$

which rearranges to give the growth rate

$$\frac{\gamma}{\omega_A} = \left[\frac{\Gamma(1/4)r_s\Delta'(r_s)}{\pi\Gamma(3/4)}\right]^{4/5} S^{-3/5}(ns)^{2/5}. \tag{107}$$

We recall that $r_s\Delta'(r_s)$ is obtained by solving Eqs. (101) and (100) in the outer region. Thus, the instability requires that $\Delta' > 0$, and this condition in turn is governed by the current profile. For the case shown in the figure (page 91-92), we have $r_s\Delta'(r_s) = 4.25058$, i.e. the mode is unstable. Taking $S = 10^8$, this gives $\gamma/\omega_A \sim 10^{-5}$, which is a slow growth rate compared to ideal growth rates (typically $\gamma/\omega_A \sim 10^{-2}$).

Two important things should be noted before concluding this section. (1) There is analytic continuation between the stability boundary of external kink mode and the tearing mode. Clearly the transition occurs as r_s (where $q(r_s) = m/n$) goes through the plasma-vacuum interface. Both modes are driven by J_ϕ'. (2) There are very important non-linear corrections, and thus the growth rates derived here are of limited importance. However, the stability boundary, defined by the sign of Δ' remains of primary importance. The Δ' remains a fundamental parameter for non-linear tearing modes (often neo-classical tearing modes).

Layer Theory: Inertia and Resistivity

$\Delta'<0$ (stable - no asymptotic solution in layer with $\gamma>0$ OR $\gamma=0$

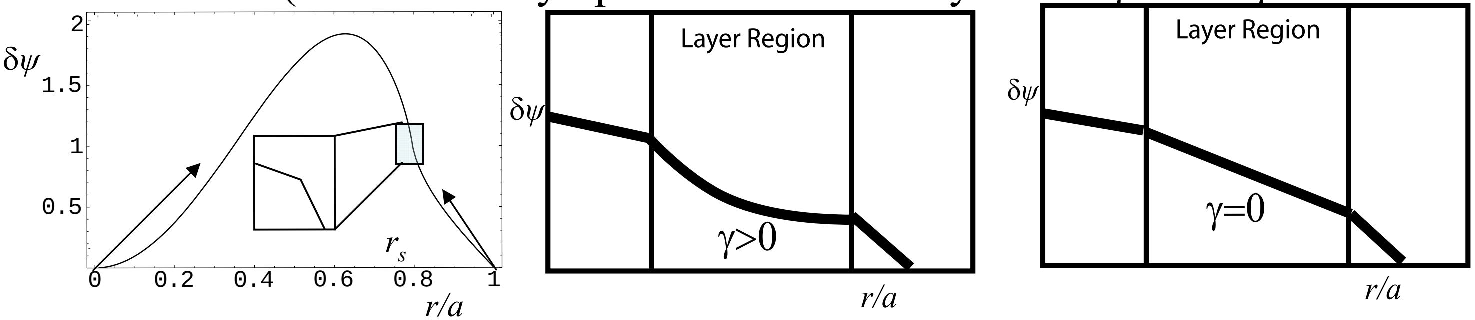

$\Delta'=0$ (marginally stable - asymptotic solution found for $\gamma=0$

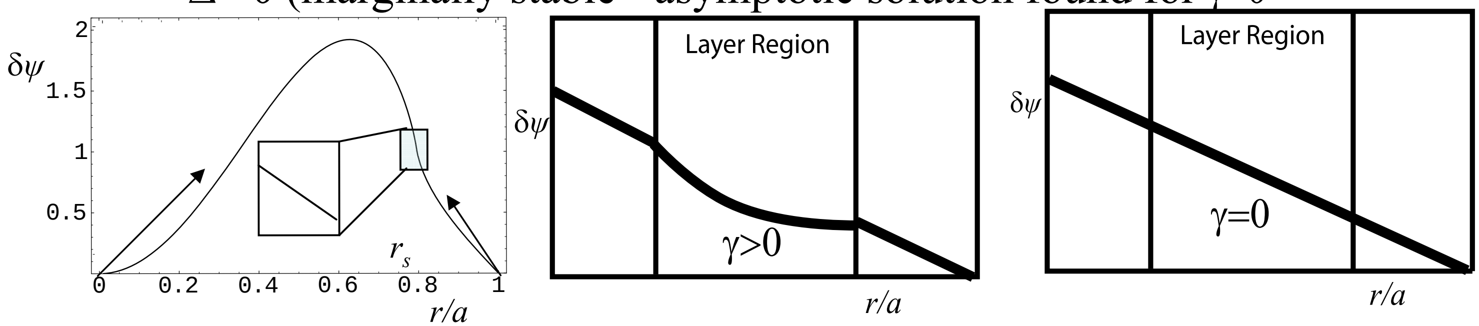

$\Delta'>0$ (unstable - asymptotic solution in layer with $\gamma>0$

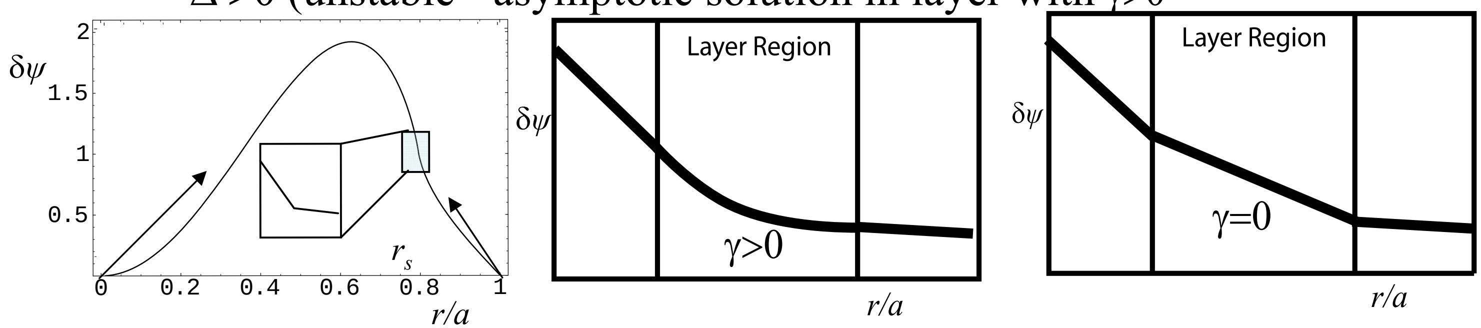

OBJECTIVE: FIND DEPENDENCY OF γ ON Δ' AND RESISTIVITY

- Week 1: Derivation and limitations of the MHD model. Conservation of Flux, The Grad-Shafranov Equation. Coordinate systems in tokamak equilibrium.
- Week 2: Tokamak equilibrium. Analytical expansions. Shafranov Shift. Shaping, and shaping penetration into the torus.
- Week 3: Linearised ideal MHD stability, energy principle, stability boundaries, ideal internal kink mode
- Week 4: External Kink modes, linear tearing modes
- week 5: Ideal singular layer calculations, magnetic islands, non-linear resistive MHD, NTMs
- Week 6: Toroidal effects: Interchange stability (Mercier) and ballooning.
- Week 7: Ballooning continued. Introduction to kinetic MHD and long mean free path parallel dynamics.

ÉCOLE POLYTECHNIQUE
FÉDÉRALE DE LAUSANNE

Layer Theory: Ideal Internal Kink Mode

Once again, as with the tearing mode, inertia is only important in the region close to the rational surface. Inclusion of a calculation in the 'internal region' enables the ideal growth rate to be obtained. If this calculation is subject to ideal MHD, the stability boundary will not be affected. Unlike the $m > 1$ tearing mode, the drive for the ideal internal kink mode instability occurs in the external (inertia free region). Clearly, for the $m > 1$ tearing mode, the external region was stabilising, and the only drive that remained was from the effect of resistivity in the inertial region. Since an ideal MHD drive exists for the internal kink mode, it is legitimate to treat the internal region as ideal, though resistive corrections are crucial near the ideal stability boundary (where the external drive $\delta W^e \approx 0$). The external drive for the ideal internal kink mode has been calculated, and was written down in Eq. (84) in the form of the potential energy associated with the external region

$$\delta W^e = (2\pi^2 R_0 B_0^2 \xi_{r0}^2 \varepsilon^4/\mu_0)\delta\hat{W}^T,$$

and the leading order radial eigenfunction was also obtained in this external region

$$\xi_{r0}^e = \begin{cases} \xi_0 \, e^{i(\theta-\phi-\omega t)} & \text{for } r \lesssim r_1 - \delta, \\ 0 & \text{for } r \gtrsim r_1 + \delta \end{cases} \tag{108}$$

It remains to calculate the displacement ξ_{r0}^s in the internal, or singular, region $r_1 - \delta < r < r_1 + \delta$, and the corresponding total energy

$$D^s = \delta K^s + \delta W^s$$

We recall from Eq. (60) that the total energy should be zero. Since the inertia in the external region is negligible, we have the important dispersion relation

$$\delta K_\perp^s + \delta W^s + \delta W^e = 0. \tag{109}$$

For the total energy and ideal displacement in the singular region, we can refer to Eqs. (94) and (95), which for $n = m = 1$, and in terms of the layer variable $x = (r - r_1)/r_1$, and expanding in $1 - 1/q = s_1 x$, and taking $r d\xi_{r0}/dr \gg \xi_{r0}$ in the layer gives:

Layer Theory: Ideal Internal Kink Mode

$$\delta W^s + \delta K_\perp^s = \frac{2\pi^2 R_0 B_0^2}{\mu_0}\epsilon_1^2 s_1^2 \int_{-\infty}^{\infty} dx \left[x^2 + \left(\frac{\gamma}{s_1\omega_A}\right)^2\right]\left(\frac{d\hat{\xi}_r^s}{dx}\right)^2 \tag{110}$$

where the integration limits are appropriate because an asymptotic match between the singular and external regions are being sought. Furthermore, from Eq. (95),

$$\frac{d}{dx}\left[\left\{\left(\frac{\gamma}{s_1\omega_A}\right)^2 + x^2\right\}\left(\frac{d\hat{\xi}_r^s}{dx}\right)\right] = 0, \tag{111}$$

giving by integration

$$\frac{d\hat{\xi}_r^s}{dx} = \frac{C}{x^2 + \left(\frac{\gamma}{s_1\omega_A}\right)^2}. \tag{112}$$

Integrating Eq. (112) with respect to x and substituting the external solutions of Eq. (108) yields the constant of integration to give

$$\frac{d\hat{\xi}_r^s}{dx} = -\frac{\xi_0}{\pi}\left(\frac{\gamma}{\omega_A s_1}\right)\frac{1}{x^2 + \left(\frac{\gamma}{\omega_A s_1}\right)^2}, \tag{113}$$

and straightforward integration of Eq. (113) gives,

$$\hat{\xi}_r^s = \frac{\xi_0}{2}\left[1 - \frac{2}{\pi}\arctan\left(x\frac{\omega_A s_1}{\gamma}\right)\right].$$

Layer Theory: Ideal Internal Kink Mode

Substituting Eq. (113) into Eq. (112) yields

$$\delta W^s + \delta K_\perp^s = 4R_0\epsilon_1^2 s_1^2 \frac{B_0^2}{\mu_0}\xi_0^2 \left(\frac{\gamma_I}{s_1\omega_A}\right)^2 \int_0^\infty \frac{dx}{x^2 + \left(\frac{\gamma_I}{s_1\omega_A}\right)^2} = 2\pi R_0 \epsilon_1^2 s_1 \frac{B_0^2}{\mu_0}\xi_0^2 \frac{\gamma_I}{\omega_A}. \qquad (114)$$

Hence, substituting this into the dispersion relation of Eq. (109), and identifying $\delta W^e = (2\pi^2 R_0 B_0^2 \xi_{r0}^2 \varepsilon^4/\mu_0)\delta\hat{W}^T$, with the normalisation defined in Eq. (84), obtains

$$\frac{\gamma_I}{\omega_A} = -\varepsilon_1^2 \frac{\pi}{s_1}\delta\hat{W}^T. \qquad (115)$$

As mentioned earlier, it is seen that the relation

$$\omega^2 \approx \frac{\delta W_{min}}{K(\xi_{min})}.$$

completely breaks down. The minimisation of δW alone does correctly recover the stability threshold, but any information regarding ω^2 has to be obtained through variation of the total energy $\delta K + \delta W$, as has been done above.

Furthermore, if one wishes to include the effect of the parallel displacement, as required for the full ideal MHD model, one simply replaces γ with $\sqrt{1+2q_s^2}\gamma = \sqrt{3}\gamma$ in all the above (see problem at the end of lecture 3, and take $q=1$). Kinetic corrections create a strong modification to the Glasser - Greene - Johnson inertial enhancement. Graves, Hastie and Hopcraft were the first to do this [PPCF 2000], and the inertial enhancement turns out to be identical to the collisonless zonal flow factor $(1+1.6q^2\epsilon^{-1/2})$, such that $\gamma \rightarrow 1+1.6\epsilon^{-1/2}\gamma$.

Layer Theory: Ideal Internal Kink Mode

To leading order, the perpendicular eigenfunction is incompressible also in the singular layer ($\nabla \cdot \xi_\perp = 0$), such that

$$\xi_\theta = -\frac{i}{m}\left(\xi_r + r\frac{d\xi_r}{dr}\right)$$

The figure plots ξ_r^s as defined above (with $\xi_0 \exp(im\theta - in\phi - i\omega t) = 1$ and ξ_θ as defined above (with $i(\xi_0/m)\exp(im\theta - in\phi - i\omega t) = 1$) with $\gamma\tau_A = 0.025$, $r_1 = 0.3$ and $s_1 = 0.35$ all radial lengths are normalised to the plasma edge radius. Also plotted is a linear expansion of the radial eigenfunction around r_1, i.e.

$$\xi_r(fit) = (r - r_1)\frac{d\xi}{dr}\bigg|_{r_1} = \frac{1}{2} - \left(\frac{r - r_1}{r_1}\right)\frac{s_1}{\pi\gamma\tau_A}$$

A characterisation of the width of the poloidal displacement, δ, is the radial distance between the locations where $\xi_r(fit)$ intersects zero and unity, divided by two, as shown in the second figure below. One then obtains:

$$\delta = \frac{\pi r_1 \gamma\tau_A}{s_1}.$$

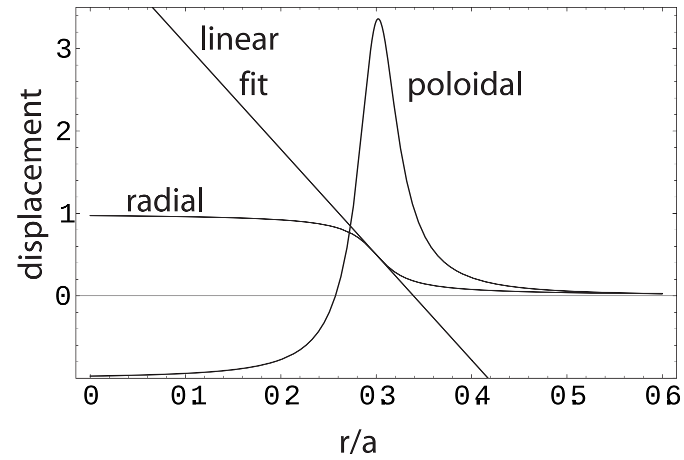

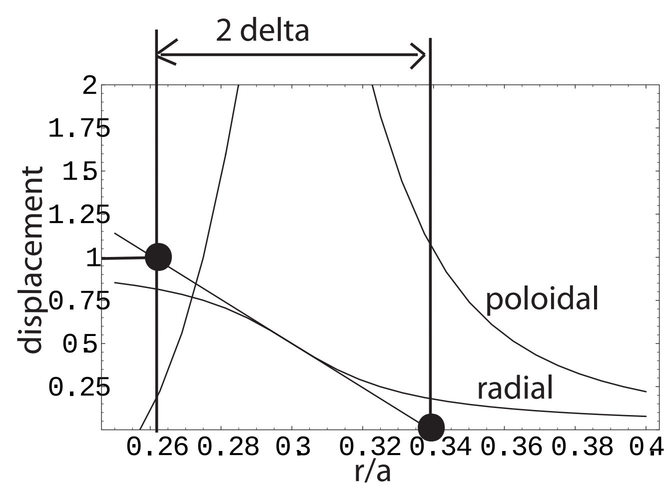

Magnetic Islands

Consider the parallel wave-number

$$k_{\parallel} = \frac{1}{R}(nq(r) - m)$$

We know that a rational surface occurs where $k_{\parallel} = 0$, i.e. at the location

$$q(r_s) \equiv q_s = m/n$$

We assume that the perturbations have the usual form $\exp(im\chi)$ where

$$\chi = \theta - \frac{n}{m}\phi = \theta - \frac{1}{q_s}\phi$$

It turns out that the angle χ is orthogonal to the magnetic field lines on the rational surface, and near orthogonal close to the rational.

Interpretation is made easier by assuming straight field line coordintates for which $q = q(r) = d\phi/d\theta$ so that a field line is described by

$$\phi = q\theta$$

This can be compared with the χ coordinate in ϕ - θ space, which is constant for

$$\phi = q_s\theta$$

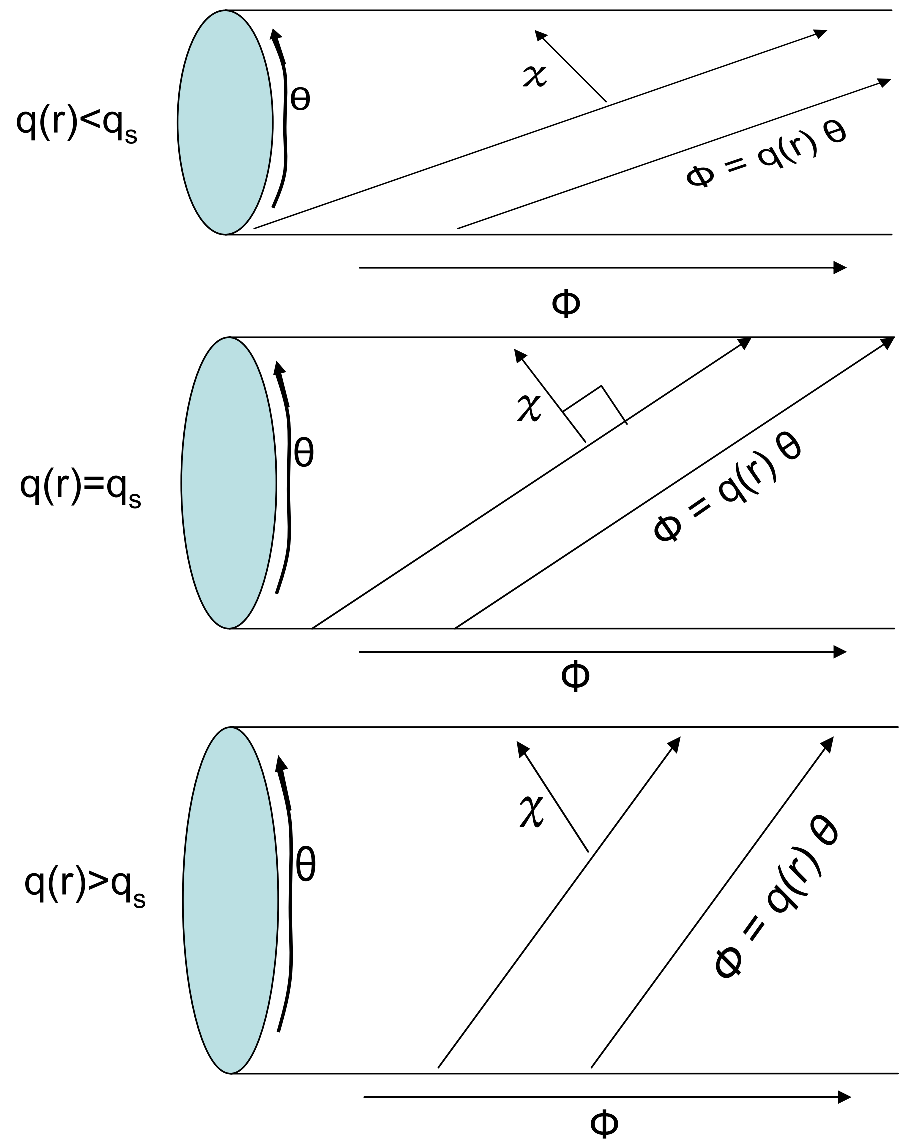

Consider now the fields in these coordinates. Now since $\boldsymbol{\nabla}\cdot\boldsymbol{B}=0$, and since $B_{\|}$ is small (it is a finite beta effect - see next chapter), and since $\partial/\partial l\ \propto k_{\|}$ (again small) then:

$$\boldsymbol{\nabla}\cdot\boldsymbol{B}_{\perp}\approx\frac{1}{r}\frac{\partial}{\partial r}(rB_r)+\frac{1}{r}\frac{\partial B_{\chi}}{\partial\chi}$$

These components of the magnetic field can then be written in terms of a flux Ψ (which comprises equilibrium and perturbed contributions) so that the above is satisfied:

$$B_r=-\frac{1}{r}\frac{\partial\Psi}{\partial\chi}\quad\text{and}\quad B_{\chi}=\frac{\partial\Psi}{\partial r}\tag{116}$$

Note that we do not use the notation δ for perturbed fields because we allow the these perturbations to become large so that a linearisation is not appropriate.

Now, we wish to establish the form of the equilibrium magnetic field in the χ direction. The equilibrium magnetic field, assuming straight field line coordinates, can be written as:

$$\boldsymbol{B}=\boldsymbol{\nabla}\beta\times\boldsymbol{\nabla}\psi=\psi'\boldsymbol{\nabla}\beta\times\boldsymbol{\nabla}r$$

where $\beta=q\theta-\phi$, and where this definition of the equilibrium poloidal flux ψ was defined in chapters 1 and 2. The equilibrium in the χ direction is simply proportional to

$$\boldsymbol{B}\cdot\boldsymbol{\nabla}\chi=-\boldsymbol{\nabla}\beta\times\boldsymbol{\nabla}\chi\cdot\boldsymbol{\nabla}\psi$$

Magnetic Islands

So that, writing χ and β in terms of θ and ϕ, and ignoring contributions due to the non-orthogonality of $\boldsymbol{\psi}$ and $\boldsymbol{\theta}$, we have

$$\boldsymbol{B}\cdot\boldsymbol{\nabla}\chi = -q\boldsymbol{\nabla}(\theta-\phi/q(r))\times\boldsymbol{\nabla}(\theta-\phi/q_s)\cdot\boldsymbol{\nabla}\psi \approx \left(1-\frac{q(r)}{q_s}\right)\boldsymbol{\nabla}\theta\times\boldsymbol{\nabla}\phi\cdot\boldsymbol{\nabla}\psi$$

Now from definition of equilibrium field we have the poloidal component of the field:

$$B_\theta = \frac{\vec{B}\cdot\boldsymbol{\nabla}\theta}{|\boldsymbol{\nabla}\theta|} = \frac{\boldsymbol{\nabla}\beta\times\boldsymbol{\nabla}\psi\cdot\boldsymbol{\nabla}\theta}{|\boldsymbol{\nabla}\theta|}$$

Using the simple result $|\boldsymbol{\nabla}\theta|^2 = 1/r^2$ eventually gives,

$$B_\chi = B_\theta\left(1-\frac{q(r)}{q_s}\right) \quad \approx \left(\frac{rB}{q}\left(1-\frac{q(r)}{q_s}\right)\right)$$

This can be expanded in terms of a 'layer' variable, $x = r - r_s$. Letting magnetic shear $s = (r/q)dq/dr$ and thus for small x (i.e. near the rational surface) we have $q = q_s(1 + s(r_s)x/r_s)$ so that for small x we have

$$B_\chi = -B_\theta\frac{s(r_s)x}{r_s}.$$

Now from Eq. (116), and integrating with respect to r we find the equilibrium and perturbed flux of the form,

$$\Psi = \Psi_0(r) + \Psi_1(r,\chi) \quad \text{with} \quad \Psi_0 = -\frac{1}{2}\left(\frac{B_\theta s}{r}\right)_{r_s} x^2$$

and where $\Psi_1(r,\chi)$ is determined from the radial component of the field in Eq. (116), which is of course does not have an equilibrium contribution.

Magnetic Islands

Hence, from the radial component of the field given in Eq. (116), i.e. $B_r = -(1/r)\partial\Psi_1(r,\chi)/\partial\chi$ AND employing the assumed form for perturbations $\sim \exp(im\chi)$ we have upon integration in χ:

$$\hat{\Psi}_1(r,\chi) = \frac{r\hat{B}_r}{m} \quad \text{with} \quad B_r = \hat{B}_r \exp(im\chi).$$

This is almost job done. Recall that $\Psi(r,\theta)$ actually maps out the trajectory of magnetic field lines (field lines lie on constant flux surfaces Ψ). So, we can rearrange to obtain for example the radial (x) position of a field line as a function of the helical angle χ. Taking real part of perturbation, we therefore have the following:

$$x^2(\Psi) = -\frac{2r^2}{s}\left(\frac{\Psi}{rB_\theta} - \frac{\hat{B}_r}{mB_\theta}\cos m\chi\right) = \frac{2r}{sB_\theta}\left(\hat{\Psi}_1 \cos m\chi - \Psi\right) \quad with \quad \hat{\Psi}_1 = \frac{r\hat{B}_r}{m}$$

This marks out the island structure. Sufficiently far from the rational, specifically for $\Psi > \hat{\Psi}_1$ we have wobbling unbroken field lines. Close to the rational surface, for which $\Psi < \hat{\Psi}_1$ the field lines are broken, to reveal island loops. For $\Psi = \hat{\Psi}_1$ we are on the separatrix of the island. Thus the full island width is

$$w = 4\left(\frac{r_s\hat{\Psi}_1}{sB_\theta}\right)^{1/2} = 4r_s\left(\frac{\hat{B}_r}{msB_\theta}\right)^{1/2} \tag{117}$$

We see that the island is enlarged for reduces poloidal field, and reduced magnetic shear (again small shear invokes weakness in the plasma configuration - this time in the nonlinear resistive MHD treatment).

Also small m leads to larger magnetic islands. It is generally found that modes with small mode numbers are the most degrading (poor transport properties due to rapid parallel motion 'across' island structure.

Magnetic Islands

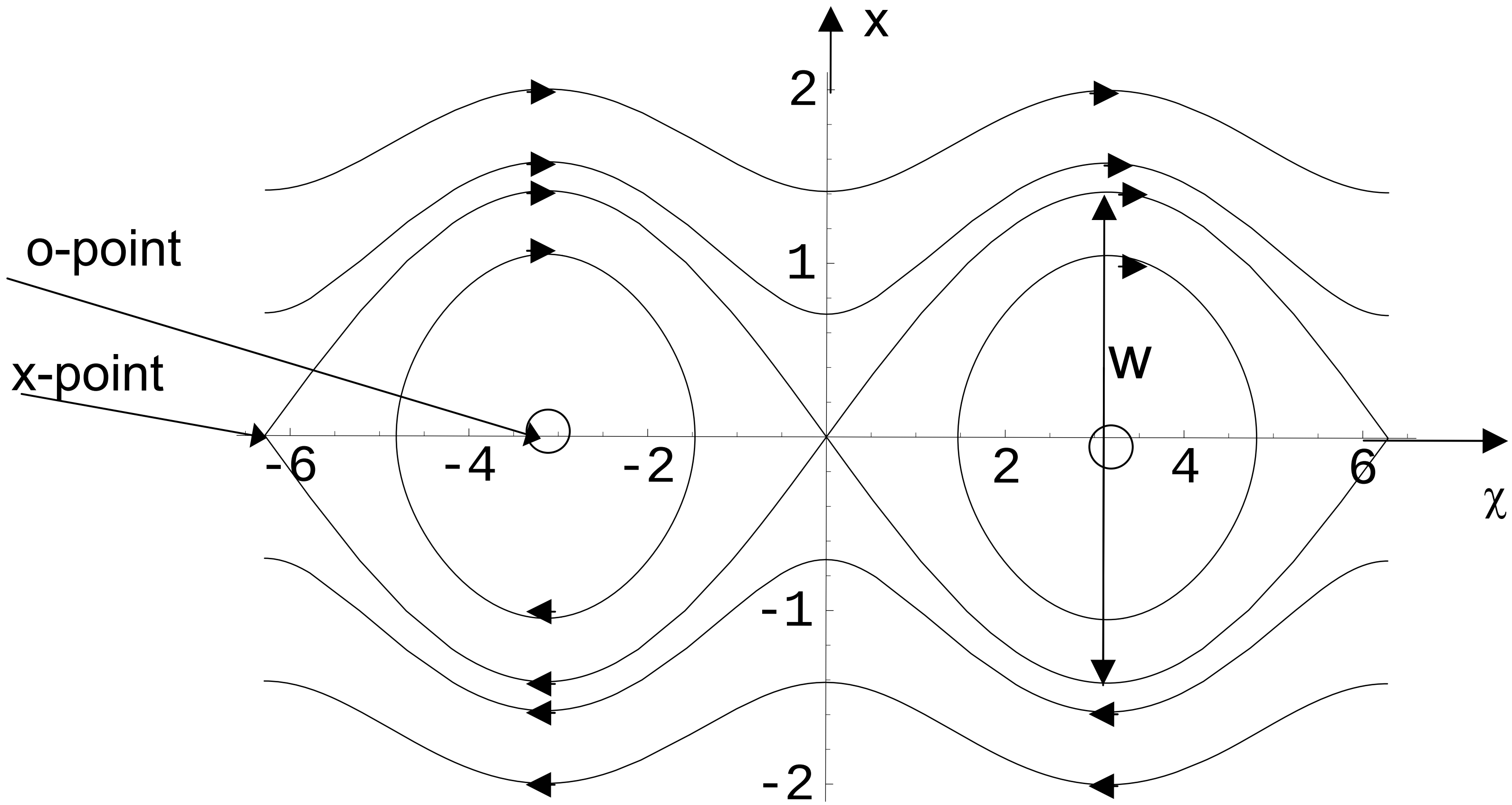

Magnetic island chain assuming poloidal mode number m=1

In this figure δB_r is constant with respect to x (and χ). Note that, there would be no island for an ideal δB_r because the radial field is zero on the rational ($x = 0$). From Eq. (79, and the last chapter we have

$$\delta B_{r0}(\text{ideal}) = -\frac{imB_0}{R_0}\left(\frac{n}{m} - \frac{1}{q}\right)\xi_{r0}(\text{ideal}) \quad \text{and} \quad \delta B_{r0}(\text{res}) = -\frac{imB_0}{R_0}\left(\frac{n}{m} - \frac{1}{q}\right)\xi_{r0}(\text{res}) - \frac{\eta}{\mu_0}\nabla^2\delta B_r(\text{res})$$

Effect of large islands on temperature profile

Recent JET PULSE 80869.

density also reduced simularly

results in reduction in beta of 30 percent

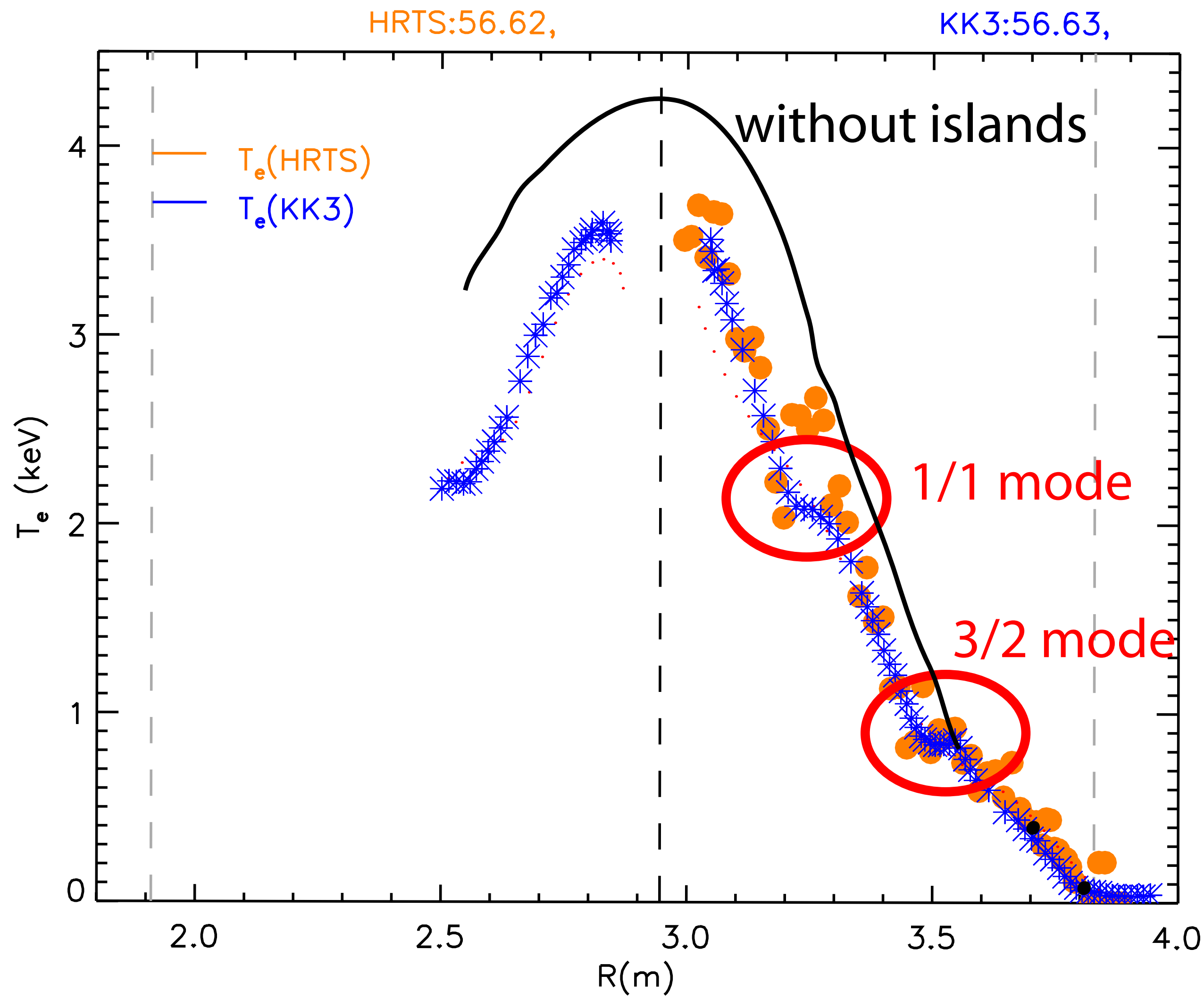

Non linear Tearing Modes, islands and NTMs

We now perform a non-linear treatment of the evolution of the magnetic field in the region of the island. This means we examine the non-linear treatment of the layer region. Consequently, in some respects, the treatment is more complicated than that undertaken in the previous chapter, BUT there is at least one simplifying feature. We will look for static or near static conditions (i.e. a saturated, or neighbouring equilibrium solution), and this means that we can drop the fluid velocity (this was kept in the linear layer treatment of the previous chapter). Note that the velocity term is small, and vanishes on the rational (proportional to magnetic operator - see structure of δB_r). If we can find a saturated non-linear solution, then this justifies the simplification of neglecting the fluid velocity.

Begin with Faraday's law

$$\frac{\partial \boldsymbol{B}}{\partial t} = -\boldsymbol{\nabla} \times \boldsymbol{E}$$

now substitute Ohms law:

$$\frac{\partial \boldsymbol{B}}{\partial t} = -\boldsymbol{\nabla} \times (\eta \boldsymbol{j}_{\text{Ohm}} - \boldsymbol{v} \times \boldsymbol{B}),$$

where $\boldsymbol{j}_{\text{Ohm}}$ is the Ohmic - MHD current. Finally we employ Amperes law $\boldsymbol{\nabla} \times \boldsymbol{B} = \mu_0 \boldsymbol{j}$, but we write the total current as the sum of Ohmic (MHD) current and non-MHD currents, or non Ohmic current (this might be an externally applied current from e.g. cyclotron heating, or from kinetic effects that generate currents that are not described by MHD (e.g. bootstrap current). So substituting $\boldsymbol{j}_{\text{Ohm}} = \boldsymbol{j} - \boldsymbol{j}_{\text{non-Ohm}} = \mu_0^{-1} \boldsymbol{\nabla} \times \boldsymbol{B} - \boldsymbol{j}_{\text{non-Ohm}}$ we have:

$$\frac{\partial \boldsymbol{B}}{\partial t} = -\boldsymbol{\nabla} \times \eta \left(\mu_0^{-1} \boldsymbol{\nabla} \times \boldsymbol{B} - \boldsymbol{j}_{\text{non-Ohm}} - \boldsymbol{v} \times \boldsymbol{B} \right) \tag{118}$$

Now a key simplification factor - ignore fluid velocity $\boldsymbol{v}$ (this term is proportional to magnetic operator $(\boldsymbol{B} \cdot \boldsymbol{\nabla})\boldsymbol{\xi}$ which in the linear treatment was expanded about x, and in any case we ultimately search for near-stationary solution) so that:

$$\frac{\partial \boldsymbol{B}}{\partial t} = -\mu_0^{-1} \boldsymbol{\nabla} \times \left[\eta \left(\boldsymbol{\nabla} \times \boldsymbol{B} - \mu_0 \boldsymbol{j}_{\text{non-Ohm}} \right) \right]. \tag{119}$$

Basic MHD Non linear Tearing Modes

In this section we drop the non-Ohmic current contribution, and thus consider only tearing modes that confirm to the self contained MHD model. Neither externally generated currents, nor currents generated by kinetic effects, are considered in this section. Hence we start with

$$\frac{\partial \boldsymbol{B}}{\partial t} = -\mu_0^{-1}\boldsymbol{\nabla}\times(\eta\boldsymbol{\nabla}\times\boldsymbol{B})$$

Taking η constant (there is also in practice an effect from a helical deformation in η, which we neglect here), then we can use $\boldsymbol{\nabla}\times(\boldsymbol{\nabla}\times\boldsymbol{\delta B})\equiv\boldsymbol{\nabla}(\boldsymbol{\nabla}\cdot\boldsymbol{\delta B})-\boldsymbol{\nabla}^2\boldsymbol{\delta B}$ and since $\boldsymbol{\nabla}\cdot\boldsymbol{B}=0$, then picking out the radial component of the field we have

$$\frac{\partial B_r}{\partial t} = \mu_0^{-1}\eta\frac{\partial^2 B_r}{\partial r^2} \tag{120}$$

We can now substitute for the radial flux (earlier section on magnetic islands) to simply give

$$\frac{\partial \Psi_1}{\partial t} = \mu_0^{-1}\eta\frac{\partial^2 \Psi_1}{\partial r^2}. \tag{121}$$

Integrating in radius across the island we have

$$\int_{r_s-w/2}^{r_s+w/2} dr\frac{\partial \Psi_1}{\partial t} = \mu_0^{-1}\eta\frac{\partial \Psi_1}{\partial r}\bigg|_{r_s-w/2}^{r_s+w/2}$$

In order to make some analytic progress we assume that the radial variation of Ψ_1 is weak compared to the radial variation of $\partial\Psi/\partial r$. (this can be verified afterwards). So we have

$$w\frac{\partial \Psi_1}{\partial t} = \mu_0^{-1}\,\eta\frac{\partial \Psi_1}{\partial r}\bigg|_{r_s-w/2}^{r_s+w/2}.$$

Basic MHD Non linear Tearing Modes

We now use the result from the derivation of the island. In particular we use $\hat{\Psi}_1(t) = Cw(t)^2$ where C is a constant in time. This easily yields

$$\frac{dw}{dt} = \frac{\eta}{2\mu_0} \frac{1}{\hat{\Psi}_1} \frac{d\hat{\Psi}_1}{dr}\bigg|_{r_s-w/2}^{r_s+w/2}.$$

The right hand side is the Δ' in the layer, but it is dependent on w (compare this with Eq. (101)) So that

$$\frac{dw}{dt} = \frac{\eta}{2\mu_0}\Delta'(w) \quad \text{with} \quad \Delta'(w) = \frac{1}{\hat{\Psi}_1} \frac{d\hat{\Psi}_1}{dr}\bigg|_{r_s-w/2}^{r_s+w/2}.$$

Now, Δ' in the layer must be identical to Δ' in the ideal MHD external region (require analytical continuation of Ψ_1. Note that, from Eq. (100), and noting that $\delta\psi \equiv \Psi_1$, we have:

$$r\frac{d}{dr}\left(r\frac{d\hat{\Psi}_1}{dr}\right) + \left(\frac{R_0}{B_0}\right)\frac{rqm\hat{\Psi}_1}{nq-m}\frac{dJ_\phi}{dr} - m^2\hat{\Psi}_1 = 0.$$

But, we must generalise the Δ' definition of Eq. (101) for non zero $\delta \equiv w$ so that in both the layer and ideal region we have:

$$\Delta'(w) = \frac{1}{\hat{\Psi}_1} \frac{d\hat{\Psi}_1}{dr}\bigg|_{r_s-w/2}^{r_s+w/2}$$

A final comment to make before we generalise this result. We are clearly interesting in the ultimate size of an island. A saturated island occurs for:

$$dw/dt = 0, \quad \text{and this in turn, for this simplified case, requires} \quad \Delta'(w) = 0.$$

Basic MHD Non linear Tearing Modes

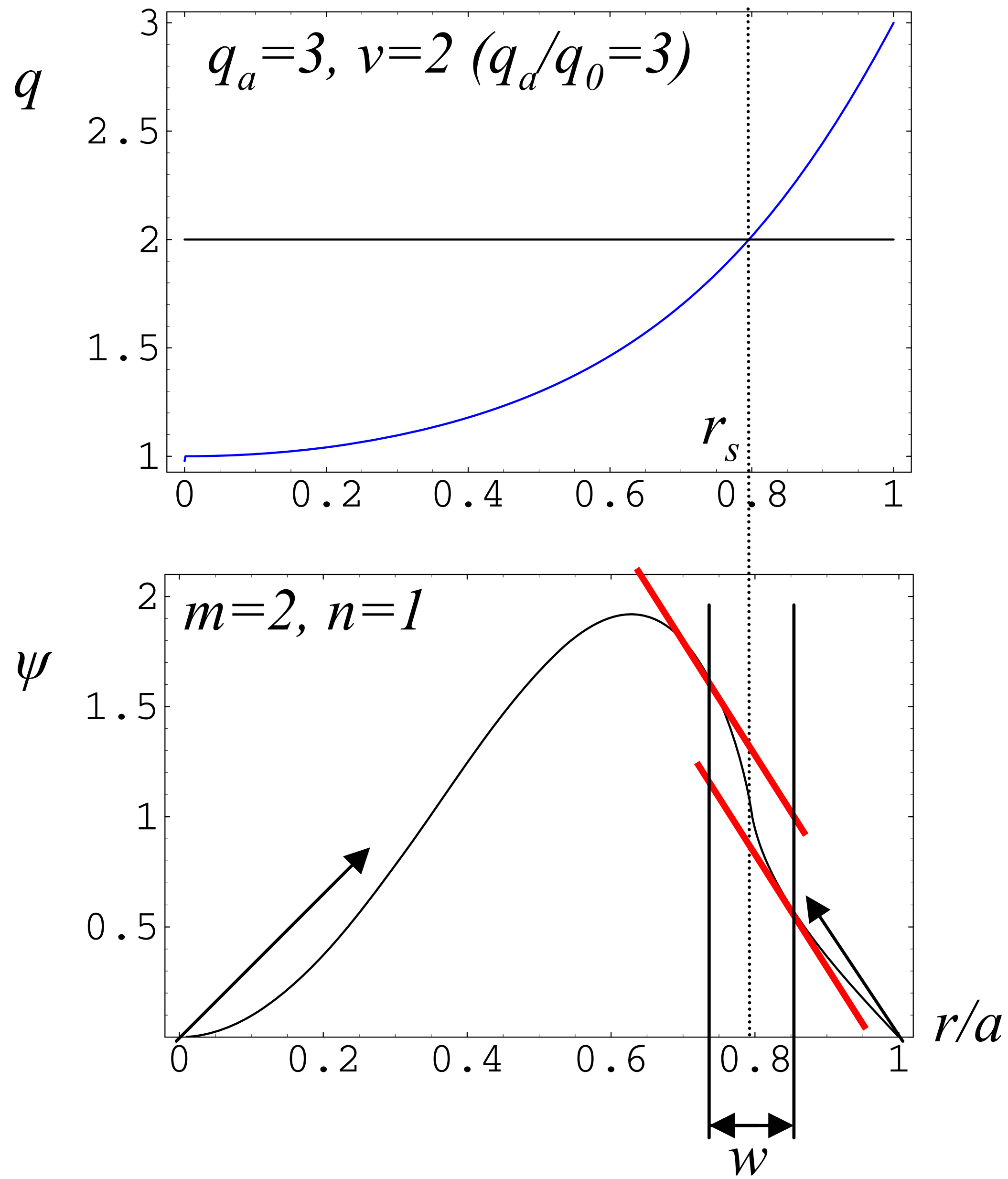

Exaggerated example Of island size *w,* depending only on Delta'(w). (Note that since w is so large, then ψ is not really constant).

NeoClassical Tearing Modes

Now we move on tearing modes in realistic tokamak plasmas. In tokamaks there are sources of current that are not contained in the closed MHD equations. We will examine the contribution of bootstrap current and how this generates neoclassical tearing modes. We will also look how we might affect tearing modes with auxiliary heating/current drive. The bootstrap current is a TOROIDAL contribution to the equilibrium current given by

$$j_{BS} \approx \frac{\epsilon^{1/2}}{B_\theta}\left(-\frac{dP}{dr}\right).$$

This is the bootstrap that we would expect before the onset of a tearing mode, i.e. at $t = 0$ we have

$$j_{non-Ohm}(t = 0) = j_{BS}$$

But, when the tearing mode is fully formed, the transport of energy and transport along the helical field lines mean that the pressure across the island vanishes, and so does the bootstrap current. Hence when the tearing mode has saturated in amplitude (when $t \to \infty$) we have:

$$j_{non-Ohm}(t \to \infty) = 0.$$

Now, in order to solve Eq. (119) we would ideally know how $j_{non-Ohm}$ changes dynamically in time. However, we can crudely approximate this dynamic evolution when solving for the helical tearing mode evolution, by writing the change in current (subscript '1') as

$$j_{1,non-Ohm} = -j_{BS}$$

So that

$$j_{non-Ohm}(t \to \infty) = j_{non-Ohm}(t = 0) + j_{1,non-Ohm}.$$

Note that here we are concentrating on the evolution of the helical perturbation. However, there is a slower evolution of equilibrium parameters even without a tearing mode. This effect is known as resistive diffusion, and the associated timescales are the longest in tokamak plasmas (in today's tokamaks a resistive diffusion of the current occurs over timescales longer than the pulse length, but it controls the current ramp during e.g. the sawtooth cycle).

NeoClassical Tearing Modes

We follow the procedure of the last section, but now use Eq. (119). i.e. from Eqs. (119), (120) and (121) we have (noting we are looking at the radial contribution to the perturbed field (or poloidal flux):

$$\frac{m}{r}\frac{\partial \Psi_1}{\partial t} = \mu_0^{-1}\eta\left(\frac{m}{r}\frac{\partial^2\Psi_1}{\partial r^2} + \mu_0[\boldsymbol{\nabla}\times(j_{1,non-Ohm}\boldsymbol{e}_\phi)]\cdot\boldsymbol{e}_r\right) = \mu_0^{-1}\eta\left(\frac{m}{r}\frac{\partial^2\Psi_1}{\partial r^2} - \mu_0[\boldsymbol{\nabla}\times(j_{BS}\boldsymbol{e}_\phi)]\cdot\boldsymbol{e}_r\right)$$

Now, we have $[\boldsymbol{\nabla}\times(j_{BS}\boldsymbol{e}_\phi)]\cdot\boldsymbol{e}_r \approx -(m/r)j_{BS}$, so that

$$\frac{\partial \Psi_1}{\partial t} = \mu_0^{-1}\eta\left[\frac{\partial^2\Psi_1}{\partial r^2} + \mu_0 j_{BS}\right]$$

We now follow the procedure of the previous section. In addition, we assume that j_{BS} has only a small variation across the island. Using the relationship for the island width w in terms of Ψ_1 given by Eq. (117) we have,

$$\frac{dw}{dt} = \frac{\eta}{2\mu_0}\left[\Delta'(w) + \mu_0 \mathrm{J}_{BS}\frac{16 r_s}{s B_\theta w}\right] = \frac{\eta}{2\mu_0}\left[\Delta'(w) + \mu_0\frac{16\epsilon_s^{1/2} r_s}{s B_\theta^2 w}\left(-\frac{dP}{dr}\right)\right].$$

This result would yield that islands grow infinitely fast for infinitely small width. However, for small island widths the bootstrap current term actually vanishes since the $1/w$ dependence should be replaced by $w/(w_a^2 + w^2)$, with w_a much smaller than the saturated NTM island width. Moreover, there is an effect derived by Glasser, Green and Johnson, which is due to toroidal effects. There is another controversial term due to polarisation current (the sign of this term has not yet been determined, so we do not consider it here. Eventually we have:

$$\frac{dw}{dt} = \frac{\eta}{2\mu_0}\left[\Delta'(w) - \frac{a_{GGJ}}{w} + a_{BS}\frac{w}{w_a^2 + w^2}\right]$$

with $-a_{GGJ}$ negative (stabilising), and a_{BS} the standard bootstrap contribution (positive and thus destabilising).

Neoclassical tearing Modes

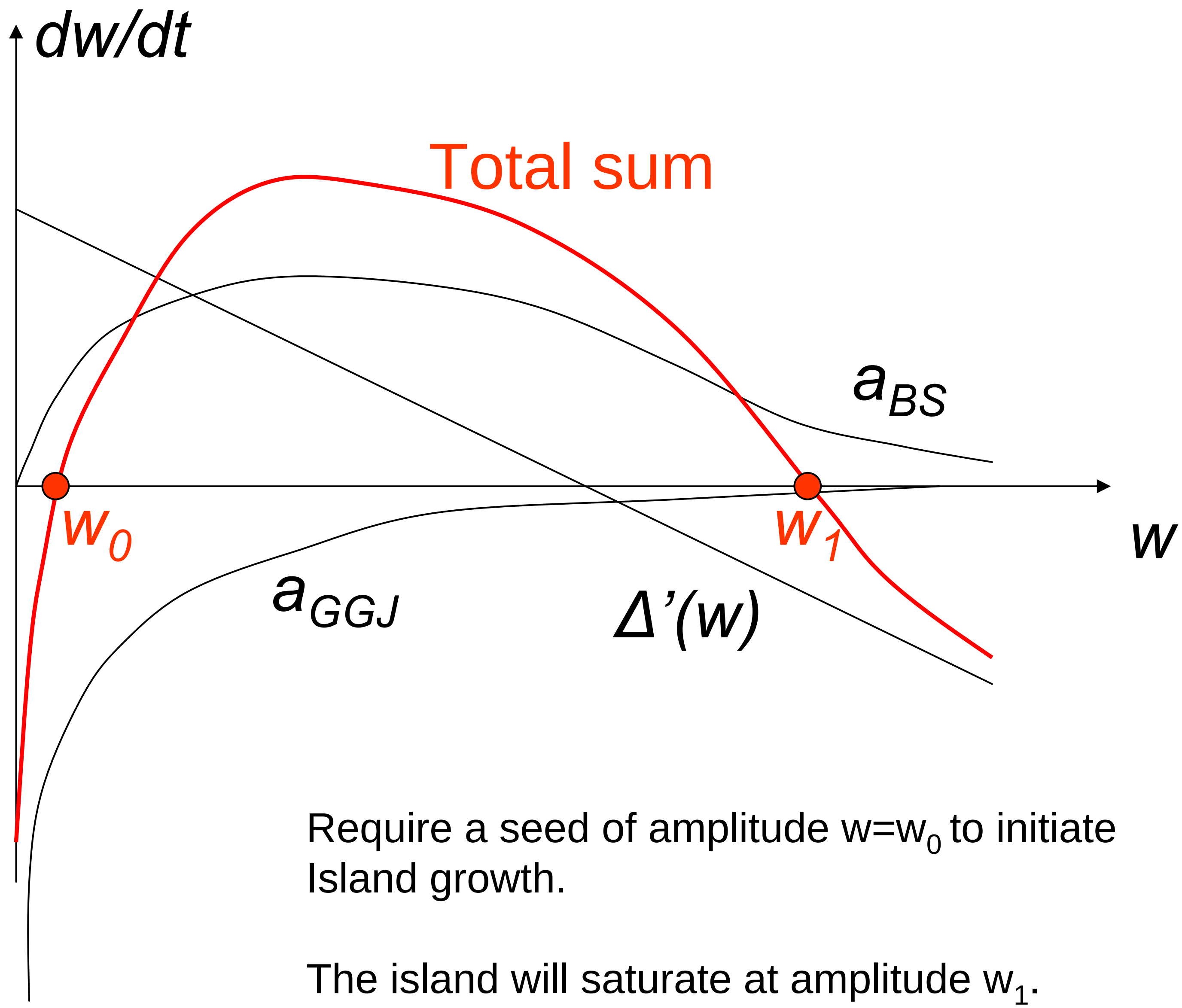

Require a seed of amplitude $w=w_0$ to initiate Island growth.

The island will saturate at amplitude w_1.

Sawtooth as a Seed to NTM

80869

420ms sawtooth triggers 3/2 NTM with beta_N=0.68
Mode locking until ICRH switch off.
Locked mode signal is small. Severe confinement degradation.

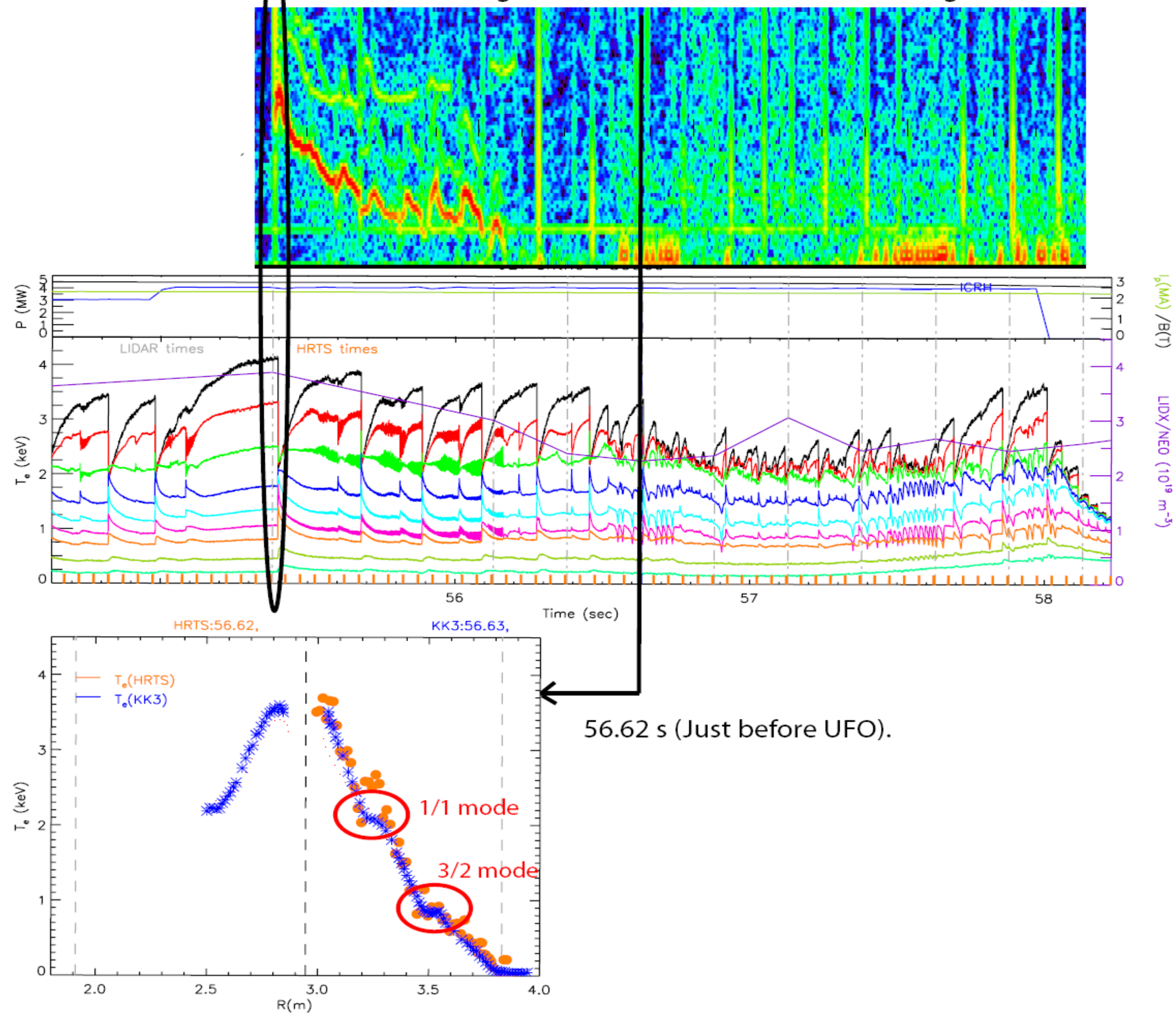

56.62 s (Just before UFO).

Current drive to affect NTM triggering

Clever approach: use localised current drive before a seed island is generated in order to increase the threshold island width w_0. But this is more difficult because we may not know where the island will generated, or when.

Standard approach: detect an NTM, then apply current drive on the island in order to reduce w_1. Either remove island (unusual), or continue to track the reduced island.

Also: localised heating: Apply heating on island. This affects all the driving terms (since they depend on pressure - even Δ' depends on pressure through the effect of temprature on resistivity, and pressure on bootstrap current and thus net current.

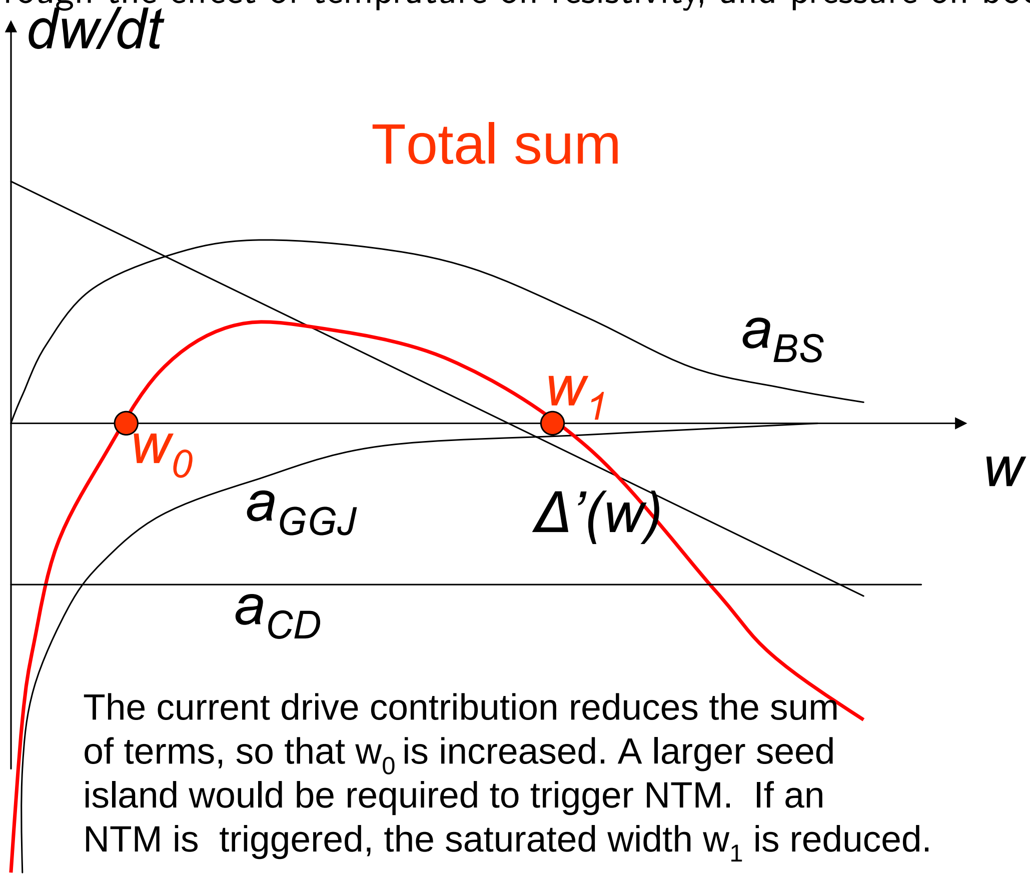

The current drive contribution reduces the sum of terms, so that w_0 is increased. A larger seed island would be required to trigger NTM. If an NTM is triggered, the saturated width w_1 is reduced.

- Week 1: Derivation and limitations of the MHD model. Conservation of Flux, The Grad-Shafranov Equation. Coordinate Systems in tokamak Equilibrium.
- Week 2: Tokamak Equilibrium. Analytical Expansions. Shafranov Shift. Shaping, and shaping penetration into the torus.
- Week 3: Linearised ideal MHD stability, energy principle, stability boundaries, compressibility etc, kinetic MHD formulation.
- Week 4: External Kink modes, linear tearing modes
- week 5: Ideal singular layer calculations, magnetic islands, non-linear resistive MHD, NTMs
- Week 6: Toroidal effects: Interchange stability (Mercier) and ballooning.
- Week 7: Ballooning continued. Introduction to kinetic MHD and long mean free path parallel dynamics.

ÉCOLE POLYTECHNIQUE FÉDÉRALE DE LAUSANNE

Importance of Magnetic Operator

We will see that in a toroidal system, a suitable coordinate system makes the stability analysis much simpler. This can be seen through the perturbation in the magnetic field, as follows.

One can always write the equilibrium magnetic field in the "Clebsch" form

$$\boldsymbol{B} = \boldsymbol{\nabla}\beta \times \boldsymbol{\nabla}\psi \tag{122}$$

where ψ is the poloidal flux, and we recall that in flux coordinates, $\boldsymbol{\nabla}\psi = \psi'\boldsymbol{\nabla}r$. Thus we see that the field is perpendicular to the ψ direction, and to the β direction, which will be defined later.

Consider now the perturbation in the magnetic field according to Eq. (52),

$$\boldsymbol{\delta B} = \boldsymbol{\nabla} \times (\boldsymbol{\xi} \times \boldsymbol{B})$$

Now consider the radial component of $\boldsymbol{\delta B}$:

$$\delta B_r \equiv \boldsymbol{\delta B} \cdot \boldsymbol{\nabla}r = \boldsymbol{\nabla}r \cdot \boldsymbol{\nabla} \times (\boldsymbol{\xi} \times \boldsymbol{B})$$

Employing the vector identity $\boldsymbol{\nabla}r \cdot (\boldsymbol{\nabla} \times \boldsymbol{D}) = \boldsymbol{\nabla} \cdot (\boldsymbol{\nabla}r \times \boldsymbol{D}) + \boldsymbol{D} \cdot (\boldsymbol{\nabla} \times \boldsymbol{\nabla}r)$ and noting that $\boldsymbol{\nabla} \times (\boldsymbol{\nabla}r) = 0$ we have

$$\delta B_r = \boldsymbol{\nabla} \cdot [(\boldsymbol{\xi} \times \boldsymbol{B}) \times \boldsymbol{\nabla}r] = \boldsymbol{\nabla} \cdot [\boldsymbol{B}(\boldsymbol{\nabla}r \cdot \boldsymbol{\xi}) - \boldsymbol{\xi}(\boldsymbol{\nabla}r \cdot \boldsymbol{B})]$$

Moreover, since $\boldsymbol{\nabla}r \cdot \boldsymbol{B} = 0$ then

$$\delta B_r = \boldsymbol{\nabla} \cdot [\boldsymbol{B}(\boldsymbol{\xi} \cdot \boldsymbol{\nabla}r)] = (\boldsymbol{\xi} \cdot \boldsymbol{\nabla}r)\boldsymbol{\nabla} \cdot \boldsymbol{B} + \boldsymbol{B} \cdot \boldsymbol{\nabla}(\boldsymbol{\xi} \cdot \boldsymbol{\nabla}r)$$

and since $\boldsymbol{\nabla} \cdot \boldsymbol{B} = 0$ then we finally obtain

$$\delta B_r = \boldsymbol{B} \cdot \boldsymbol{\nabla}(\boldsymbol{\xi} \cdot \boldsymbol{\nabla}r) = \boldsymbol{B} \cdot \boldsymbol{\nabla}\xi_r$$

Importance of Magnetic Operator

The important operator $\boldsymbol{B}\cdot\boldsymbol{\nabla}$ is known as the Magnetic Operator. Note that we haven't yet employed the Clebsch field yet. We have only used the field identity $\boldsymbol{\nabla} r\cdot\boldsymbol{B}=0$. If we know assume the Clebsch field, then we arrive at the analogous result, after using $\boldsymbol{\nabla}\beta\cdot\boldsymbol{B}=0$ to obtain for the other perpendicular component of the field,

$$\boldsymbol{\delta B}\cdot\nabla\beta=\boldsymbol{B}\cdot\boldsymbol{\nabla}(\boldsymbol{\xi}\cdot\boldsymbol{\nabla}\beta),$$

where we note that the total perturbed perpendicular field strength is

$$\delta B_{\perp}^2=\delta B_r^2+\frac{(\boldsymbol{\delta B}\cdot\nabla\beta)^2}{(\boldsymbol{\nabla}\beta)^2}.$$

Let us now consider the magnetic operator. Writing

$$\boldsymbol{\nabla}=(\boldsymbol{\nabla}\psi)\frac{\partial}{\partial\psi}+(\boldsymbol{\nabla}\Omega)\frac{\partial}{\partial\Omega}+(\boldsymbol{\nabla}\phi)\frac{\partial}{\partial\phi} \tag{123}$$

where Ω is not necessarily the same as θ defined in lecture 1. Now, choose to apply the form for $\boldsymbol{B}$ given in Eq. (22), $\boldsymbol{B}=F\boldsymbol{\nabla}\phi+\boldsymbol{\nabla}\psi\times\boldsymbol{\nabla}\phi$ so that

$$\boldsymbol{B}\cdot\boldsymbol{\nabla}=F\boldsymbol{\nabla}\phi\cdot\left[(\boldsymbol{\nabla}\psi)\frac{\partial}{\partial\psi}+(\boldsymbol{\nabla}\Omega)\frac{\partial}{\partial\Omega}+(\boldsymbol{\nabla}\phi)\frac{\partial}{\partial\phi}\right]+(\boldsymbol{\nabla}\psi\times\boldsymbol{\nabla}\phi)\cdot\left[(\boldsymbol{\nabla}\psi)\frac{\partial}{\partial\psi}+(\boldsymbol{\nabla}\Omega)\frac{\partial}{\partial\Omega}+(\boldsymbol{\nabla}\phi)\frac{\partial}{\partial\phi}\right].$$

Writing the Jacobian of the ϕ,Ω,ψ system as $\mathcal{J}_\Omega=|\boldsymbol{\nabla}\psi\times\boldsymbol{\nabla}\Omega\cdot\boldsymbol{\nabla}\phi|^{-1}$, and recalling that $\boldsymbol{\nabla}\phi^2=R^{-2}$ then

$$\boldsymbol{B}\cdot\boldsymbol{\nabla}=\frac{F}{R^2}\left[\frac{\partial}{\partial\phi}+\frac{R^2}{F\mathcal{J}_\Omega}\frac{\partial}{\partial\Omega}\right].$$

Importance of Magnetic Operator

Now , what is $R^2/(F\mathcal{J}_\Omega)$? From the cylindrical analysis of the previous chapter where we found that $\delta B_r \propto (n - m/q)$, we would expect $R^2/(F\mathcal{J}_\Omega) \approx q$. From lecture 1, one finds that

$$q_l \equiv \frac{d\phi}{d\Omega} = \frac{\boldsymbol{B}\cdot\boldsymbol{\nabla}\phi}{\boldsymbol{B}\cdot\boldsymbol{\nabla}\Omega} = \frac{F\mathcal{J}_\Omega}{R^2},$$

so that

$$\boldsymbol{B}\cdot\boldsymbol{\nabla} = \frac{F}{R^2}\left[\frac{\partial}{\partial\phi} + \frac{1}{q_l}\frac{\partial}{\partial\Omega}\right] = \frac{1}{\mathcal{J}_\Omega}\left[q_l\frac{\partial}{\partial\phi} + \frac{\partial}{\partial\Omega}\right].$$

It will now be clear that it is advantageous to choose a straight field line system, for which $q = q_l$. Let us see what happens if we don't choose a straight field line system. Choose e.g. the system employed in lecture 2, so that $\mathcal{J}_\Omega = J$ where $\mathcal{J}$ is defined in Eq. (31), and R given by Eq. (24) to give

$$q_l(r,\theta) \approx q(r)\left\{1 - (\epsilon + \Delta')\cos\theta + \sum_{m=2}^{\infty}\left(S'_m - (m-1)\frac{S_m}{r}\right)\cos(m\theta)\right\},$$

and now letting $\xi_r = \xi_0\exp(-in\phi + im\theta)$ we obtain

$$\delta B_r \approx -i\frac{\xi_r F}{R^2}\left[n - \frac{m}{q(r)}\left\{1 + (\epsilon + \Delta')\cos\theta - \sum_{m=2}^{\infty}\left(S'_m - (m-1)\frac{S_m}{r}\right)\cos(m\theta)\right\}\right]$$

which is quite a mess. If on the other had we Fourier analyse the modes in a straight field line system (r, Ω, ϕ), where $\xi_r = \xi_0\exp(-in\phi + im\Omega)$ and $q(r) = q_l(r)$ we will have

$$\mathcal{J}_\Omega = \frac{qR^2}{F}, \quad \boldsymbol{B}\cdot\boldsymbol{\nabla} = \frac{F}{R^2}\left[\frac{\partial}{\partial\phi} + \frac{1}{q(\psi)}\frac{\partial}{\partial\Omega}\right] = \frac{1}{\mathcal{J}_\Omega}\left[q(\psi)\frac{\partial}{\partial\phi} + \frac{\partial}{\partial\Omega}\right] \quad \text{and thus} \quad \delta B_r \approx -i\frac{\xi_r F}{R^2}\left[n - \frac{m}{q(r)}\right]$$

Straight Field Line Coordinates

Clearly in the straight field line coordinate system we have the jacobian

$$\mathcal{J}_\Omega = \frac{R(\Omega, r)^2 q(\psi)}{F(r)} = |\nabla\psi \times \nabla\Omega \cdot \nabla\phi|^{-1}.$$

Ω can be obtained in terms of the angle θ via equating the volume element

$$d^3x = \mathcal{J}(\theta) dr\, d\theta\, d\phi = \mathcal{J}_\Omega d\psi\, d\Omega\, d\phi,$$

giving

$$d\Omega = d\theta \frac{\mathcal{J}(\theta)}{\mathcal{J}_\Omega}\left(\frac{dr}{d\psi}\right) \quad \text{and} \quad \Omega(\theta) = \int_\theta d\theta\, \frac{\mathcal{J}(\theta)}{\mathcal{J}_\Omega \psi'},$$

where $\psi' = d\psi(r)/dr$. Now the poloidal dependence in $\mathcal{J}_\Omega$ is entirely contained in R^2, so that

$$\Omega = \left(2\pi \Big/ \int_0^{2\pi} d\theta\, \frac{\mathcal{J}(\theta)}{R^2}\right) \int_0^\theta d\theta\, \frac{\mathcal{J}(\theta)}{R^2}.$$

From the results of lecture 2 (Eq. (31)), we therefore have

$$\Omega(\theta) = \theta - \varepsilon(\epsilon + \Delta')\sin\theta + \varepsilon \sum_{m=2}^{\infty} \frac{1}{m}\left(S'_m - (m-1)\frac{S_m}{r}\right)\sin(m\theta) + O(\varepsilon^2),$$

which can easily be inverted to obtain $\theta(\Omega)$

$$\theta(\Omega) = \Omega + \varepsilon(\epsilon + \Delta')\sin\Omega - \varepsilon \sum_{m=2}^{\infty} \frac{1}{m}\left(S'_m - (m-1)\frac{S_m}{r}\right)\sin(m\Omega) + O(\varepsilon^2),$$

$$d^3x = d\psi\, d\Omega\, d\phi \mathcal{J}_\Omega = \frac{rR^2}{R_0} dr\, d\Omega\, d\phi$$

Localised Pressure Driven Modes

As we have seen, the most unstable modes will tend to be aligned to the field lines $m \approx nq$. We require that our localised modes vary strongly only perpendicularly to the field lines $\boldsymbol{k}_\perp \gg 1/a$, while varying slowly, on the scale of the machine size, along the field lines ($k_\parallel \sim 1/a$). We implement this ordering by means of an eikonal representation for $\boldsymbol{\xi}_\perp$ [Ref. Connor, Hastie and Taylor, 1978]:

$$\boldsymbol{\xi}_\perp(\psi,\Omega,\phi) \to \boldsymbol{\xi}_\perp(\psi,\Omega,\beta) = \hat{\boldsymbol{\xi}}_\perp(\psi,\Omega)\exp(in\beta), \quad \text{with} \quad \boldsymbol{B}\cdot\boldsymbol{\nabla}\beta(\psi,\Omega,\phi) = 0$$

It is found that the most unstable localised pressure driven modes have large n (infinite n are the most unstable in a static (non rotating) equilibrium). As a result, $\exp(-in\beta)$ is a rapidly varying function in β (though beta itself is essentially constant along the field line), while $\hat{\boldsymbol{\xi}}_\perp$ is a slowly function of θ (compared to the variation of $\exp(-in\beta)$ in β. Consequently, $\boldsymbol{\xi}_\perp$ varies strongly across the field lines, via the $n\Omega$ contribution to $n\beta$. Along the field lines the $\boldsymbol{\xi}_\perp$ varies slowly: β will be exactly constant along the field lines, but there will be a slow variation along the field lines through the Ω variation contained in $\boldsymbol{\xi}_\perp$. For the straight field line system already described, it is straightforward to show that

$$\beta = q(\psi)\Omega - \phi,$$

this ensures that the Clebsch definition (Eq. (122)) of the field $\boldsymbol{B} = \boldsymbol{\nabla}\beta\times\boldsymbol{\nabla}\psi$ and the definition of the field given in Eq. (22), $\boldsymbol{B} = F\boldsymbol{\nabla}\phi + \boldsymbol{\nabla}\psi\times\boldsymbol{\nabla}\phi$, with jacobian $\mathcal{J}_\Omega$, are identical. Thus, also, the requirement $\boldsymbol{B}\cdot\boldsymbol{\nabla}\beta(\psi,\Omega,\phi) = 0$ is obvious.

We are now ready to consider the potential energy δW of the internal plasma region. Consider just the perpendicular potential energy

$$\delta W_\perp = \int d^3x \left[\delta B_\perp^2 + B^2\left(\boldsymbol{\nabla}\cdot\boldsymbol{\xi}_\perp + 2\boldsymbol{\xi}_\perp\cdot\boldsymbol{\kappa}\right)^2 - 2(\boldsymbol{\xi}_\perp\cdot\boldsymbol{\nabla}P)(\boldsymbol{\kappa}\cdot\boldsymbol{\xi}_\perp^*) - J_\parallel(\boldsymbol{\xi}_\perp^*\times\boldsymbol{e}_\parallel)\cdot\boldsymbol{\delta B}_\perp\right] \quad (124)$$

Localised Pressure Driven Modes

The large quantity $\boldsymbol{\nabla}\beta$ does not enter the field line bending energy as one can see by inspecting the perpendicular components of $\boldsymbol{\delta B}$. e.g. since $\delta B_r = \boldsymbol{B}\cdot\boldsymbol{\nabla}(\boldsymbol{\xi}\cdot\boldsymbol{\nabla}r)$, and $\boldsymbol{B}\cdot\boldsymbol{\nabla}\beta = 0$ then $\delta B_r = \exp(in\beta)\cdot\boldsymbol{\nabla}(\hat{\boldsymbol{\xi}}\cdot\boldsymbol{\nabla}r)$ and thus,

$$\delta B_\perp = \exp(in\beta)\left[\boldsymbol{\nabla}\times(\hat{\boldsymbol{\xi}}_\perp\times\boldsymbol{B})\right]_\perp .$$

The energy becomes

$$\delta W_\perp = \frac{1}{2}\int d^3x\,[\delta B_\perp^2 + B^2\left(in\boldsymbol{\nabla}\beta\cdot\hat{\boldsymbol{\xi}}_\perp + \boldsymbol{\nabla}\cdot\hat{\boldsymbol{\xi}}_\perp + 2\hat{\boldsymbol{\xi}}_\perp\cdot\boldsymbol{\kappa}\right)^2 - 2(\hat{\boldsymbol{\xi}}_\perp\cdot\boldsymbol{\nabla}P)(\boldsymbol{\kappa}\cdot\hat{\boldsymbol{\xi}}_\perp^*) - J_{\|}(\hat{\boldsymbol{\xi}}_\perp\times\boldsymbol{e}_{\|})\cdot\boldsymbol{\delta B}_\perp\exp(-in\beta)]$$

We note at this point something of concern: the toroidal wavenumber, n, still appears in the field compression term $B^2\left(in\boldsymbol{\nabla}\beta\cdot\hat{\boldsymbol{\xi}}_\perp + \boldsymbol{\nabla}\cdot\hat{\boldsymbol{\xi}}_\perp + 2\hat{\boldsymbol{\xi}}_\perp\cdot\boldsymbol{\kappa}\right)^2$, and with large n, this would lead to a massive stabilising energy contribution $(n^2/2)\int d^3x\,B^2|\boldsymbol{\nabla}\beta\cdot\hat{\boldsymbol{\xi}}|^2$. In order to keep this term finite, the perturbation must be of the form

$$\hat{\boldsymbol{\xi}}_\perp = \hat{\boldsymbol{\xi}}_{\perp 0} + \frac{\hat{\boldsymbol{\xi}}_{\perp 1}}{n}, \quad \text{with} \quad \hat{\boldsymbol{\xi}}_{\perp 0} = \frac{X}{B}\boldsymbol{e}_{\|}\times\boldsymbol{\nabla}\beta$$

where $X(\psi,\Omega)$ is a new scalar function (a stream function) which is independent of $\hat{\boldsymbol{\xi}}_{\perp 1}$. The term of concern $in\boldsymbol{\nabla}\beta\cdot\hat{\boldsymbol{\xi}}_\perp$ is now finite even for infinite n, since $\hat{\boldsymbol{\xi}}_{\perp 0}$ is perpendicular to $\boldsymbol{\nabla}\beta$. Meanwhile, taking the infinite limit of n enables $\boldsymbol{\delta B}_\perp$ to be written in a simplified form (independent of $\hat{\boldsymbol{\xi}}_{\perp 1}$):

$$\begin{aligned}
\boldsymbol{\delta B}_\perp &= \{\boldsymbol{\nabla}\times[(X\boldsymbol{e}_{\|}\times\boldsymbol{\nabla}\beta)\times\boldsymbol{e}_{\|}]\}_\perp \\
&= \{\boldsymbol{\nabla}\times(X\boldsymbol{\nabla}\beta)\}_\perp \equiv \boldsymbol{\nabla}\times(X\boldsymbol{\nabla}\beta) - \boldsymbol{e}_{\|}[\boldsymbol{e}_{\|}\cdot\boldsymbol{\nabla}\times(X\boldsymbol{\nabla}\beta)] \\
&= (\boldsymbol{e}_{\|}\cdot\boldsymbol{\nabla}X)\boldsymbol{e}_{\|}\times\boldsymbol{\nabla}\beta.
\end{aligned}$$

Localised Pressure Driven Modes

The $J_{\|}$ term vanishes for infinite n (so that dependence on $\hat{\boldsymbol{\xi}}_{\perp 1}$ vanishes) because $\hat{\boldsymbol{\xi}}^*_{\perp 0} \times \boldsymbol{e}_{\|} = (X^*/B)\boldsymbol{\nabla}\beta$, and this is clearly perpendicular to the recent definition of $\boldsymbol{\delta B}_{\perp}$. Consequently we obtain the energy

$$\begin{aligned}\delta W &= \frac{1}{2}\int d^3x \left[\frac{1}{B^2}|\boldsymbol{B}\cdot\boldsymbol{\nabla}X|^2|\boldsymbol{e}_{\|}\times\boldsymbol{\nabla}\beta|^2 + \right.\\ &\left. B^2\left|i\hat{\boldsymbol{\xi}}_{\perp 1} + \boldsymbol{\nabla}\cdot\hat{\boldsymbol{\xi}}_{\perp 0} + 2\hat{\boldsymbol{\xi}}_{\perp 0}\cdot\boldsymbol{\kappa}\right|^2 - \frac{2}{B^4}(\boldsymbol{B}\times\boldsymbol{\nabla}\beta\cdot\boldsymbol{\nabla}P)(\boldsymbol{B}\times\boldsymbol{\nabla}\beta\cdot\boldsymbol{\kappa})|X|^2\right].\end{aligned}$$

Now, $\hat{\boldsymbol{\xi}}_{\perp 1}$ appears only in the stabilising field compression term, and so we are free to minimise this term with respect to $\hat{\boldsymbol{\xi}}_{\perp 1}$. The term is minimised to zero with $\hat{\boldsymbol{\xi}}_{\perp 1} = i(\boldsymbol{\nabla}\cdot\hat{\boldsymbol{\xi}}_{\perp 0} + 2\hat{\boldsymbol{\xi}}_{\perp 0}\cdot\boldsymbol{\kappa})$. Finally, we see some more simplifications: since $\boldsymbol{\nabla}\beta$ is perpendicular to $\boldsymbol{B}$, and moreover, both are perpendicular to $\boldsymbol{\nabla}P(\psi)$, then, since X is independent of ϕ, or β, then $\boldsymbol{B}\cdot\boldsymbol{\nabla}X = \mathcal{J}_\Omega^{-1}\partial X/\partial\Omega$, thus giving,

$$\delta W = \pi\int d\psi\, d\Omega\mathcal{J}_\Omega\left[\left(\frac{\boldsymbol{\nabla}\beta}{B\mathcal{J}_\Omega}\right)^2\left|\frac{\partial X}{\partial\Omega}\right|^2 - 2\left(\frac{\boldsymbol{B}\times\boldsymbol{\nabla}\beta\cdot\boldsymbol{\nabla}P}{B^2}\right)\left(\frac{\boldsymbol{B}\times\boldsymbol{\nabla}\beta\cdot\boldsymbol{\kappa}}{B^2}\right)|X|^2\right] \tag{125}$$

Let us now address and simplify the second term in δW, the so called interchange term. Employing the Clebsch field:

$$\begin{aligned}\frac{\boldsymbol{B}\times\boldsymbol{\nabla}\beta\cdot\boldsymbol{\nabla}P}{B^2} &= \frac{[(\boldsymbol{\nabla}\beta\times\boldsymbol{\nabla}\psi)\times\boldsymbol{\nabla}\beta]\cdot\boldsymbol{\nabla}P}{(\boldsymbol{\nabla}\beta\times\boldsymbol{\nabla}\psi)\cdot(\boldsymbol{\nabla}\beta\times\boldsymbol{\nabla}\psi)}\\ &= \frac{\left[(\boldsymbol{\nabla}\beta)^2\boldsymbol{\nabla}\psi - (\boldsymbol{\nabla}\beta\cdot\boldsymbol{\nabla}\psi)\boldsymbol{\nabla}\beta\right]\cdot\boldsymbol{\nabla}P}{(\boldsymbol{\nabla}\beta)^2(\boldsymbol{\nabla}\psi)^2 - (\boldsymbol{\nabla}\beta\cdot\boldsymbol{\nabla}\psi)^2}\\ &= \frac{dP}{d\psi}\quad\text{by employing}\quad \boldsymbol{\nabla}P = \boldsymbol{\nabla}\psi\,\frac{dP}{d\psi}\end{aligned}$$

Localised Pressure Driven Modes

Moreover, the following quantity is fondly known as the 'weird' (w) component of the curvature by that of the field:

$$\begin{aligned}\kappa_w &= \frac{\boldsymbol{B}\times\boldsymbol{\nabla}\beta\cdot\boldsymbol{\kappa}}{B^2}\\ &= \frac{[(\boldsymbol{\nabla}\beta\times\boldsymbol{\nabla}\psi)\times\boldsymbol{\nabla}\beta]\cdot\boldsymbol{\kappa}}{(\boldsymbol{\nabla}\beta\times\boldsymbol{\nabla}\psi)\cdot(\boldsymbol{\nabla}\beta\times\boldsymbol{\nabla}\psi)}\\ &= \frac{\left[(\boldsymbol{\nabla}\beta)^2\boldsymbol{\nabla}\psi-(\boldsymbol{\nabla}\beta\cdot\boldsymbol{\nabla}\psi)\boldsymbol{\nabla}\beta\right]\cdot\boldsymbol{\kappa}}{(\boldsymbol{\nabla}\beta)^2(\boldsymbol{\nabla}\psi)^2-(\boldsymbol{\nabla}\beta\cdot\boldsymbol{\nabla}\psi)^2}\end{aligned}$$

Now from force balance it is straightforward to show that the curvature vector:

$$\boldsymbol{\kappa}\equiv(\boldsymbol{e}_\parallel\cdot\boldsymbol{\nabla})\boldsymbol{e}_\parallel=\left(\frac{1}{B^2}\right)[\boldsymbol{\nabla}-\boldsymbol{e}_\parallel(\boldsymbol{e}_\parallel\cdot\boldsymbol{\nabla})]\left(\frac{B^2}{2}+P(\psi)\right)\quad\text{where}\quad\boldsymbol{e}_\parallel=\frac{\boldsymbol{B}}{B}.$$

We do not need to worry about subtracting the parallel derivative in B^2 from $\boldsymbol{\nabla}$ because the required operation on $\boldsymbol{\kappa}$ in $\boldsymbol{B}\times\boldsymbol{\nabla}\beta\cdot\boldsymbol{\kappa}$ is perpendicular to $\boldsymbol{B}$. So we can use

$$\boldsymbol{\nabla}\left(\frac{B^2}{2}+P\right)=\left(\boldsymbol{\nabla}\psi\frac{\partial}{\partial\psi}+\boldsymbol{\nabla}\Omega\frac{\partial}{\partial\Omega}\right)\left(\frac{B^2}{2}+P\right)$$

which gives,

$$\kappa_w=\frac{1}{B^2}\left[\frac{[(\boldsymbol{\nabla}\beta)^2(\boldsymbol{\nabla}\psi)^2-(\boldsymbol{\nabla}\beta\cdot\boldsymbol{\nabla}\psi)^2]\frac{\partial}{\partial\psi}+[(\boldsymbol{\nabla}\beta)^2\boldsymbol{\nabla}\psi\cdot\boldsymbol{\nabla}\Omega-(\boldsymbol{\nabla}\beta\cdot\boldsymbol{\nabla}\psi)(\boldsymbol{\nabla}\beta\cdot\boldsymbol{\nabla}\Omega)]\frac{\partial}{\partial\Omega}}{(\boldsymbol{\nabla}\beta)^2(\boldsymbol{\nabla}\psi)^2-(\boldsymbol{\nabla}\beta\cdot\boldsymbol{\nabla}\psi)^2}\right]\left(\frac{B^2}{2}+P\right)\tag{126}$$

Localised Pressure Driven Modes

And therefore we have

$$\kappa_w = \left(\frac{1}{B^2}\right)\left[\frac{\partial}{\partial\psi} + \left\{\frac{(\nabla\beta)^2\nabla\psi\cdot\nabla\Omega - (\nabla\beta\cdot\nabla\psi)(\nabla\beta\cdot\nabla\Omega)}{B^2}\right\}\frac{\partial}{\partial\Omega}\right]\left(\frac{B^2}{2} + P\right) \tag{127}$$

We note that the correction contained in Eq (127) is due to non-orthogonality in Ω and ψ (which is small but present for straight field line coordinates, and magnetic coordinates (Boozer) and for the analytical equilibrium coordinates described in lecture 2). Substituting κ_w into δW we finally have the compact expression:

$$\delta W = \pi \int d\psi\, d\Omega \mathcal{J}_\Omega \left[\left(\frac{\nabla\beta}{B\mathcal{J}_\Omega}\right)^2\left|\frac{\partial X}{\partial\Omega}\right|^2 - 2\kappa_w\frac{dP}{d\psi}|X|^2\right]. \tag{128}$$

There are some important properties to note at this point. Firstly, the expression for δW, and the corresponding, forthcoming, Euler equation, can undergo simple redefinition of the poloidal coordinate, since $\mathcal{J}_\Omega d\Omega$ and $\mathcal{J}_\Omega^{-1}\partial/\partial\Omega$ is independent of the poloidal coordinate. Note that when transforming to a new angle, the same new Ω definition must be used in Eq. (127) for κ_w.

Moreover, and more importantly, δW contains only one variable, X, and its derivative along the field lines (in Ω). The problem is one dimensional because is does not contain and radial derivatives. We can therefore consider a potential energy functional on each flux surface separately:

$$\delta W_\psi = \int d\Omega \mathcal{J}_\Omega \left[\left(\frac{\nabla\beta}{B\mathcal{J}_\Omega}\right)^2\left|\frac{\partial X}{\partial\Omega}\right|^2 - 2\kappa_w\frac{dP}{d\psi}|X|^2\right]. \tag{129}$$

The ballooning Equation

One can now minimize δW_ψ with respect to X in order to find the solution satisfying the equation of motion. Thus is done again by Euler-Lagrange:

$$\frac{1}{\mathcal{J}_\Omega}\frac{\partial}{\partial\Omega}\left[\left(\frac{\boldsymbol{\nabla}\beta}{B}\right)^2\frac{1}{\mathcal{J}_\Omega}\frac{\partial}{\partial\Omega}|X|\right]+2\kappa_w\frac{dP}{d\psi}|X|=0, \tag{130}$$

where again we note the independence of the definition of the poloidal angle Ω.

If we employ the angle $\Omega\to\theta$ where θ is the angle used in the large aspect ratio expansion of the equilibrium of lectures 1 and 2, then the Jacobian is $\mathcal{J}_\Omega\approx rR_0/\psi'$, where $\psi'=d\psi/dr$. Using this definition, Eq. (130) becomes the famous Ballooning equation in large aspect ratio,

$$\frac{\partial}{\partial\theta}\left[\left\{1+(s\theta-\alpha\sin\theta)^2\right\}\frac{\partial}{\partial\theta}|X|\right]+\alpha\left[\cos\theta-\epsilon\left\{1-\frac{1}{q^2}(1-\alpha\cos\theta)\right\}+\sin\theta(s\theta-\alpha\sin\theta)\right]|X|=0 \tag{131}$$

In this expression shaping effects have been neglected ($S_m=0$), pressure gradients have been allowed to be large, while the pressure itself remains of conventional order so that

$$\alpha\equiv-\frac{2q^2R_0}{B_0^2}\frac{dP}{dr}\sim O(\epsilon^0),\quad \text{while}\quad \frac{2P}{B_0^2}\sim O(\epsilon^2).$$

One then finds that

$$\Delta'\sim\epsilon,\quad \text{and}\quad r\Delta''=\alpha+O(\epsilon^1)$$

so that, in the final equation, Δ' has been dropped, and $r\Delta''$ has been replaced with α everywhere.

The ballooning Equation

Intermediate results required in this analytic expansion of the ballooning equation are

$$\nabla\beta = \nabla r\frac{\partial\beta}{\partial r} + \nabla\theta\frac{\partial\beta}{\partial\theta} + \nabla\phi\frac{\partial\beta}{\partial\phi} \quad \text{giving} \quad \nabla\beta = -\left(\nabla\phi + a\nabla r - b\nabla\theta\right)$$

with

$$\beta \equiv q(\psi)\,\Omega(\theta) - \phi \quad \text{where} \quad \Omega(\theta) = \theta - (\epsilon + \Delta')\sin\theta .$$

Thus

$$a = -\frac{\partial\beta}{\partial r} = q\sin\theta\frac{d}{dr}(\epsilon+\Delta') - \frac{q}{r}s[\theta - (\epsilon+\Delta')\sin\theta] \quad \text{and} \quad b = \frac{\partial\beta}{\partial\theta} = q[1-(\epsilon+\Delta')\cos\theta],$$

giving,

$$|\nabla\beta|^2 = |\nabla\phi|^2 + a^2|\nabla r|^2 + b^2|\nabla\theta|^2 - 2ab\nabla r\cdot\nabla\theta = \frac{q^2}{r^2}\left[1 + \Big(s\theta - r\Delta''\sin\theta) + O(\epsilon)\Big)^2\right]$$

Also, in the definition of κ_w we require

$$(\nabla\beta)^2\nabla\psi\cdot\nabla\theta - (\nabla\beta\cdot\nabla\psi)(\nabla\beta\cdot\nabla\theta) = \left[|\nabla\phi|^2\nabla r\cdot\nabla\theta - ab(\nabla r\cdot\nabla\theta)^2 + ab|\nabla r|^2|\nabla\theta|^2\right],$$

so that

$$(\nabla\beta)^2\nabla\psi\cdot\nabla\theta - (\nabla\beta\cdot\nabla\psi)(\nabla\beta\cdot\nabla\theta) \approx \psi' ab|\nabla r|^2|\nabla\theta|^2 = \psi'\frac{q^2\psi'}{r^3}\left[\sin\theta(\epsilon + r\Delta'') - s\theta + O(\Delta') + O(\epsilon^2)\right]$$

Another quantity that is required in κ_w is

$$\boldsymbol{\kappa}\cdot\nabla r = \frac{1}{B^2}\frac{\partial}{\partial r}\left(\frac{B^2}{2} + P\right) \approx \frac{1}{B_0^2}\frac{dP}{dr} + \frac{R^2}{2}\frac{\partial}{\partial r}\left[\left(\frac{R_0}{R}\right)^2\left(1 + F_2 + \frac{\epsilon^2}{q^2(1-\Delta'\cos\theta)}\right)\right]$$

The ballooning Equation

But,

$$\frac{dF_2}{dr} = -\frac{1}{B_0^2}\frac{dP}{dr} - \frac{r}{R_0^2 q^2}(2-s) \quad \text{giving} \quad \boldsymbol{\kappa}\cdot\boldsymbol{\nabla} r = \frac{1}{B^2}\frac{\partial}{\partial r}\left(\frac{B^2}{2}+P\right) \approx \kappa_{rR} + \kappa_{rr}$$

where we break these terms down respectively as toroidal (κ_{rR}) and poloidal (κ_{rr}) curvature contributions projected in the direction of the minor radius:

$$\kappa_{rR} \approx \frac{R^2}{2}\frac{\partial}{\partial r}\left(\frac{1}{R}\right)^2 = -\frac{1}{R}\frac{\partial R}{\partial r} \approx -\frac{1}{R_0}\left(\cos\theta - \epsilon\cos^2\theta\right)$$

and

$$\kappa_{rr} = -\frac{\epsilon}{R_0 q^2}(1 - r\Delta''\cos\theta).$$

We note that in a cylinder (screw pinch approximation) we do not have the toroidal curvature (κ_R), so that

$$\boldsymbol{\kappa}\cdot\boldsymbol{\nabla} r(cyl) = \kappa_{rr}(\text{with } \Delta''=0) = -\frac{\epsilon}{R_0 q^2}$$

Meanwhile,

$$\boldsymbol{\kappa}\cdot\boldsymbol{\nabla}\theta \approx \left(\frac{1}{r^2}\right)\frac{1}{2B^2}\frac{\partial B^2}{\partial\theta} \approx \frac{1}{rR_0}\sin\theta$$

and combining with $(\boldsymbol{\nabla}\beta)^2\boldsymbol{\nabla}\psi\cdot\boldsymbol{\nabla}\theta - (\boldsymbol{\nabla}\beta\cdot\boldsymbol{\nabla}\psi)(\boldsymbol{\nabla}\beta\cdot\boldsymbol{\nabla}\theta)$, makes a crucial contribution to κ_w, eventually yielding

$$\kappa_w = -\frac{1}{\psi' R_0}\left[\cos\theta - \epsilon\left\{1 - \frac{1}{q^2}(1 - r\Delta''\cos\theta)\right\} + \sin\theta(s\theta - r\Delta''\sin\theta)\right]. \tag{132}$$

The ballooning Equation

There are two important things to note here. First, in a cylinder (screw pinch) one obtains simply,

$$\kappa_w(cyl) = -\frac{1}{\psi' R_0}\left[\epsilon\frac{1}{q^2}\right].$$

Meanwhile, if we assume toroidal geometry, but ignore the 'weird' component of κ_w in this coordinate system, i.e. if we simply take

$$\kappa_w(\text{toroidal-incorrect}) = \frac{1}{B^2}\frac{\partial}{\partial\psi}\left(\frac{B^2}{2}+P\right) = \frac{1}{\psi'}\boldsymbol{\kappa}\cdot\boldsymbol{\nabla} r$$

then one would obtain the intuitive, but crucially incorrect result

$$\kappa_w(\text{toroidal-incorrect}) = -\frac{1}{\psi' R_0}\left[\cos\theta - \epsilon\left(\frac{1}{2}-\frac{1}{q^2}\right) - \frac{\epsilon}{2}\left(\cos 2\theta + \frac{2\alpha}{q^2}\cos\theta\right)\right].$$

In the above incorrect definition of κ_w, ballooning contributions involving s and α are absent, and even more importantly, the Mercier coefficient (term proportional to ϵ in the above) is wrong.

By assuming the correct definition of κ_w given by Eq. (132), one now easily obtains the large aspect ratio tokamak ballooning equation with circular cross section of Eq. (131), by also noting that $\psi' = rB_0/q$.

The Suydam Criterion

From the ballooning equation of Eq. (131), one can easily obtain the Suydam Criterion, which is the stability criteria for localised pressure driven instability in a cylindrical screw-pinch. Simply take the cylindrical approximation for κ_w, and take $\Delta' = 0$ and $r\Delta'' = 0$ in $\boldsymbol{\nabla}\beta$. Then, we have the ballooning equation in a cylinder:

$$\frac{\partial}{\partial\theta}\left[\left\{1+(s\theta-0\alpha\sin\theta)^2\right\}\frac{\partial|X|}{\partial\theta}\right]+\alpha\left[0*\cos\theta-\epsilon\left(0*1-\frac{1-0\alpha\cos\theta}{q^2}\right)+0\sin\theta(s\theta-\alpha\sin\theta)\right]|X|=0 \tag{133}$$

i.e. for $\theta \gg 1$,

$$\frac{\partial}{\partial\theta}\left[\theta^2\frac{\partial}{\partial\theta}|X|\right]+D_S|X|=0 \quad \text{with} \quad D_S=\frac{\epsilon}{s^2}\alpha\left[\frac{1}{q^2}\right] \tag{134}$$

This equation has solution

$$X = c_+\theta^{\lambda_+} + c_-\theta^{\lambda_-} \quad \text{with} \quad \lambda_\pm = -\frac{1}{2} \pm \sqrt{\frac{1}{4} - D_S}$$

The criteria for instability turns out to be given by the condition that both the solutions for X are physical (not infinite) for large θ, and that the solutions are oscillatory in θ (see lecture 6). Thus the condition for instability is:

$$D_S > \frac{1}{4} \quad \text{or} \quad 4\epsilon\alpha\left[\frac{1}{q^2}\right] > s^2$$

Intuitive explanation for this stability criteria is simple. Magnetic curvature in a cylinder points radially inwards, and coupling this effect with the radial pressure gradient, is destabilising (the interchange term in δW is proportional to $\boldsymbol{\kappa}\cdot\boldsymbol{\nabla}P$. The effect of field line bending is stabilising, except on the rational surface. However, the magnetic shear ensures that the region with poor field line bending is strongly localised. So, magnetic shear is stabilising. So, it is seen that magnetic shear off-sets the destabilising role of pressure and magnetic curvature.

The Mercier Criterion

We now wish to generalise the criterion for interchange instability, in a tokamak. This is done by considering the ballooning equation, and removing (averaging over) all the periodic terms. This is considered to be the asymptotic ($\theta \gg 1$) behaviour of the solution to $X(\theta)$. Hence we have

$$\frac{\partial}{\partial\theta}\left[\left\{1*0+(s\theta-0\alpha\sin\theta)^2\right\}\frac{\partial}{\partial\theta}|X|\right]+\alpha\left[0\cos\theta-\epsilon\left(1-\frac{1-0\alpha\cos\theta}{q^2}\right)+0\sin\theta(s\theta-\alpha\sin\theta)\right]|X|=0. \tag{135}$$

which is simply,

$$\frac{\partial}{\partial\theta}\left[\theta^2\frac{\partial}{\partial\theta}|X|\right]+D_M|X|=0 \quad \text{with} \quad D_M=-\frac{\epsilon}{s^2}\alpha\left[1-\frac{1}{q^2}\right]. \tag{136}$$

Clearly the solution to X has the same form as the cylindrical result,

$$X=c_+\theta^{\lambda+}+c_-\theta^{\lambda-} \quad \text{with} \quad \lambda_\pm=-\frac{1}{2}\pm\sqrt{\frac{1}{4}-D_M}$$

The criteria for instability turns out to be given by the condition that both the solutions for X are physical (not infinite) for large θ, and that the solutions are oscillatory in θ (see lecture 6). Thus the condition for instability is:

$$D_M>\frac{1}{4} \quad \text{or} \quad 4\epsilon\alpha\left[\frac{1}{q^2}-1\right]>s^2$$

It is seen that stability to interchange modes in a tokamak with circular cross section is assured in the region in the plasma where $q>1$ regardless of the pressure gradient. The region where $q>1$ has 'average' curvature which is favourable. In this region, the 'average' κ_{rR} curvature points outward (stabilising if $P,<0$ as is usual) more strongly than the inward pointing κ_r destabilising (cylindrical) curvature. The region where $q<1$ has 'average' curvature which is unfavourable. Elongation tends to move the region of unfavourable to curvature to $q>1$ (it is destabilsing), while triangularity does the opposite. Finally, it is important to note that the sawtooth instability could be linked to the interchange mode, and that the sawtooth removes plasma from the region $q<1$.

Magnetic Curvature in a Tokamak

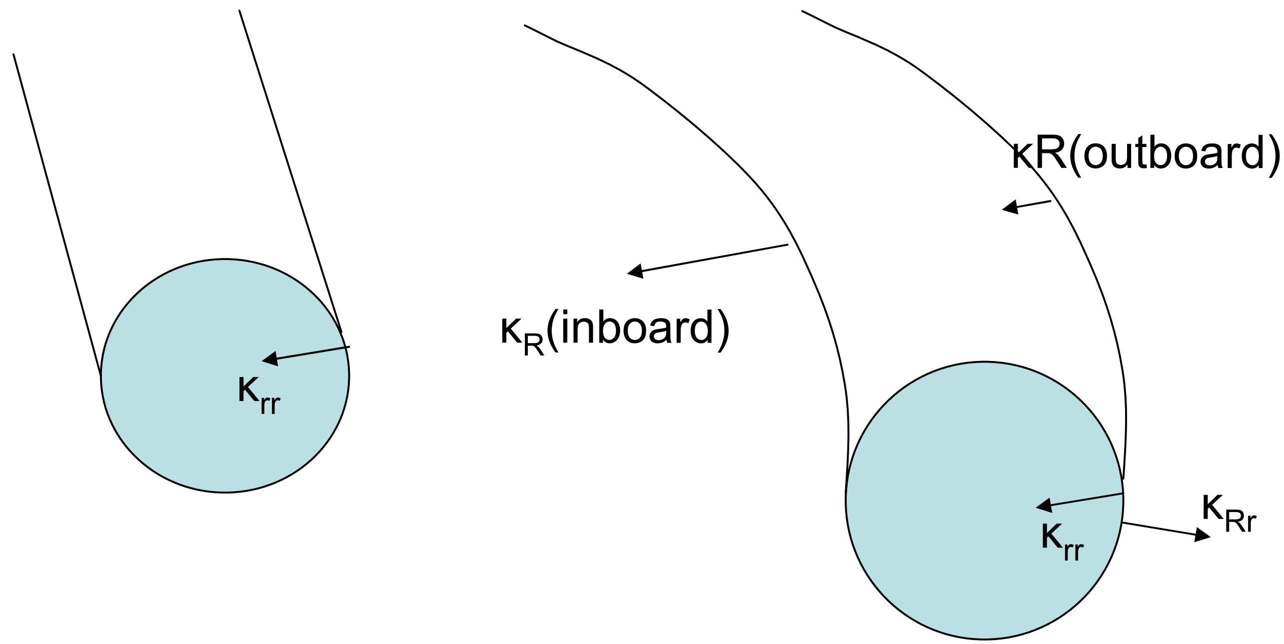

Finally, note that if we had used the intuitive curvature

$$\kappa_w(\text{toroidal-incorrect}) = \frac{1}{B^2}\frac{\partial}{\partial\psi}\left(\frac{B^2}{2} + P\right) = \frac{1}{\psi'}\boldsymbol{\kappa}\cdot\boldsymbol{\nabla} r$$

in the Mercier criterion, then for our chosen coordinate system, this would have led to a crucial error in the stability criteria, such the unfavourable curvature would correspond to the region where $q > 2^{1/2}$, since one would have

$$4\epsilon\alpha\left[\frac{1}{q^2} - \frac{1}{2}\right] > s^2.$$

- Week 1: Derivation and limitations of the MHD model. Conservation of Flux, The Grad-Shafranov Equation. Coordinate Systems in tokamak Equilibrium.
- Week 2: Tokamak Equilibrium. Analytical Expansions. Shafranov Shift. Shaping, and shaping penetration into the torus.
- Week 3: Linearised ideal MHD stability, energy principle, stability boundaries, compressibility etc, kinetic MHD formulation.
- Week 4: External Kink modes, linear tearing modes
- week 5: Ideal singular layer calculations, magnetic islands, non-linear resistive MHD, NTMs
- Week 6: Toroidal effects: Interchange stability (Mercier) and ballooning.
- Week 7: Ballooning continued. Recap of the Course

Periodicity and Ballooning Representation

We recall that the ballooning equation was derived by using an eikonal representation for $\boldsymbol{\xi}_\perp$ [Ref. Connor, Hastie and Taylor, 1978]:

$$\boldsymbol{\xi}_\perp(\psi,\Omega,\beta)=\hat{\boldsymbol{\xi}}_\perp(\psi,\Omega)\exp(in\beta),\quad \text{with}\quad \boldsymbol{B}\cdot\boldsymbol{\nabla}\beta(\psi,\Omega,\phi)=0$$

Let us consider the periodicity of $\exp(in\beta)$ where $\beta=\Omega q(\psi)-\phi$. It is clear that

$$\exp(in\beta)=\exp[inq(\psi)\Omega-in\phi]$$

is not periodic in θ except on a rational surface $q=m/n$. For example

$$\beta(\Omega+2\pi,\phi)=\beta(\Omega,\phi)-2\pi q(\psi)$$

and

$$\exp[in\beta(\Omega+2\pi,\phi)]=\{\cos[2\pi nq(\psi)]-i\sin[2\pi nq(\psi)]\}\ \exp[in\beta(\Omega,\phi)]$$

It was realised by Connor, Hastie and Taylor that since the eikonal gives the solution along the field line (represented by β), then the boundary conditions on the scalar function $X(\Omega)$ should not be applied at $\Omega=\pm\pi$. Since the solution is along the field line, we are free to consider the angle Ω to be a generalised coordinate, mapping out the entire length of a field line, from minus infinity, to plus infinity.

Periodicity and Ballooning Representation

An equilibrium magnetic field line is constrained to lie on a flux surface (constant pressure surface). The relevant boundary condition on $X(\Omega)$ must be such that a physical solution is single valued at all points on the toroidal surface defined by ψ. Consider now a Fourier decomposition of $X(\Omega)$. Let

$$\tilde{X}(\Omega) = \sum_{m=-\infty}^{\infty} x_m \exp(im\Omega) \quad \text{with} \quad x_m = \int_{-\infty}^{\infty} d\Omega\, X(\Omega) \exp[-im\Omega].$$

Clearly, $\tilde{X}(\Omega)$ is single valued on the toroidal surface (from $-\pi$ to π). Now, $\tilde{X}(\Omega)$ is considered to be the physical solution, adhering to a single valued solution, and is defined within $-\pi < \Omega < \pi$. Meanwhile, the representation of $\tilde{X}$, by X, defined in the interval $-\infty < \Omega < \infty$ using the eikonal formulation, is called the ballooning representation.

Consider now the potential energy δW given by Eq. (128), or indeed, the radially localised potential energy δW_ψ given by Eq. (129). The latter, written in terms of $\hat{X}$, is simply,

$$\delta W_\psi \propto \int_{-\pi}^{\pi} d\Omega \mathcal{J}_\Omega \left[\left(\frac{\nabla \beta}{B \mathcal{J}_\Omega} \right)^2 \left| \frac{\partial \tilde{X}}{\partial \Omega} \right|^2 - 2\kappa_w \frac{dP}{d\psi} |\tilde{X}|^2 \right].$$

But, in the ballooning representation, this is exactly the same as

$$\delta W_\psi \propto \int_{-\infty}^{\infty} d\Omega \mathcal{J}_\Omega \left[\left(\frac{\nabla \beta}{B \mathcal{J}_\Omega} \right)^2 \left| \frac{\partial X}{\partial \Omega} \right|^2 - 2\kappa_w \frac{dP}{d\psi} |X|^2 \right].$$

Convergence of $\int_{-\infty}^{\infty} d\Omega |X|^2$ requires that $|X| \lesssim \Omega^{-1/2}$. This forms the boundary condition for X, i.e. that the solution remains physical (finite energy).

Ballooning Structure

Consider the interchange contribution to the energy, i.e.

$$\int_{-\infty}^{\infty} d\Omega \mathcal{J}_\Omega \left(-2\kappa_w \frac{dP}{d\psi} |X|^2 \right).$$

Since P' is negative, then the minimising solution for X takes a ballooning form. This can be seen by noting that $\kappa_w = (\psi' R_0) \cos\Omega$ to leading order. i.e. the interchange term is minimised by having X large near $\Omega = 0$, and X small for large $|\Omega|$.

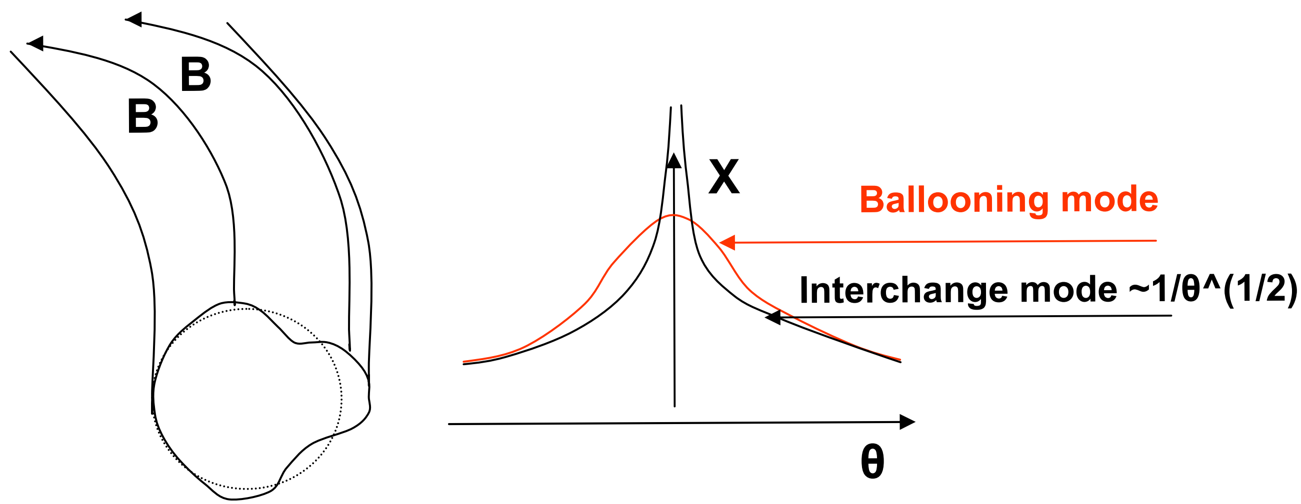

Ballooning Structure

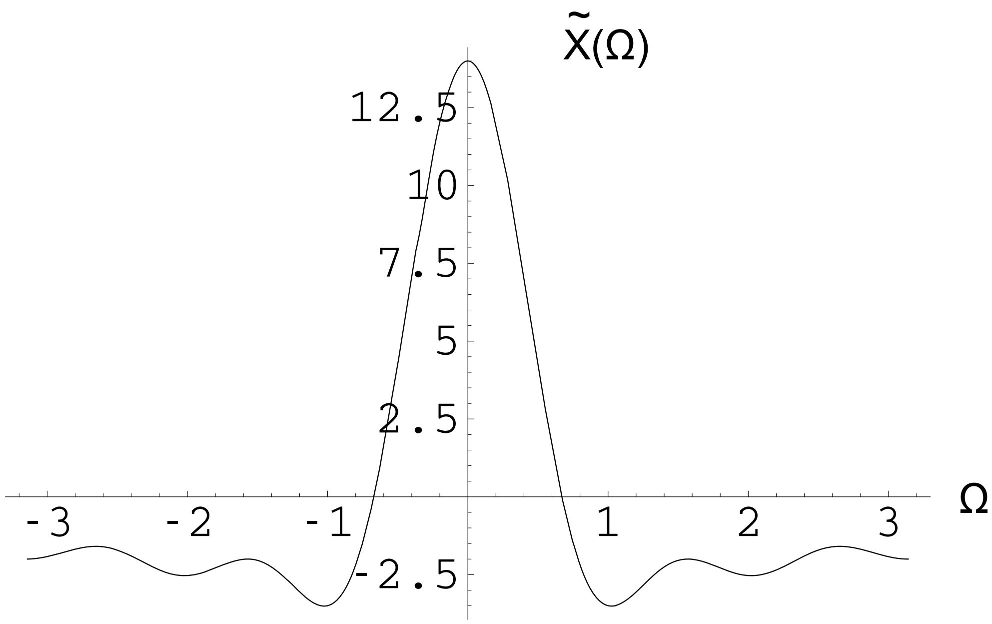

$\tilde{X}(\Omega) = 4\mathrm{Cos}\Omega + 4\mathrm{Cos}2\Omega + 3\mathrm{Cos}3\Omega + \mathrm{Cos}5\Omega$

Interchange at large θ

Consider two neighbouring surfaces ψ_0 and ψ_1, and their corresponding the functional $X_{0,1} = \hat{X}_{0,1}\exp(-in\beta_{0,1})$. Writing $q(\psi_1) = q(\psi_0) + \Delta q$ one then has

$$X_1 = \hat{X}_1 \exp(in\beta_0)\exp(-in\Delta q\Omega),$$

and since the poloidal and radial variation in $\hat{X}$ is slow, then

$$X_1 \approx X_0 \exp(-in\Delta q\Omega),$$

Thus, it is seen that X_1 and X_0 differ by a factor $\exp(-in\Delta q\Omega)$, which can be very large for large n and large Ω. Hence, where there is non-zero magnetic shear, the radial variation of X is primarily contained in β.

Stability to interchange modes is concerned with the stability corresponding to the large Ω behaviour of X in the ballooning representation, and is therefore associated with the local behaviour in ψ. The result will usually be an underestimate of instability. The procedure is to

1) Solve the ballooning equation for large Ω.

2) Assume that the large Ω solution is valid for all Ω. This identifies the eigenfunction everywhere.

3) Obtain the condition for marginal stability by imposing physical boundary conditions

Interchange at large θ

Simply write the ballooning equation (Eq. 131) in the form:

$$\frac{d}{d\theta}\left[f\frac{dX}{d\theta}\right] + gX = 0$$

and we let

$$f = a + b\theta + c\theta^2 \quad \text{and} \quad g = d + e\theta$$

where a, b, c, d and e are periodic functions of θ (see R.B. White, Toroidally Confined Plasmas, 2nd ed.).

Now it is the secular dependence (long trend in θ) that needs to be captured in the large θ solution of X. We also know that we require $X \lesssim \theta^{-1/2}$. We write X as an expansion in a large variable (reciprocal Taylor expansion):

$$X = \theta^p \left[X_0(\theta) + \frac{X_1(\theta)}{\theta} + \frac{X_2(\theta)}{\theta^2}\right]$$

where again, X_0, X_1 and X_2 contain periodic, but no secular dependence, in θ. We must solve for X_0, X_1 and X_2 by substitution into the ballooning equation, and examination of coefficients in the resulting power series. Substitution of X_0, X_1 and X_2 into the ballooning equation then yields the power index p (student exercise).

The result is

$$X = \theta^p[1 + O(1/\theta)] \quad \text{with} \quad p = -\frac{1}{2} \pm \sqrt{\frac{1}{4} - D_M}$$

where

$$D_M = \left\langle \frac{\hat{e}}{c} \right\rangle - \left\langle \frac{\hat{e}}{c} \right\rangle^2 + \left\langle \frac{1}{c} \right\rangle \left(\left\langle \frac{\hat{e}\hat{e}}{c} \right\rangle + \langle d \rangle - \langle \hat{e} \rangle \right) \quad , \quad \hat{e} = \int_0^\theta d\theta\, e, \quad \text{and} \quad \langle X \rangle = \frac{1}{2\pi}\int_0^{2\pi} d\theta\, X$$

Interchange at large θ

If a well behaved solution exists the system is ballooning unstable. We require that both of these well behaved solutions are physical. Note that if $D_M < 1/4$, one of the solutions will give rise to $p > -1/2$, and hence the energy will be infinite.

On the other hand, if $D_M > 1/4$, then p is complex, and both solutions are well behaved:

$$\theta^p = \theta^{-1/2}\,\theta^{\pm i|D_M - 1/4|}$$

This result is oscillatory in D_M (and in r or ψ as we postulated earlier), since

$$\theta^p = \theta^{-1/2}\,\theta^{\pm i|D_M-1/4|} = \theta^{-1/2}\exp\left[\ln\left(\theta^{\pm i|D_M-1/4|}\right)\right] = \theta^{-1/2}\exp\left[\pm i|D_M - 1/4|\ln\theta\right].$$

Substituting for the coefficients (see Eq. 131) $a = 1+\alpha^2\sin^2\theta$, $b = -2\alpha s\sin\theta$, $c = s^2$, $d = \alpha[\cos\theta - \epsilon[1-(1-\alpha\cos\theta)/q^2)] - \alpha\sin^2\theta]$ and $e = \alpha s\,\sin\theta$ one ends up with

$$D_M = \frac{\alpha}{s^2}\epsilon\left(\frac{1}{q^2}-1\right)$$

or the condition for instability,

$$4\alpha\epsilon\left(\frac{1}{q^2}-1\right) > s^2$$

which is the condition that pressure driven interchange can overcome magnetic field line bending stabilisation.

Ballooning effects not captured by large θ interchange assumption

It is clear that magnetic shear is stabilising. This is not surprising because, in order to minimise magnetic field line bending stabilisation, instabilities tend to align themselves with the equilibrium field on a given flux surface. The magnetic shear determines the rate at which the mode and the equilibrium magnetic field become misaligned on neighbouring flux surfaces.

A feature that is missing from the large θ treatment is the role of poloidally localised magnetic shear. These effects are taken care in the general ballooning equation of Eq. (131) via $\alpha \sin\theta$. In order to see the effect of local shear, we should first examine the local q defined above in Eq. (15), and in the last lecture:

$$q_l \equiv \frac{d\phi}{d\Omega} \approx q(r)\left\{1 - (\epsilon + \Delta')\cos\theta\right\},$$

if circular (unshaped, $S_m = 0$) flux surfaces are assumed. Hence the local shear

$$s_l(r,\theta) = \frac{r}{q_l}\frac{dq_l}{dr} = s(r) - \alpha(r)\cos\theta + O(\epsilon) \quad \text{for} \quad \Delta' \sim \epsilon \quad \text{and} \quad r\Delta'' = \alpha + O(\epsilon).$$

The stabilising effect of shear is reduced at $\theta = 0$ as α is increased. This ensures that ballooning modes, are more unstable than interchange modes at small to moderate α. This local shear effect, and its impact on magnetic field line bending, is averaged over when taking the large θ assumption of interchange modes.

Interestingly however, by further increase in α, the local minimum in s_l, and the minimum in field line bending stabilisation, occurs at larger values of θ (region of improved curvature). As a result, very large values of α can yield a second region of stability to the ballooning mode. In this parameter range, the ballooning mode has no pressure driven trigger. The interchange instability, on the other hand, would be strongly unstable.

Ballooning Stability Diagram

Conventional pressure and q profiles chosen.
q>1, so Mercier stability everywhere

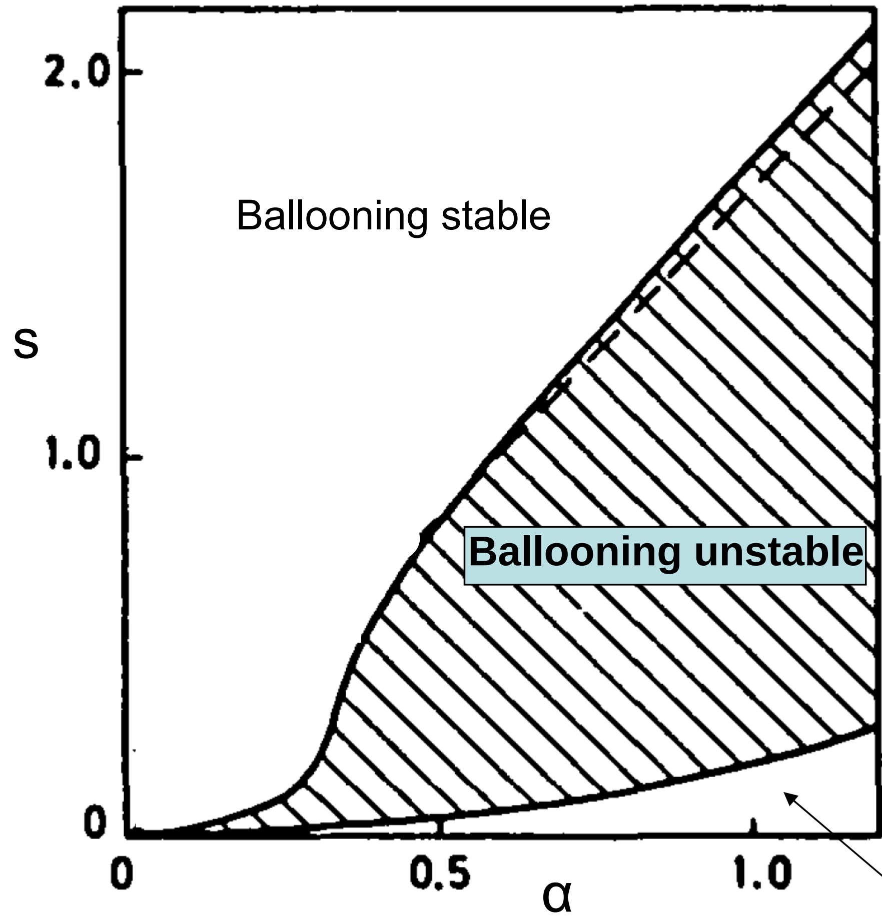

Second region of ballooning stability

Recap of Key Results

Chapter 1 - MHD and Equilibrium

The perpendicular MHD equations were derived from a guiding centre model. The parallel momentum equation and the equation of state (closing the fluid system of equations) is more difficult to justify in a near-collisionless plasma. Nevertheless, these two approximations do not enter MHD static equilibrium, and moreover, they are not very restrictive for instabilities existing in a static equilibrium that are close to marginal stability.

The conservation of flux: in ideal MHD, field lines are frozen into the fluid. Resistive effects (included in non-deal Ohm's law) allow field lines to 'tear' through the fluid. In the ideal MHD model the concept of conservation of flux helps us to understand how instabilities can be damped or prevented. In particular, if the fluid displacement associated with an instability has a wave-vector component which is parallel to the equilibrium magnetic field, then the frozen in theorem requires that the fluid displacement must bend the magnetic field lines. The latter requires energy, and thus damps the perturbation.

MHD Equilibrium: Without equilibrium flow, the equilibrium state has vanishing time dependence. As such, the momentum equation simply yields the force balance equation $\boldsymbol{J} \times \boldsymbol{B} = \boldsymbol{\nabla} P$. Certain properties of this equation yield obvious results. In particular, current and magnetic field lines lie on constant pressure surfaces. In toroidal geometry, these surfaces are called flux surfaces.

In a tokamak (toroidal geometry, with axis-symmetric toroidal field) force balance yields the Grad-Shafranov equation. The result is independent of the system of coordinates, allowing the most convenient coordinate system to be chosen (depending on the eventual application). It is seen that the equilibrium can be defined upon knowledge of the pressure profile, the current profile and the outer boundary shape.

Recap of Key Results

The Fourier components of the Grad-Shafranov equation can identified. The $\cos(0\theta)$ contribution yields the lowest order force balance in the $\nabla\psi$ (or ∇r) direction. This equation enables the derivation of the total toroidal magnetic field including the diamagnetic effect of the pressure on the toroidal field. Derivation of the poloidal field then enables the total magnetic field strength to obtained in toroidal geometry. The pressure also enters the poloidal field through its dependence on the local field line pitch q_l, and in turn, through the Shafranov shift. The net effect of pressure (and shaping) on the field strength was seen to impact particle trapping.

The $\cos\theta$ component of the Grad-Shafranov equation describes force balance in the ∇R direction. A differential equation for the Shafranov shift Δ can be derived. It is seen that Δ shifts nested flux surfaces. The source of the shift can be easily seen in terms of a tyre tube force (effect of pressure), and a hoop force (effect of current).

The $\cos m\theta$ (with $m > 2$) components of the Grad-Shafranov equation describe the penetration of the shaping from the boundary into the core. It is seen that to leading order, the differential equation just depends on the q profile. The magnetic shear is seen to impact on the shaping penetration. In a region of shear free plasma, the elongation parameter κ is a constant with respect to r (thus remaining non-zero on the magnetic axis), while the triangularity parameter δ scales linearly with r, thus vanishing on the magnetic axis.

Recap of Key Results

Chapter 3 - Linearised MHD

Linear MHD equations. Fluid and electromagnetic quantities are all perturbed. Ohms law and Faradays law enables electro-magnetic perturbations to be written in terms of a fluid displacement. The linearised normal mode equation, involving just the fluid displacement $\boldsymbol{\xi}$, can the be obtained.

It is possible to obtain a conservation of energy equation. For many applications, this serves as a dispersion relation. A property of this equation is that the square of the eigenvalue ω is real. This means that in the ideal MHD model, modes are either purely growing (or decaying), or they are purely oscillating (not growing or decaying).

The energy method is seen to reproduce the normal mode equation (the linearised equation of motion). This involves minimisation of the total energy with respect to the displacement for constant mode frequency of growth rate. Convenient Euler-Lagrange equations can then be developed for many applications.

The energy principal is the most straightforward means of accessing stability. It involves employing trial functions to inspect the corresponding sign of the potential energy δW. If $\delta W < 0$ for any physically reasonable trial function, the system is unstable. A mathematical equivalent to the trial function method is to minimise δW with respect to $\boldsymbol{\xi}$, usually by solving Euler-Lagrange equations. The energy principle, unlike the energy method above, does not provide information regarding the growth rate (only provides the sign of ω^2).

A convenient form for δW can be derived. Close to marginal stability it is seen that the parallel component of the displacement does not enter δW. The remaining δW contributions can be written in a convenient form involving the two perpendicular components of $\boldsymbol{\xi}$. One term is associated with field line bending. It is usually strong stabilising, except near a rational surface. All the MHD instabilities studied in this course develop where field line bending stabilisation is minimal. Another stabilising term corresponds to the energy necessary to compress the magnetic field and describes the major potential energy contribution to magnetosonic waves. A term proportional to the pressure gradient is responsible for ballooning and interchange instabilities. It is destabilising if $\boldsymbol{\nabla} P$ and $\boldsymbol{\kappa}$ are parallel (unfavourable curvature). Finally, a 'kink' term can be identified corresponding to the free energy arising from the current. Pages 63-66 give a description of kinetic-MHD considerations.

Recap of Key Results

Chapter 3 continued - Current Driven Instabilities in a Tokamak

The remainder of chapter is primarily concerned with the field line bending contribution, and the kink contribution to δW (an exception to this is the internal kink mode where the interchange term also features - though we don't derive this). In this chapter true toroidal effects on the instabilities do not feature at the leading order. Screw pinch approximation is sufficient.

Inverse aspect ratio expansions enable analytic derivation. The largest term yields perpendicular incompressibility. At order ϵ^2, field line bending and the kink contributions compete. Minimisation of δW can be obtained via an Euler-Lagrange equation for the eigenfunction (radial displacement).

Rational surfaces: It is seen why rational surfaces, where $q = m/n$ minimise field line bending stabilisation. On the rational surface the parallel wave-vector vanishes, so a perturbation can oscillate without having to bend the magnetic field lines.

$m = 1$ is seen to be a special mode number where the curvature of the magnetic field lines in the poloidal plane is matched by the mode structure. As result, field lines do not bend in the poloidal plane, and the corresponding field line bending is lost. One has to go to higher order in the inverse aspect ratio in order to solve the internal kink mode problem, and it is seen that for $n = 1$ there is an analogous loss of field line bending in the toroidal direction. The internal kink mode is thought to be responsible for the sawtooth oscillation.

Recap of Key Results

chapter 4: The external kink mode: This mode is one of the main candidates for tokamak disruption. A generalised δW treatment involving the plasma-vacuum interface, and the vacuum region is required for treating these instabilities. It is found that the external contribution to δW is destabilising for modes with $q_a < m/n$, where q_a is safety factor at the plasma-vacuum interface. The mode will be stable if the field line bending stabilisation can compensate for a destabilising external region. Whether this is the case depends on the current profile in the core region. Enhanced global shear (e.g. measured through q_a/q_0) is stabilising.

chapter 4: Inertia and Resistivity: In the region close to a rational surface the effect of inertia must be included. This treatment is required if ideal growth rates are sought, or if resistivity is important.

Tearing modes: It was shown that internal kink modes with $m > 1$ are marginally stable. Additional physics is required in order to access stability. This additional physics primarily comes in the form of a generalised Ohm's law, namely 'resistive Ohm's law.'

It is found that the growth rate of the tearing mode is proportional to the tearing mode parameter Δ' (not to be confused with the Shafranov shift). The tearing mode parameter is determined by the current profile in the ideal region, on either side of the narrow resistive region close to the rational surface. The growth rate is proportional to Δ', and hence a mode will be unstable is $\Delta' > 0$, and this in turn generally happens when there is large global shear. The non-linear version of this instability is identified with neo-classical tearing modes, which has a strong impact on plasm confinement, and can give rise to disruptions.

It turns out that the linear tearing mode, and the external kink modes are analytically continuous across the boundary in q_a. For a sufficiently large global shear, the external kink is unstable for $q_a < m/n$ (external mode), and the tearing mode is unstable for $q_a > m/n$.

Recap of Key Results

The growth rate of the internal kink mode can be obtained by considering the effect of inertia in a narrow layer region. The calculation yields an unexpected relationship between the growth rate and δW (a linear relationship).

We are able to derive the structure of magnetic islands. We write down the radial position of a field line as a function of the helical angle χ. It is parameterized in terms of the total magnetic flux (constant along a field line), and the amplitude of the radial field perturbation. The radial field perturbation can only create an island if resistivity is non-zero (since the radial field is zero on a rational surface in an ideal plasma).

We derive the equation that describes the evolution of the width of an island. We are especially interested in identifying saturated states, for which w does not evolve in time. These are of course new resistive MHD equilibria (non-linear saturated states). It is found that the non-linear state is determined by $\Delta'(w)$ evaluated in the ideal region.

By including bootstrap current, and upon consideration of the effect of bootstrap on the pressure, we eventually obtain the Modified Rutherford equation. It is found that a seed island is required in order for the island to grow to a (non-zero) saturated state.

Recap of Key Results

The Clebsch form of the magnetic field and straight field line coordinates enables us to write the magnetic operator in a convenient form. It is seen that the perpendicular components of the perturbed magnetic field vanish on a rational surface.

If we expect an instability to be highly radially localised (close to a rational surface) an eikonal approach is useful. This allows a clear separation of the dynamics along the field, and across the field.

The ballooning equation is obtained in a form where the poloidal field can me redefined arbitrarily. Consequently, one can then make progress analytically by employing the coordinates used in chapters 1 and 2 for the large aspect ratio expansion of the equilibrium.

To obtain the ballooning equation, one needs to obtain δW including full toroidal effects. All of the four terms in the convenient form for δW have to be minimised. The interchange term involves the the weird component of the curvature. Compared to a screw pinch (cylindrical geometry) this definition of the curvature is very different in a tokamak. In the latter, one has both the curvature in the $\boldsymbol{\nabla} R$ direction as well as the $\boldsymbol{\nabla}\boldsymbol{\psi}$ direction. As a result, the tokamak is more stabilising to interchange modes (Mercier criterium) than in a cylinder (Suydam criterium).

Recap of Key Results

Chapter 7 - Interchange and Ballooning continued

It was found that the eikonal approach apparently yields periodicity problems.

One can get around this problem via the concept of the ballooning representation, where the poloidal angle is allowed to be a stretched coordinate which maps out the real axis $-\infty < \Omega < \infty$. A boundary condition is identified which ensures that the energy associated with a ballooning perturbation is not infinite.

A means of analysing the stability of the ballooning equation is to examine the large Ω secular structure of the mode. This turns out to be the treatment required for a proper examination of an interchange mode.

The interchange instability condition turns out to be the condition that both interchange solutions remain physical (finite energy). It is found that the magnetic shear is stabilising, while negative pressure gradients are destabilising.

A ballooning mode is usually more unstable than an interchange mode. A ballooning mode takes into account the effect of local (poloidally localised) shear, which is generally less in the region of poor curvature (outboard side). However, pressure can be stabilising if (negative) pressure gradients are large enough (second region of stability).

Interchange instabilities are associated with the lowest order stability criteria in a confined plasma. The tokamak would be expected to be stable to interchange modes at 'all times'. Note however that there are important kinetic corrections to interchange modes. These can be stabilising or destabilising depending on the properties of the population of 'energetic' particles.

High n ballooning instabilities are micro-instabilities. They typically have very short toroidal and poloidal wave lengths, and are highly localised radially. High n ballooning instabilities are linked with cross-field transport. Moderate n ballooning instabilities are associated with edge localised modes.